CO_2/HCO_3^-/PH SENSING SOLUBLE ADENYLYL CYCLASE REGULATES LYSOSOMAL PH

A Dissertation

Presented to the Faculty of the Weill Cornell Graduate School

of Medical Sciences

in Partial Fulfillment of the Requirements for the Degree of

Doctor of Philosophy

by

Nawreen Rahman

February 2016

CO_2/HCO_3^-/PH SENSING SOLUBLE ADENYLYL CYCLASE REGULATES LYSOSOMAL PH

Nawreen Rahman, Ph.D.

Cornell University 2016

Lysosomes, the degradative organelle of the endocytic and autophagic pathways, function at an acidic pH, but the molecular processes that determine lysosomal pH are not understood. In particular, no lysosomal pH sensitive signaling enzymes have yet been identified. Here we show genetically and pharmacologically that in the absence of bicarbonate (HCO_3^-) regulated soluble adenylyl cyclase (sAC), lysosomes fail to properly acidify leading to accumulation of autophagic vacuoles (AVs). Due to the ubiquitous presence of carbonic anhydrases (CAs), which instantaneously equilibrate carbon dioxide (CO_2), HCO_3^-, and intracellular pH (pH_i), sAC serves as a physiological sensor of HCO_3^-, CO_2, and pH_i. We show that sAC's role in lysosomal acidification is dependent upon its regulation by intracellular HCO_3^- in a CA dependent manner, consistent with sAC serving as a pH sensor regulating lysosomal pH. Thus, sAC is the first, and thus far only known, pH regulated signaling enzyme that affects lysosomal pH. Because intracellular vesicles like lysosome are functionally dependent upon acidification, this work has broad implications.

BIOGRAPHICAL SKETCH

Nawreen Rahman was born in Dhaka, Bangladesh in 1984. She spent the first 16 years of her life in Dhaka, Bangladesh, before moving to England in 2000 and finishing her high school from King George V College in 2002. From 2002-2006, Nawreen attended Oxford University where she was enrolled in a joint Bachelors/Master program and graduated with a MBioch degree in Molecular and Cellular Biochemistry. She completed her Masters thesis under the guidance of Dr. Edith Sim studying the expression and biochemistry of azoreductase from *P. aeruginosa*. While in university, Nawreen was involved in running the Oxford University Scientific Society (OUSS) with finally being elected as the President of the society in 2005. Nawreen moved to United States and in 2007 she accepted a position as a Research Technician at Weill Cornell Medical College in the laboratory of Dr. Gunnar Gouras. There, she had the opportunity to do research in Alzheimer's Disease and co-authored publications in peer reviewed journals. Dr. Gouras' laboratory is also where Nawreen found her love of microscopy that she was able to incorporate to her graduate studies. In the summer of 2009, Nawreen joined the Neuroscience program of Weill Cornell Graduate School of Medical Sciences and pursued her thesis work in the laboratory of Drs. Lonny Levin and Jochen Buck. Over the past five years, Nawreen studied the role of soluble adenylyl cyclase in regulating lysosomal acidification. She received a pre-doctoral Ruth L. Kirschstein National Research Service Award (F31) from the National Institutes of Health (NIH) to help with her research.

DEDICATION

I would like to dedicate my thesis to my parents Arifur Rahman and Raihana Rahman and my incomparable husband Shafat Zaman. I would not have been able to complete this chapter of my life without your constant love, support and understanding. I thank my parents especially for flying half way across the world to babysit my 3 month-old son, Aydin Sharief Zaman, while I come back to work to finish my studies.

ACKNOWLEDGMENTS

I would like to thank my mentors, Drs. Lonny Levin and Jochen Buck, for all their support and guidance over the years. With their unique approach to science, their generosity, open-mind and sense of humor, they have not only guided me through this challenging part of my life, but made it seem effortless while doing so. Thank you not only for open door policy that lead to hours of discussions in all sort of random topics including science, politics and sometime fashion trends. I will always be thankful for their patient instruction and editorial skill as they helped me in my progression into a better scientific writer. It was no small task to be sure. I would also like to thank my committee members, Drs. Fred Maxfield, Teresa Milner and Giovanni Manfredi for time, dedication and scientific input and for making sure my progress is right on track.

Thank you to all the members of the Levin Buck Laboratory, past and present. A special thanks to Dr. Jon Zippin who is always willing to talk science and give constructive criticism. A big thank you to all the other members of the lab, who became my family away from home. Eric Salazar, Jacob Bitterman, Lavoisier Ramos, Jennifer Martinez, Jonathan Chen, Nicole Ramsey, Ken Hess, Elisabeth Wondimu: Thank you for making my time in and outside lab very entertaining and enjoyable. Thank you to our lab manager and research technicians, Heather Patrick, Ana Diaz, and Archana Vishwanath for doing a great job and making sure the lab is running smoothly. It has been a pleasure working with all of you and your support and friendship is greatly appreciated.

I would especially like to thank Drs. Gunnar Gouras, Davide Tampellini and Estibaliz Capetillo-Zarate who first taught me how to start thinking like a scientist and treated me more as a graduate student and not as a research technician. Thank you for taking the time to explain the principle behind each and every experiment we were performing and help me design experiments and teach me the importance of proper controls.

Last but not the least I would like to thank my parents and brothers, for putting up with my absent mindedness, missed calls and constantly showering me with your unconditional love and understanding. Thank you for travelling half way across the world to look after my son, so that I can finish my graduate career.

To my husband and best friend, Shafat Zaman, thank you for your love and support over the years, as well as putting up with my short temper and frustrations during the bad months (of which there were many). You have always encouraged me and been my personal cheerleader during the highs and lows of my research career.

Lastly, to my son, Aydin Zaman: You have given a new significance to my life and made my life more meaningful and beautiful. You are my shining star!

TABLE OF CONTENTS

LIST OF FIGURES

ABBREVIATIONS

AC	Adenylyl cyclases
AD	Alzheimers Disease
AKAP	A-kinase anchor proteins
AMRF	Action myoclonus renal failure syndrome
AP1	Adaptor protein 1
APL	Autophagolysosomes
ATP	Adenosine triphosphate
β-GC	β-glucocerebrosidase
bp	Base-pair
CA	Carbonic anhydrases
cAMP	Cyclic 3', 5'-adenosine monophosphate
CAP	Catabolite gene activator protein
CatD	Cathepsin D
cDNA	Complementary DNA
CI-M6PR	Cation-independent mannose-6-phosphate receptor
ClC	Chloride Channel
CLEAR	Coordinated lysosomal expression and regulation
CMA	Chaperone mediated autophagy
CNG	Cyclic nucleotide gated ion channels
CO_2	Carbon Dioxide
DMEM	Dulbecco's modified Eagle medium
DNA	Dioxyribonucleic Acid
EE	Early Endosomes
EEA 1	Early Endosome Antigen 1
EPAC	Exchange proteins activated by cAMP
ER	Endoplasmic Reticulum

FBS	Fetal Bovine Serum
FTD	Frototemporal Disease
GAP	GTPase activating protein
GD	Gaucher Disease
GDP	Guanosine Diphosphate
GEF	Guanine exchange factor
GGA	Golgi-associated, Gamma-adaptin ear-containing, ADP ribosylation factor binding protein
glc	Glucose
GlcNac	*N*-acetylglucosamine
GPCR	G-protein coupled receptor
GTP	Guanosine Triphosphate
HCN	Hyperpolarization-activated cyclic nucleotide-gated channels
HCO_3^-	Bicarbonate
HOPS	Homotypic fusion and vacuole protein sorting
kDa	Kilo Dalton
Km	Michaelis Menten constant
KO	Knock Out
LAMP-1	Lysosomal associated membrane protein-1
LAMP-2	Lysosomal associated membrane protein-2
LE	Late Endosomes
LIMP-1	Lysosomal integral membrane protein-1
LIMP-2	Lysosomal integral membrane protein-2
LMP	Lysosomal membrane proteins
LSD	Lysosomal storage disorders
LysoT	LysoTracker
M-6-P	Mannose-6-phosphate
M6PR	Mannose-6-phosphate receptor
MEF	Mouse embryonic fibroblasts

NCL	Neuronal Ceroid Lipofuscinoses
NGF	Neurotrophin growth factor
NGS	Normal Goat Serum
NSF	N-ethylmaleimide sensitive factor
OSTM1	Osteopetrosis associated transmembrane protein 1
P/S	Penicillin/streptomycin
PBS	Phosphate Buffered Saline
PBST	Phosphate Buffered Saline Tween
PD	Parkinson's disease
PDE	Phosphodiesterases
PFA	Paraformaldehyde
PKA	Protein kinase A
PS	Presenilin
RAVE	Regulator of the ATPase of vacuolar and endosomal membranes
RNA	Ribonucleic Acid
RPE	Retinal pigmented epithelium
RT-PCR	Reverse transcriptase Polymerease chain reaction
sAC	Soluble adenylyl cyclase
sAC_{fl}	sAC full length
sAC_t	sAC truncated
SDS	Sodium Dodecyl sulphate
SDS PAGE	SDS-Polyacrylamide Gel Electrophoresis
SNAP	Soluble NSF attachment proteins
SNARE	Soluble N- ethylmaleimide–sensitive factor attachment protein receptor
TBST	Tris Buffered Saline Tween
TFEB	Transcription factor EB
TGN	Trans Golgi Network

tmAC	Transmembrane adenylyl cyclases
TNF	Tumor Necrosis Factor
TPC-2	Two pore channel
TRPML-1	Transient receptor potential cation channel, mucolipin subfamily
TSE	Tubular sorting endosomes
V-ATPase	Vacoular ATPase
VAMP-7	Vesicle-associated membrane protein 7
Vmax	Maximum velocity
WT	Wild Type

CHAPTER ONE: INTRODUCTION

1. Lysosomes

1.1 An Overview

Lysosomes, first discovered more than 50 years ago by Christian De Duve (de Duve, 2005),(Bainton, 1981) are single membrane bound organelles that are present in all nucleated eukaryotic cells. Lysosomes constitute up to 5% of the intracellular volume of a cell and are heterogeneous in size and morphology. Lysosome size, shape, and number per cell varies between cell types; they may be spherical, ovoid, or tubular in shape, and may differ between 0.1 to 2 μm in size (Luzio et al, 2014).

When studied by electron microscopy, lysosomes often appear to contain electron dense deposits and membrane whorls (a membranous structure that appears to be multi lamellar or arranged in spirals when observed in cross section) (Klumperman & Raposo, 2014). Within a few years of their discovery, lysosomes were quickly recognized to be the terminal degradative compartments of the endocytic pathway; they are also required for degradation of intracellular materials that is sequestered during the process of autophagy (discussed in Section 1.3.3).

The most acidic organelles of the cell, lysosomes have a luminal pH of 4.5-5, which is maintained by an adenosine triphosphate (ATP)-dependent proton pump. The low pH supports optimal activity of lysosomal hydrolases, which are responsible for breaking down proteins and cellular components within the lysosomal lumen. The

lysosomal membrane, which acts as a barrier to separate these catabolic enzymes from other cell constituents to prevent their degradation, does not just act as a mechanical barrier. It is also responsible for establishment of the pH gradient between the lysosomal lumen and the cytoplasm and for transport of degradation products into the cytoplasm. It also facilitates transfer of materials across the lysosomal membrane by mediating the fusion of endosomes or their organelles as well as selective transport processes. Kinetic studies of radiolabeled metabolites into lysosomes have demonstrated the existence of more than 20 lysosomal membrane proteins (Luzio et al, 2014).

1.2 Lysosomal Proteins

A schematic view is shown in **Figure 1.1** of a lysosome with some of the lysosomal membrane proteins (relevant to the project) which regulate communication between the lysosomal lumen and the cytosol.

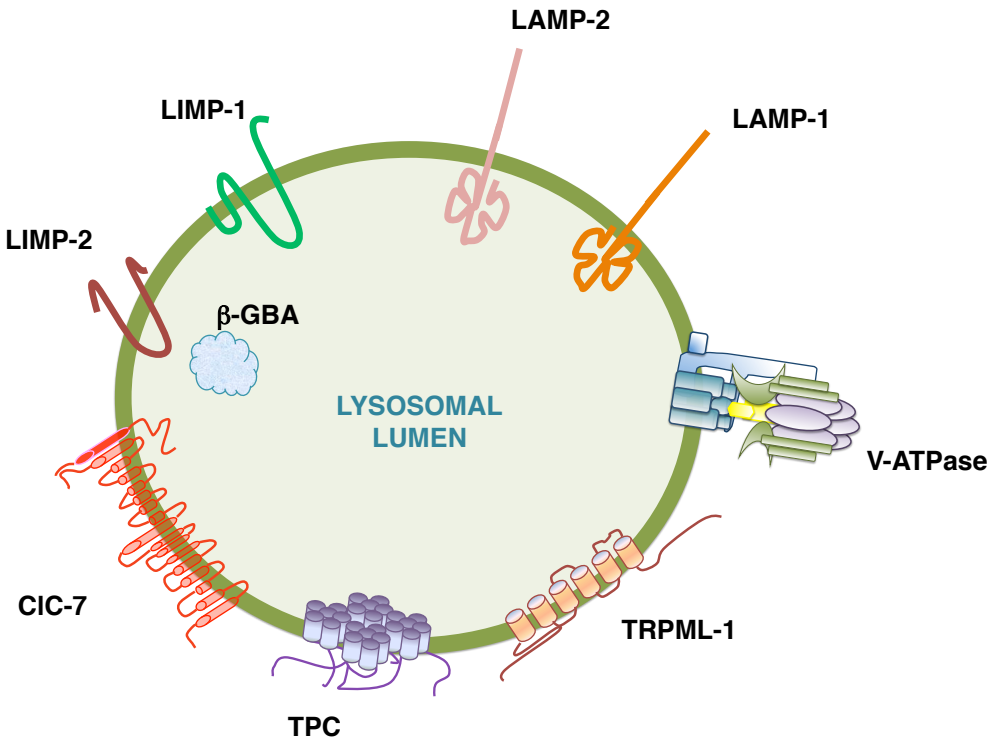

Figure 1.1: Representative lysosomal membrane proteins. Schematic drawing of the topology of the major integral membrane proteins LAMP-1, LAMP-2, LIMP-1 and LIMP-2. β-GC is indicated as a ligand for LIMP-2. The multimeric V-ATPase, essential for acidification of the lysosomal lumen and three lysosomal membrane transporters thought to be involved in counterion conductance are depicted.

1.2.1 LAMP-1 and LAMP-2

One salient feature of lysosomal membrane proteins is their high carbohydrate content. Integral lysosomal membrane proteins are heavily glycosylated on their luminal domains. The heavy glycosylation renders lysosomal membrane proteins resistant to degradation by lysosomal hydrolases. Their abundance is so high that they form a coat on the inner surface of the lysosomal membrane and serve as a protective barrier against lysosomal hydrolases, thus playing a critical role in the maintenance of the structural integrity and stability of the lysosome (Saftig &

Klumperman, 2009).

Among the most abundant lysosomal membrane proteins are the lysosomal associated membrane proteins LAMP-1 and LAMP-2, which account for more than 50% of all lysosomal proteins. Both LAMP-1 and LAMP-2 have their N termini directed towards the luminal side, span the membrane once and have short cytoplasmic C-termini. The N-termini are heavily glycosylated. They are among the most densely glycosylated proteins known with modifications contributing about 60% of the total mass of the glycoproteins. Whereas the transmembrane segments of the lysosomal membrane proteins are putatively involved in direct transport events across membrane, the short cytoplasmic tails usually mediate contact to other cytosolic proteins and organelles (Saftig & Klumperman, 2009).

Mice deficient in either LAMP-1 (Andrejewski et al, 1999) or LAMP-2 (Tanaka et al, 2000) are both viable and fertile. However mice deficient in both LAMP-1 and LAMP-2 (Eskelinen et al, 2004) have an embryonic lethal phenotype, suggesting that the two lysosomal membrane associated proteins share common functions *in vivo*. Of the two, LAMP-2 seems to have more specific functions. Mice deficient for LAMP-2 have a more severe phenotype relative to mice with LAMP-1 deficiency. Mutations in the mouse LAMP-2 gene result in the accumulation of autophagic vacuoles in heart and skeletal muscles (Tanaka et al, 2000). These phenotypes replicate the symptoms in human patients suffering from Danon disease (a disease caused by

primary deficiency in LAMP-2) (Nishino et al, 2000), a fatal cardiomyopathy and myopathy.

1.2.2 LIMP-1 and LIMP-2

Lysosomal integral membrane proteins (LIMPs) are also ubiquitously expressed on lysosomal membranes, but they are less abundant than LAMPs. LIMP-1 (CD63) spans the lysosomal membrane four times, whereas LIMP-2 spans the membrane only once. The N and C termini of both proteins are located in the cytoplasm and these proteins also highly glycosylated within the lysosomal lumen (Saftig et al, 2010). LIMP1 (CD63) knockout mice appear to have normal lysosomal function, but they have higher fecal water content and altered kidney function including increased urinary flow, water intake, and reduced urine osmolality. In their kidney collecting duct principle cells, CD63-deficient mice exhibit abnormal intracellular lamellar inclusions, indicating that fusion or sorting at the apical membrane might be impaired (Schroder et al, 2009).

LIMP-2 is thought to be involved in lysosome/endosome biogenesis. Overexpression of LIMP-2 results in the accumulation of large vacuoles that share features with both early and late endosomes, as well as lysosomes. These vacuoles are not electron dense and only contain luminal membrane, suggesting that invagination of intercellular vesicles may be impaired (Saftig et al, 2010).

Multiple ligands have been described to bind to LIMP-2, including β-glucocerebrosidase (β-GC; the lysosomal enzyme defective in Gaucher Disease (GD)) (Reczek et al, 2007). Binding of β-GC to LIMP-2 occurs early in the biosynthetic pathway at the endoplasmic reticulum (ER) at neutral pH. The β-GC /LIMP-2 complex is then transported from the Trans Golgi Network (TGN) and endosomes to the lysosomes, where the acidic pH of the lysosomes causes β-GC to dissociate from LIMP-2. Lack of LIMP-2 results in missorting of β-GC to the extracellular space and ER associated degradation. LIMP-2 may also function in the ureter and the kidney, in the inner ear and in the myelination of peripheral nerves. In humans, LIMP-2 mutations are known to cause progressive myoclonus epilepsy associated with renal failure (action myoclonus renal failure syndrome, AMRF) (Berkovic et al, 2008).

1.2.3 V-ATPase

In addition to these major lysosomal membrane proteins, there are also other less abundant membrane proteins that are expressed in a cell-specific or tissue specific manner. The conserved V-ATPase is also located on the lysosomal membrane (discussed in further details in Section 1.5 and 1.6) and is an essential protein that is required to maintain the lysosomes at an acidic pH.

1.2.4 ClC-7

ClC (Chloride Channel) antiporters have been primarily implicated in intra-vesicular transport along the endosomal-lysosomal pathway. Disruption of some of the intracellular ClCs affects acidification of their respective compartments. The ubiquitously expressed ClC-7 resides on late endosomes/lysosomes (Braun, 2008) as well as in the ruffled border of osteoclasts, where it is necessary for the acidification of the bone lacuna during the process of bone resorption (Kornak et al, 2001). While the role of ClC-7 in the acidification of this extracellular compartment has been shown, the role of ClC-7 in regulating lysosomal pH remains to be seen (Graves et al, 2008),(Lange et al, 2006),(Kasper et al, 2005),(Poet et al, 2006).

ClC-7 is found in the lysosomal membrane in a heterodimeric complex with Ostm-1 (osteopetrosis associated transmembrane protein 1), which is important for proper trafficking of CLC-7 to the lysosomes, stability and ion transport activity (Lange et al, 2006). ClC-7 knockout mice die within 30 days of birth (Kornak et al, 2001). Their pathology reveals severe osteopetrosis (hyper calcification of bone) leading to growth retardation and deformation as well as severe degeneration of the brain and retina. Quantitative analysis of lysosomal acidification show no change in lysosomal pH (Lange et al, 2006). However, in ClC-7 KO cells of living mice, although endocytic uptake is unaffected, the degradation of the endocytosed protein is significantly decreased (Wartosch et al, 2009). Despite the unaltered steady-state pH

in ClC-7 knockout lysosomes, ClC-7-mediated chloride transport may have an impact on the kinetics of acidification, e.g., during vesicle maturation. It is hypothesized the ClC-7 may utilize the pH gradient to maintain Cl^- in the lysosome at a concentration higher than the equilibrium concentration. Thus, counter-ions other than chloride might provide the electrical shunt for the proton pumping. Therefore it is conceivable that the chloride concentration is decreased in ClC-7-deficient lysosomes.

1.2.5 TRPML-1

Whereas there are well-established transporters/channels for anion movement across the lysosomal membrane for counterion conductance, candidates for the cation transporting candidates are more tentative. One such candidate is the cation channel TRPML-1 (transient receptor potential cation channel, mucolipin subfamily), which has been shown to play a role in Ca^{2+} release from the lysosomal lumen (Zhang et al, 2009). TRPML-1 is encoded by the gene MCOLN1, which is mutated in the lysosomal storage disease, mucolipidosis type IV. This autosomal recessive disease is characterized by a slow but progressive neurodegenerative phenotype (Altarescu et al, 2002). The TRPML 1 is localized to the lysosomes although its role in the lysosome is not completely understood. Disruption of the protein has revealed conflicting results; it has been shown to increase , decrease or even maintain lysosomal pH (Mindell, 2012).

1.2.6 TPC

There are two isoforms of TPC (two pore channel), TPC-1 and TPC-2. TPC-2 is a cation channel that was shown to localize to the lysosome and play a role in Ca^{2+} release from the lysosomal lumen (Calcraft et al, 2009). However, recent studies have shown TPC-2 to be a ATP and pH-sensitive Na^{+} channel as well (Cang et al, 2013). However, TPC double knock out cells show a role in acidification of lysosomes in starvation-induced autophagy; TPC-2 knockout cells grown in the presence of sufficient nutrients have normal lysosomal pH.

1.2.7 Cathepsins

Cathepsins are lysosomal hydrolytic proteases belonging to the aspartic, cysteine and serine proteinase family. The name Cathepsin derives from the Greek verbs to digest (cata-) and to boil (-hepsin). Many lysosomal proteases are ubiquitously expressed, like the aspartic proteinase Cathepsin D or the cysteine proteinases Cathepsin B, H and L; others have a more tissue specific expression pattern. Cathepsin expression patterns can differ by cell type or due to different physiological conditions (Ishidoh & Kominami, 2002).

Cathepsins are translated as pre-proenzymes and transferred to the Golgi apparatus. In the Golgi, they are processed into pro-enzymes, which have low enzymatic activities, and they are modified with sugar moieties containing mannose-

6-phosphate (M-6-P). Via its interaction with mannose-6-phosphate receptor (M6PR), the pro-enzymes are transported by vesicular trafficking to the lysosomes where they undergo further maturation to have full enzymatic activity. Inadequate processing of lysosomal cathepsins can result in cell death. Thus processing and activation of lysosomal proteases are tightly regulated by intra-organellar environment, such as intra organellar pH, membrane protein compositions, glycosyl side chains of membrane protein and lipid composition of organellar membranes. For example, Cathepsin D (CatD), is translated as pre-pro CatD (**Fig. 1.2**), which is transferred through the Golgi apparatus as pro-CatD with a molecular mass of 54 kDa. The mature form of CatD that is localized to the lysosomes exists in both the single chain form with a molecular mass of 44 kDa and two types of double chain forms with molecular masses of approximately 32 kDa and 7 kDa. The processing of the single chain form to double chain forms is tissue specific; for example, the two double chain forms are found in liver whereas the single chain is detected in spleen (Ishidoh & Kominami, 2002).

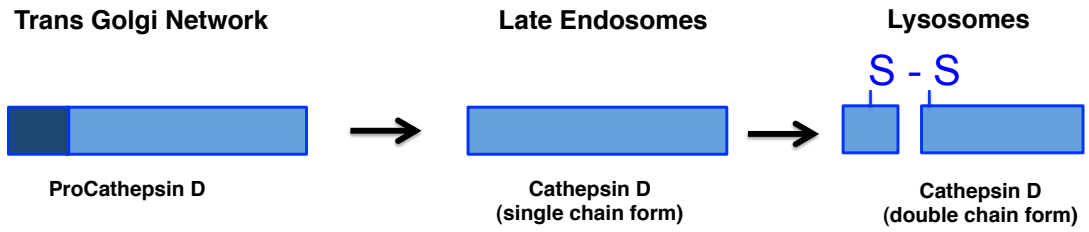

Figure 1.2: Processing and activation of lysosomal protease, Cathepsin D: Dark blue (inactive forms) and light blue (active forms) bars indicate the propeptide regions and the mature active form of Cathepsin D, respectively. Arrows indicate the processing pathways.

1.3 Biogenesis of lysosomes

Lysosome biogenesis requires the integration of both the biosynthetic and the endocytic pathways of the cell.

1.3.1 Biosynthetic pathway to the lysosomes

1.3.1.1 Biosynthesis and transport of lysosomal soluble proteins:

Lysosome biosynthesis requires the coordinated transcription of genes encoding for lysosomal proteins. Many lysosomal enzymes and membrane proteins have a palindromic 10 base-pair (bp) GTCACGTGGAC motif, named the coordinated lysosomal expression and regulation (CLEAR) element (Sardiello et al, 2009), in their promoter region that can bind to transcription factor EB (TFEB). When inactive, TFEB is highly phosphorylated and is localized to the cytosolic surface of the lysosomes. Under specific condition, such as starvation or lysosomal dysfunction, TFEB is dephosphorylated and rapidly translocates to the nucleus, resulting in synthesis of lysosomal membrane proteins, hydrolases and other proteins found within lysosomes (Settembre et al, 2013).

Lysosomal proteins synthesized by ribosomes attached to the rough endoplasmic reticulum (ER), usually contain an N-terminal signal sequence of 20-25 amino acids, which directs their translocation into the ER lumen. Following insertion,

the signal sequence is cleaved and the trafficked proteins undergo N-glycosylation on asparagine residues within the sequence Asn-X-Ser/Thr. This *N*-glycosylation step consists of addition of mannose-rich oligosaccharide chains containing three glucose (Glc), nine mannose (Man), and two *N*-acetylglucosamine (GlcNac) residues (Glc3Man9GlcNac2). Once glycosylated, these lysosomal proteins are then transferred to the Golgi by vesicular transport (Braulke & Bonifacino, 2009).

There are multiple pathways by which lysosomal proteins can reach the lysosome from the Golgi (**Figure 1.3**): mannose-6-phosphate receptor (M6PR) dependent and M6PR independent pathway.

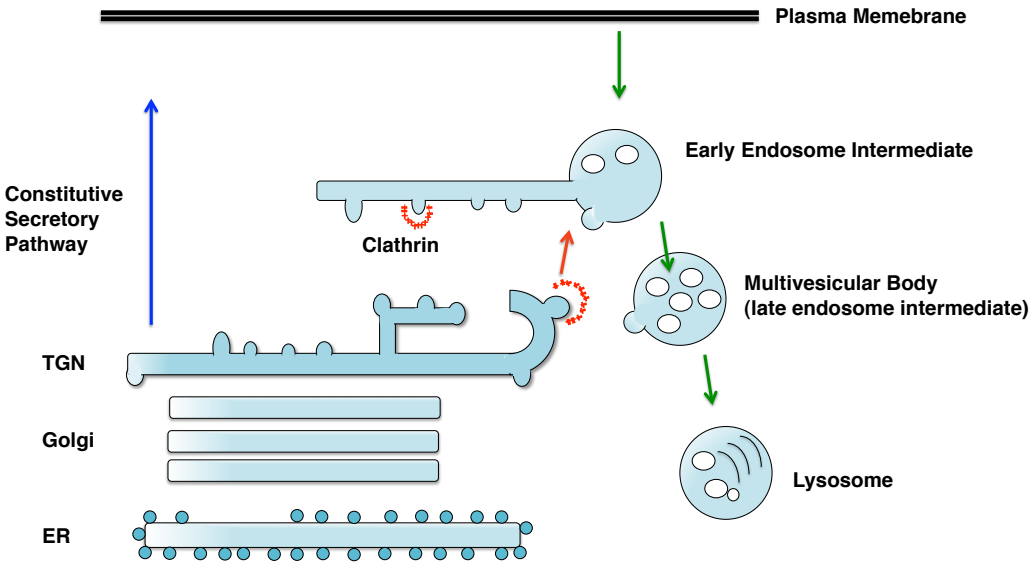

Figure1.3: Possible pathways by which lysosomal hydrolases can reach the lysosomes. Lysosome biogenesis requires a concerted interaction between the biosynthetic and the endocytic pathways. Lysosomes receive cargo for degradation as well as newly synthesized lysosomal proteins from the endocytic pathway (green arrows). Lysosomal proteins are synthesized in the endoplasmic reticular (ER) and are transported through the Golgi into the *trans*-Golgi network (TGN). From the TGN, lysosomal proteins can follow the constitutive secretory pathway (blue arrow) to the plasma membrane and subsequently reach the lysosomes by endocytosis (indirect pathway). However, lysosomal hydrolases can also follow a direct intracellular route (red arrow) to the endo-lysosomal system. One of the best-characterized intracellular pathways is the clathrin-dependent transport of lysosomal hydrolases by mannose-6-phosphate receptors (M6PR). Adapted from (Saftig & Klumperman, 2009)

1.3.1.1(i) M6PR dependent transport

The best-characterized pathway is the M6PR-dependent transport of lysosomal hydrolases. Once in the *cis*-Golgi, lysosomal hydrolases acquire M6P residues on their oligosaccharide chains that results in the separation of the

glycoproteins that are destined for the lysosome from the secretory glycoproteins.

The M6P residues on lysosomal proteins are recognized by two distinct M6PRs with molecular masses of 46 kDa (M6PR-46 or cation-dependent M6PR, CD-M6PR), and 300 kDa (M6PR-300 or cation-independent M6PR, CI-M6PR) (Ghosh et al, 2003). Both M6PRs are type I transmembrane glycoproteins. Distinct lysosomal hydrolases can exhibit different affinities for CD-M6PR and CI-M6PR.

Considerable research has gone into understanding the machinery involved in M6PR trafficking. In the TGN, the cargo-loaded MPRs are sorted into clathrin-coated vesicles for transport to endosomes, using AP-1 (adaptors proteins 1) and GGAs (Golgi-associated, Gamma-adaptin ear-containing, ADP ribosylation factor binding protein) that interact with specific motifs in the cytoplasmic tails of the M6PRs. Once the MPR-hydrolase complex is packaged into clathrin coated vesicles and trafficked to endosomes, they dissociate from their receptors due to luminal acidic pH (pH~5-6). Once dissociated, the receptors recycle back to the TGN. It is not known exactly where in the endocytic pathway the M6PRs deliver their bound ligands. Immunoelectron microscopy for M6PR and LAMP-1, a late endosome marker has demonstrated large amount of M6PR is colocalized with LAMP-1 positive organelles. (Kornfeld & Mellman, 1989). The low pH of late endosomes (~5.5) has also been shown to be optimal for the dissociation of the ligands from M6PR. However, live cell imaging as well as the observation that there is relatively equal distribution of M6PRs on early and late endosomes suggest that early endosomes can also be the point of

entry (Waguri et al, 2003).

A small fraction of newly synthesized enzymes escape binding to M6PRs in the Golgi, and instead are transported to the plasma membrane. This fraction is secreted and can bind M6PRs present on plasma membranes of neighboring cells, where it is subsequently endocytosed. This indirect transport of lysosomal proteins might differ depending on the enzyme and cell type studied. In fibroblasts for instance, about 10% of β-hexosaminidase is secreted before its delivery to lysosomes (Vladutiu & Rattazzi, 1979).

1.3.1.1(ii) M6PR independent transport

Although the M6PR route is one of the best-characterized routes for the delivery of lysosomal soluble enzymes, it is not the only route available. This became apparent in patients with I-cell disease (also known as Mucolipidosis type II), where lysosomal hydrolases do not acquire M6P tags because of a deficiency in *N*-acetylglucosamine-phosphotransferase activity. In these patients, some cells such as the hepatocytes and lymphocytes, still contain a significant number of soluble hydrolases in their lysosomes (Waheed et al, 1982).

Recently, the lysosomal integral membrane protein type 2 (LIMP-2), a heavily glycosylated type III transmembrane protein has been identified as an M6PR-independent lysosomal targeting receptor (Reczek et al, 2007). LIMP-2 was found to

be a specific receptor for β-glucocerebrosidase (β-GC). β-GC binds to LIMP-2 in the ER and is directly targeted to the lysosomes. In cells lacking LIMP2, β-GC is secreted even while most lysosomal hydrolases are successfully delivered to the lysosomes.

Another candidate for an alternative receptor protein is sortilin, a type I transmembrane glycoprotein which has been reported to mediate lysosomal trafficking of prosaposin and acid sphingomyelinase (Canuel et al, 2009).

1.3.1.2 Biosynthesis and transport of lysosomal membrane proteins (LMP)

The M6PR pathway is important for delivering soluble hydrolases to the lysosomes. Lysosomal membrane proteins (LMPs) are not modified with M6P groups, and thus, do not depend upon M6PR sorting. Instead, LMPs contain sorting signals in their cytosolic tails that mediate endosomal and lysosomal targeting (van Meel & Klumperman, 2008). Most targeting signals belong to the YXX Ø (e.g., LAMP1, LAMP2 and LIMP1) or [DE]XXXL[LI] (e.g., LIMP2) motifs. Similar to lysosomal soluble hydrolases, lysosomal targeting of newly synthesized LMPs can occur via either direct or indirect routes. In the direct pathway, LMPs are transported intracellularly from the TGN to the endo-lysosomal system. The indirect pathway involves transport from the TGN to the plasma membrane along the constitutive secretory pathway, followed by endocytosis and lysosome delivery. Newly synthetized LAMPs and LIMPs are mainly transported directly to the lysosome without appearing at the cell surface. Targeting signals allow lysosomal membrane

proteins to use the AP-1–clathrin and GGA–clathrin dependent exits from the TGN.

Lysosomal targeting of multi-protein complexes, including ion channels, exhibits an additional level of complexity because different subunits may be targeted independently. Increasing evidence indicates the existence of multiple additional or alternative pathways for the transport of both lysosomal hydrolases and lysosomal membrane proteins, which may enter the endo-lysosomal system at different stages of maturation (Braulke & Bonifacino, 2009).

1.3.2 Endocytic pathway to the lysosomes

The degradative endocytic pathway starts at the plasma membrane and leads to the generation of lysosomes. Between the plasma membrane and the lysosome, the endocytosed cargo goes through a range of endosomal intermediates that differ from each other by their content, morphology, pH and the kinetics by which endocytic tracers reach each of these compartments (van Meel & Klumperman, 2008). A schematic of endocytosed material from the plasma membrane to the lysosomes is shown below (**Figure 1.4**).

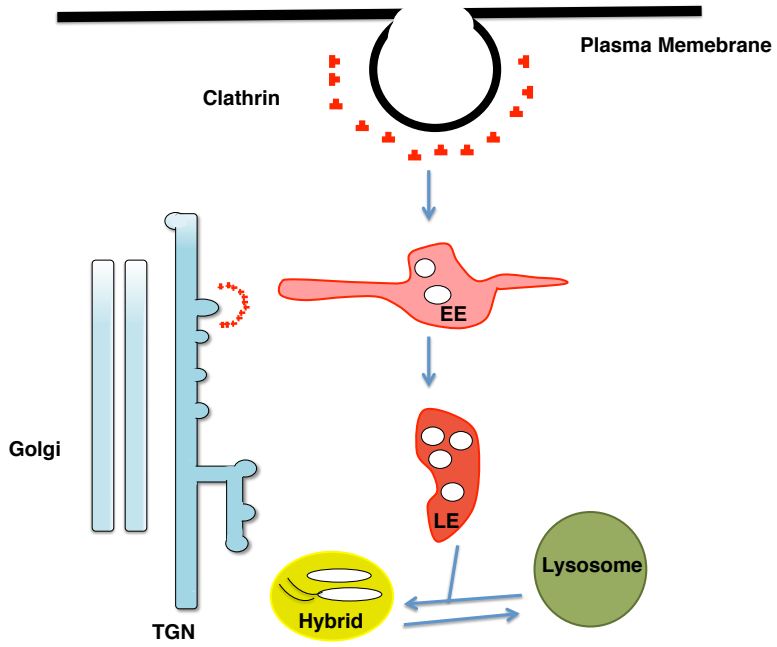

Figure 1.4: Simplistic view of the endocytic pathway. Lysosomes are the terminal compartments of the endocytic pathway. Molecules are endocytosed from the plasma membrane and are delivered to the lysosomes via the early endosomes (EE) and late endosomes (LE). Following lysosome fusion with late endosomes to form a hybrid organelle, lysosomes are reformed by a condensation process.

1.3.2.1 Early endosomes to late endosomes

At the most basic level, after internalization, endocytosed macromolecules are delivered first to early endosomes (EE). From here, they may recycle back to the plasma membrane or to other internal sites in the cell, or they may continue to late endosomes (LE) and subsequently to lysosomes for degradation. The early endosome is a major sorting compartment of the endocytic pathway; the acidic pH of its lumen causes many ligands to dissociate from their receptors defining it as a hotspot for recycling receptors. EEs contain a vacuolar part from which a reticulum of

multi branching tubules emerges called tubular sorting endosomes (TSE). Generally, cargo destined for lysosomes remain in the vacuole whereas cargo to be recycled enters the TSE. The time of delivery to each compartment can vary between cell types and between cells in culture and in living tissues (Saftig & Klumperman, 2009).

Early endosomes differ from late endosomes in their luminal pH: while EEs have a pH ~6, the lumen of LEs are more acidic with pH ~5-6. EE and LE also express distinct biological markers. For example, EEs are marked by the presence of a small GTPase of the Rab family, Rab5, and its effector protein EEA1 (early endosome antigen 1). In contrast, LEs express small GTPases of the Rab family, Rab7 and Rab11.

The mechanism by which EEs become LEs has been a subject of debate with two models emerging: a maturation model and a model in which endocytic carrier vesicles, formed from early endosomes bud off and transfer cargo to late endosomes. Live imaging studies, demonstrating that large (400-800 nm) vesicles arise from a dynamic endosome network and undergo a conversion from a Rab5-positive organelle into a Rab7-positive organelle, have helped reconcile these two models. This maturation process is regulated by the HOPS (homotypic fusion and vacuole protein sorting) complex, which has been identified as a guanine exchange factor (GEF) complex for Rab7 that is also able to interact with Rab5 (Rink et al, 2005).

1.3.2.2 Late endosomes to lysosomes

The mechanism for transferring cargo from LEs to lysosomes is also controversial as depicted in **Figure 1.5**. Among the theories being proposed, include (Luzio et al, 2014):

1. Maturation: where endosomes become lysosomes
2. Vesicular transport: where vesicles carry cargo from endosomes to lysosomes
3. Kiss and Run: where a continuous cycles of transient contact or 'kisses' between endosomes and lysosomes occur, during which material is transferred between organelles and each contact is followed by a dissociation or 'run'
4. Direct fusion: where a fusion of the endosomes to the lysosomes occurs to form a hybrid organelle
5. Fusion-fission: where a variation of fusion and kiss and run occurs, in which lysosomes reform from hybrid organelles as a result of fission events.

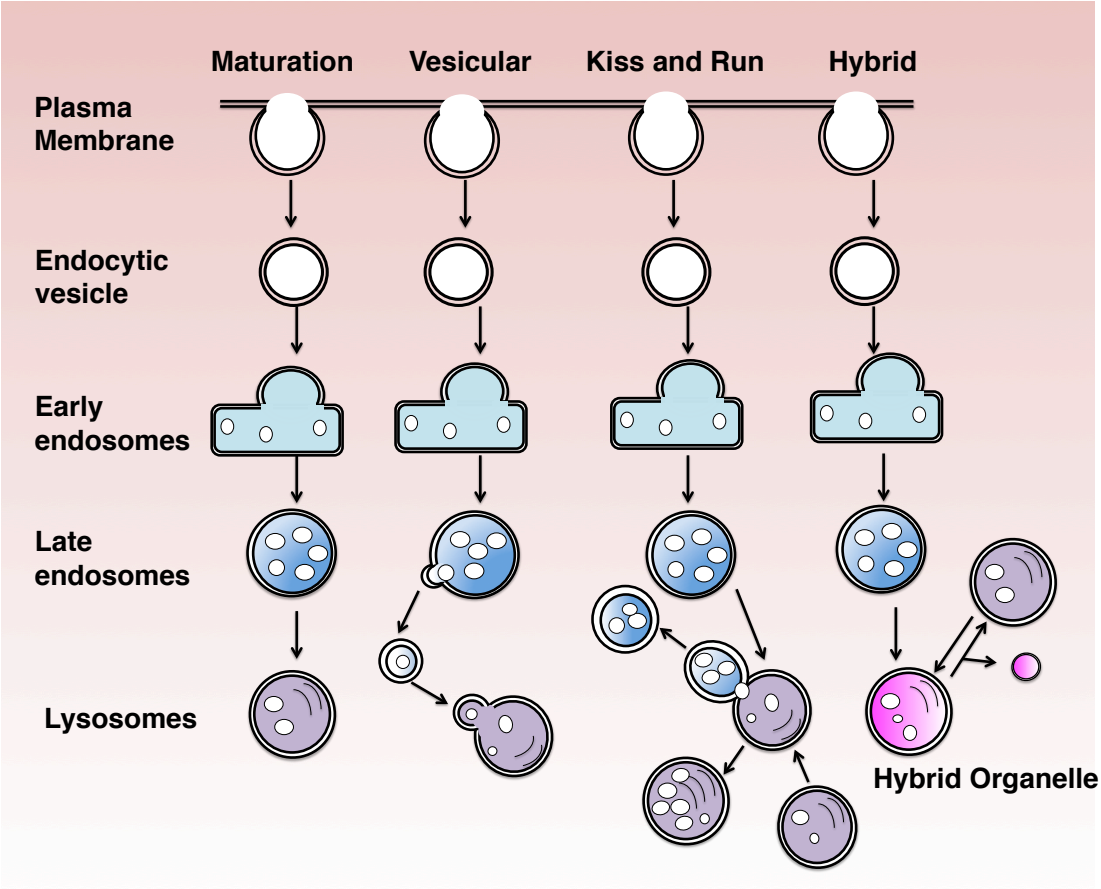

Figure 1.5: Models for delivering cargo from the late endosomes to the lysosomes. Endocytic cargo is internalized from the plasma membrane into early endosomes and then to late endosomes. Late endosomes deliver their cargo to the lysosome for degradation. Different models have been proposed on how cargo is trafficked from the late endosomes to the lysosomes. In the first model (maturation), late endosomes mature into lysosomes by the gradual addition of lysosomal components and removal of late endosomal components. In the second vesicular model, vesicles bud off from the late endosomes and fuse with the lysosomes thus delivering cargo to the lysosome. In the third, kiss and run model, late endosomes and lysosomes transiently fuse (kiss), allowing for exchange of contents between the two compartments before departing again (run). In the fourth and final model, the hybrid model, late endosomes and lysosomes fuse permanently to form a hybrid organelle that contains both components of the late endosomes and lysosomes. Lysosomes are then reformed by the selective retrieval of lysosome contents as a result of fission events. Adapted from (Luzio et al, 2007)

Recent studies using time-lapse microscopy have revealed that both kissing and direct fusion events contribute to the mixing of content between endosomes and lysosomes (Bright et al, 2005). Fusion of endosomes with lysosomes creates a hybrid organelle, which degrades a majority of the cargo. This late endosome-lysosome fusion shares common features with other fusion events in the secretory and endocytic pathway including the requirement of N-ethylmaleimide sensitive factor (NSF), soluble NSF attachment proteins (SNAP), and a small GTPase from within the Rab family, probably Rab7. These fusion events typically occur in three sequential events (Bright et al, 2005):

1. Tethering: mostly like accomplished by the HOPS complex.
2. Forming trans-SNARE (soluble N- ethylmaleimide–sensitive factor attachment protein receptor) complex: Syntaxin-8, Syntaxin-7 and VTI1B (vesicle transport through interaction with T-SNAREs homolog 1B) on the late endosome membrane assembles with VAMP7 (vesicle-associated membrane protein 7) on the opposing lysosomal membrane.
3. Membrane fusion: most likely dependent on the release of Ca^{2+} from the lumen of the fusing organelles and calmodulin.

Continuous fusion of late endosomes and lysosomes to create hybrid organelles will deplete both compartments if there is no recovery process. Although poorly understood, lysosomes must reform from these hybrid organelles, and this process would require content condensation, removal of endosome-specific proteins, and

recycling of the SNAREs. Lysosomes can be reformed in a cell free system, and under these conditions, content condensation is dependent on a proton pumping V-ATPase and luminal Ca^{2+} (Pryor et al, 2000). This view of endosome maturation, where lysosomes are fusogenic, hybrid-forming organelles, is consistent with other roles of lysosomes, which fuse with phagosomes, autophagosomes and/or plasma membranes under appropriate conditions.

1.3.3 Autophagy pathway to the lysosomes

Autophagy is an intracellular catabolic process where cytoplasmic components are delivered to the lysosomes for degradation. Three different types of autophagic pathways are known: macroautophagy, microautophagy and chaperone mediated autophagy (CMA) (Klionsky, 2007).

In macroautophagy, a double membrane structure (called phagophore) elongates to engulf a portion of cytoplasm that then fuses to itself to form a double membrane structure called autophagosome. Although still controversial, the membrane of the phagophore is thought to be derived from the endoplasmic reticulum (ER) and/or the trans-Golgi and endosomes. Autophagosomes fuse with lysosomes, forming autophagolysosomes (APL), where the cytosolic contents are degraded by lysosomal hydrolases. In microautophagy, a portion of the cytosol is directly engulfed by the lysosomes via invagination of the lysosomal membrane. And finally, CMA involves selective transport of proteins containing a pentapeptide

signaling motif (KFERQ) into the lysosome via a receptor consisting of a chaperone, hsc70, and the lysosomal membrane protein LAMP2A.

Macroautophagy (hereafter referred to as autophagy) is the predominant form of autophagy. There is a family of autophagy related genes or ATGs. Approximately 35 ATGs have been shown to be involved in autophagy in yeast. Although complex, the molecular circuitry and signaling pathways regulating autophagy can be simplified into five key steps as shown in **Figure 1.6** (Glick et al, 2010):

(a) phagophore formation or nucleation;
(b) Atg5–Atg12 conjugation, interaction with Atg16L and multimerization at the phagophore;
(c) LC3 lipidation and insertion into the phagophore membrane;
(d) engulfment of random or selective targets for degradation; and
(e) fusion of the autophagosome with the lysosome (autophagolysosome) followed by proteolytic degradation by lysosomal proteases of engulfed cargoes.

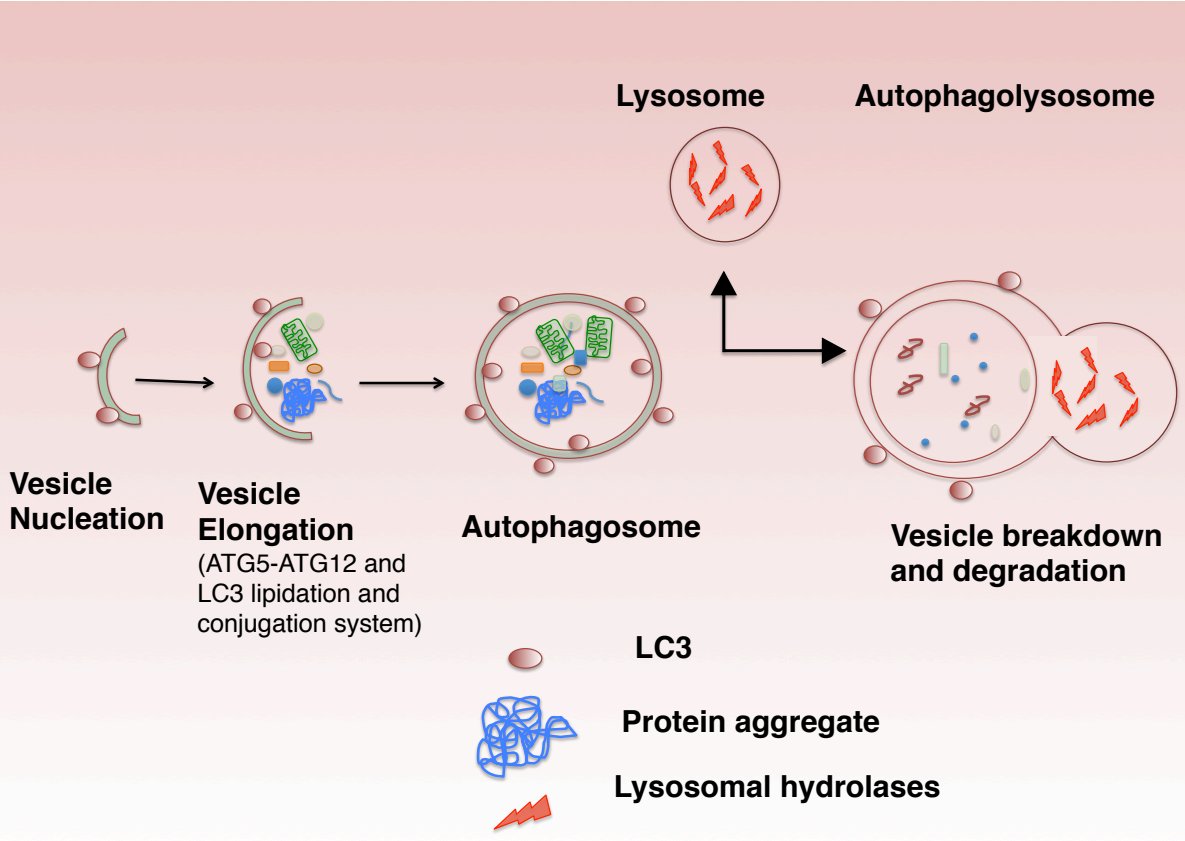

Figure 1.6: Schematic diagram of the steps of autophagy. Autophagy begins with the formation of an isolation membrane (vesicle nucleation step). The concerted action of the autophagy core machinery proteins (including ATG5-ATG-12 and LC3 lipidation) at the phagophore assembly site is thought to lead to the expansion of the phagophore into an autophagosome (vesicle elongation). The autophagosome can either non-specifically engulf bulk cytoplasm or target specific cargo. When the outer membrane of the autophagosome fuses with an with a lysosome, it forms an autolysosome where the sequestered material is degraded (vesicle breakdown and degradation) and recycled.

1.4 Methods for studying lysosome biology

Lysosomes can be studied in cultures by employing a variety of method:

1.4.1 Identifying lysosomes in live cells

1.4.1.1 LysoTracker staining

LysoTrackers (Life Technologies) are a family of weak amines that are largely unprotonated at physiological pH. They are readily cell permeable and can easily enter organelles. However, once inside acidic organelles, such as lysosomes, LysoTracker dyes get protonated and become trapped. Counting LysoTracker puncta or measuring intensity provides an assessment of organellar pH. LysoTracker dyes are available in different fluorescent colors including red, which decreases problems with the cell's autofluorescence. Because loading conditions differ between cell types, labeling intracellular organelles requires varying incubation time to optimize signal (Wolfe et al, 2013).

1.4.1.2 Dextran or BSA labeling

Lysosomes can be labeled in live cells by targeting a labeled fluorophore to the lysosomes via fluid phase endocytosis. Fluorescent dextran or BSA is particularly useful for this method because they are not degraded inside lysosomes. Loading of

dextran or BSA differs between cell types, but this method routinely takes longer than LysoTracker labeling because dextran/BSA needs to traffic through the endosomal pathway to the lysosomes. To “chase” the probe to the lysosomes, cells must be washed well with dextran free media. The appropriate chase time varies in different cell types, and shorter chase periods can be used to label earlier endocytic organelles. Dextran/BSA are available conjugated to a variety of different fluorescent colors that can be used to qualitatively asses lysosome status.

1.4.1.3 pH sensitive Dextran

A more sophisticated type of dextran bead can be used to quantitatively measure lysosomal pH. Conjugating both a pH insensitive rhodamine and a pH sensitive fluorescein to the dextran bead allows simultaneous identification and pH measurement. With decreasing pH, the pH–sensitive fluorescein (green) fluorescence is quenched, while the pH insensitive rhodamine (red) fluorescence remains unchanged; thus, the green/red ratio can be used to identify each lysosome and determine its specific pH (Majumdar et al, 2007).

1.4.2 Identifying lysosomes in fixed cells

1.4.2.1 Immunofluorescence

Fixing cells prior to analysis, helps define a snapshot of the cells at the time of fixation. Both LysoTracker and dextran fluorophore are commercially available in fixable formats. While fixation might be associated with artifact or loss of signal of the fluorophore, fixation affords the opportunity to double label the cells with lysosomal protein markers. There are a number of characteristic membrane-associated proteins that can be used to identify different organelles of the endocytic pathway. For example, lysosome associated membrane proteins, LAMP-1 and LAMP-2 are the most commonly labeled proteins for identifying lysosomes. They can be localized using antibodies or fluorescent recombinant proteins such as green fluorescent protein (i.e., GFP-LAMP-1).

1.4.2.2 Electron Microscopy

Finally, lysosomes can be readily identified ultrastructurally by electron microscopy via their characteristic appearance (Peters et al, 1991). The degraded components inside lysosomes generally appear electron dense under the scope. Distinguishing autolysosomes from lysosomes is problematic, but lysosomes are generally smaller in size (250-400 nm) compared to autolysosomes (range from 500 nm to 1.5 μm) (Mizushima et al, 2002).

1.5 Mechanism of lysosomal acidification: V-ATPase

An acidic environment is optimal for the acidic hydrolases active in the lysosome, and maintenance of acidic lysosomal pH is a necessary homeostatic cellular function. At the heart of maintaining this acidic environment is the V-ATPase, a multi subunit complex that functions as a ATP-driven proton pump.

V-ATPases possess two domains that operate by a rotary mechanism. The V1 domain is a complex of ~650 KDa, located on the cytoplasmic side of the membrane; it carries out ATP hydrolysis. The V0 domain is a membrane embedded complex of ~260 KDa that is responsible for the translocation of protons from the cytoplasm to the lysosomal lumen (Forgac, 2007).

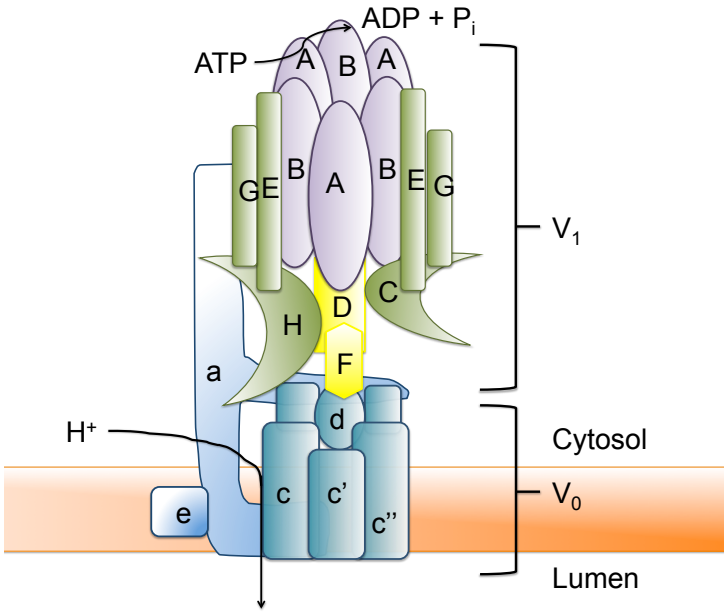

Figure 1.7: Structure of the proton-pump V-ATPase. The V-ATPase is composed of a peripheral V1 domain (shown in purple, green and yellow) and an integral V0 domain (shown in shades of blue). The hexamer in V1 domain of alternating A and B subunits participate in ATP binding and hydrolysis. The V0 domain includes a proteolipid ring structure comprising the c, c', and c'' subunits alongside subunits a and e. The central stalk is composed of subunits D and F from V1 and subunit d from V0. The peripheral stalk consists of subunits C, E, G, H from V1 and subunit a V0. Proton translocation occurs through two hemi-channels in subunit a that coordinate with the proteolipid ring (refer to the main text for details). The schematic is adapted from the model presented in (Forgac, 2007)

The V1 domain is composed of eight different subunits (A,B,C,D,E,F,G,H) while V0 has six different subunits (a,d,e,c c' and c'') (**Figure 1.7**). The core of V1 is a hexameric complex of alternating A and B subunits which participate in ATP binding and hydrolysis. The V0 domain consists of a ring of hydrophobic proteolipid containing subunits (c,c' and c") adjacent to subunits a and e. V1 and V0 are connected via central and peripheral stalks. The central stalk is composed of subunits D and F of V1 and d from V0. The peripheral stalk is composed of C, E, G

and H from V1 and the N-terminal domain of subunit a from V0. These stalks couple ATP hydrolysis to proton translocation. The central stalks serves as a rotor that couples energy released from ATP hydrolysis to the rotation of the proteolipids ring in V0. The peripheral stalk serves as a stator; it prevents the rotation of A3B3 head of V1 during ATP hydrolysis.

The V0 a subunit possesses two hemi channels and a buried arginine residue crucial for proton translocation across the membrane. One of the hemi-channels faces the cytosol while the other faces the lumen of the lysosome. Protons are transferred via carboxyl groups on glutamate residues within the proteolipid subunits in a coordinated fashion that provides the basis of proton translocation by the V-ATPase. Briefly, protons entering the cytoplasmic side of the hemi channels in the V0a subunit protonate carboxyl groups of buried glutamate residues in the proteolipids subunits. These resides remain protonated as a result of their forced rotation into the hydrophobic bilayer. ATP hydrolysis by the A3B3 head of the V1 domain drives rotation of the central rotor, and as the ring rotates, the protonated carboxyl group is brought to the lumen where it faces the hemi-channels. Once there, the V0a subunit arginine residue stabilizes the charged form of the carboxyl group, allowing release of the proton into the luminal hemi-channel and finally into the luminal space. This rotation also bring the carboxyl group of the next proteolipid subunit into contact with the cytoplasmic hemi channel allowing for another proton to enter the channel perpetuating the catalytic cycle and driving the directional movement of protons into the lysosomal lumen (Forgac, 2007).

There are three catalytic nucleotide binding sites of V1 and six to ten protonatable sites in the V0 proteolipid ring; thus, the H+/ATP stoichiometry for the V-ATPase is predicted to be between 2 and 3.3. This value is in reasonable agreement with the measured value in isolated yeast vacuoles. Two specific inhibitors of V-ATPase, bafilomycin A1 and concanamycin, prevent rotation of the complex, which obstructs proton translocation.

1.6 Regulation of V-ATPase

The V-ATPase moves protons across membranes in multiple different contexts. Different intracellular organelles are maintained at distinct pH values. Lysosomes are the most acidic compartment within the cell. Late endosomes are less acidic than lysosomes, but they are more acidic than early endosomes and compartments within the trans-Golgi network. Even less acidic are other Golgi compartments. Some cells, like the renal intercalated cells and the clear cells of the epididymis use the V-ATPase to translocate proton across their plasma membranes without affecting the acidity of their intracellular organelles (Pastor-Soler et al, 2003). To accomplish these myriad tasks, V-ATPase activity is tightly regulated by different cellular mechanisms, which is briefly described and illustrated schematically below (**Figure 1.8**).

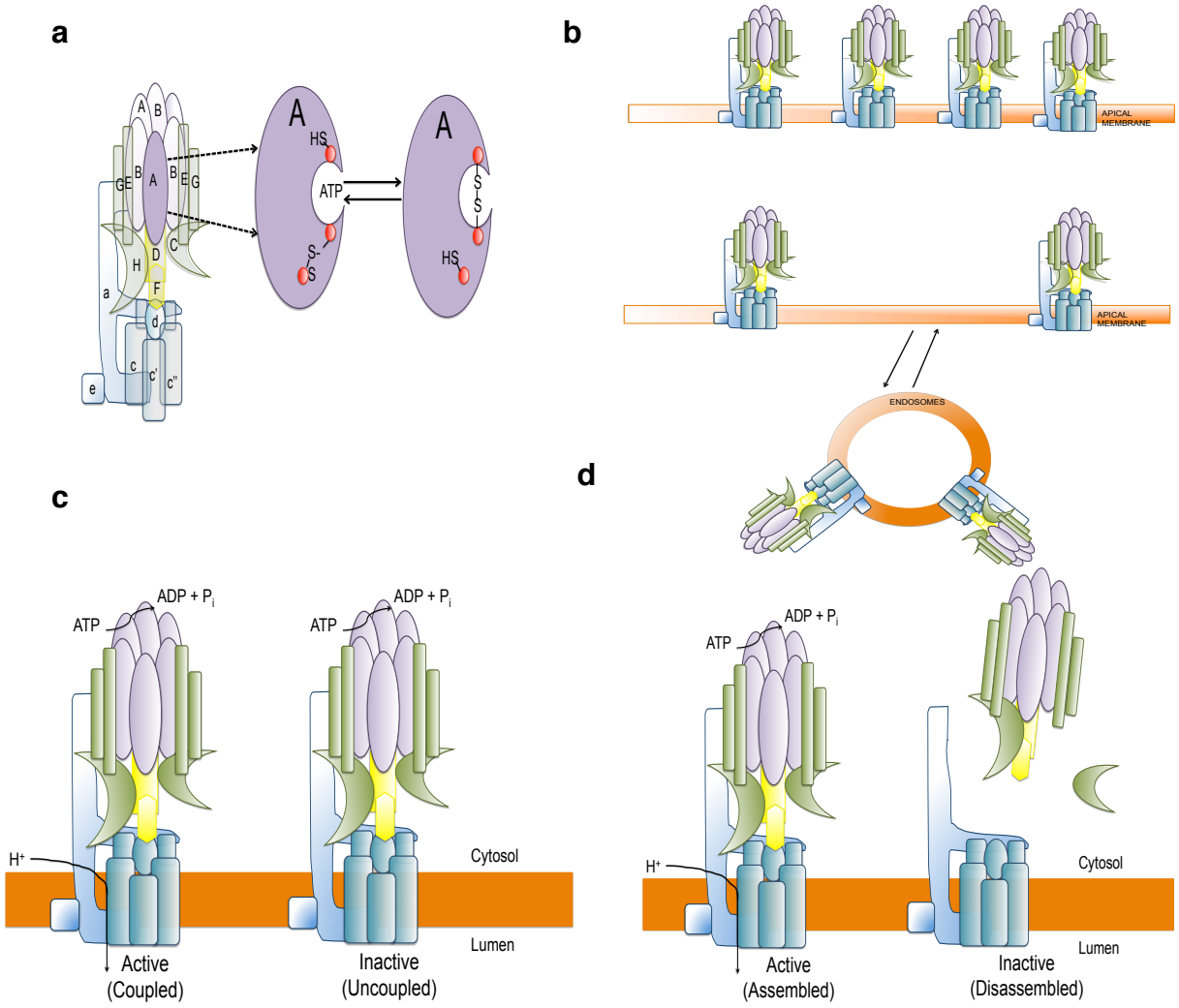

Figure 1.8 Regulation of V-ATPase **(a)** Reversible disulphide bond: The formation of a reversible disulfide bond between a highly conserved cysteine residue (red circle) in the catalytic site of subunit A prevents ATP hydrolysis and thus proton translocation. **(b)** Proton pump density: In selected epithelial cells, change in pump density through fusion of vesicles containing V-ATPase to the cell membrane modulates acid secretion. Increase in pump density is correlated wit an increased acid secretion. **(c)** Coupling efficiency: ATP hydrolysis and proton transport can be changed to modulate coupling efficiency. An extreme example will be a completely uncoupled complex when ATP hydrolysis does not result in any proton translocation. **(d)** Reversible dissociation of the V0 and V1 domain: Well characterized in yeast, the V1 and V0 domain can dissemble in response to glucose starvation. This has been also shown in mammalian dendritic cells where the physical uncoupling is used to restrict lysosomal acidification capacity in immature dendritic cells. Adapted from (Cipriano et al, 2008)

1.6.1 Regulation of V-ATPase by reversible disulphide bond formation

One mechanism of control involves reversible disulphide bond formation between conserved cysteine residues at the catalytic site of the V-ATPase (Cipriano et al, 2008). V-ATPase activity is inhibited by a disulphide bond between a highly conserved cysteine in the catalytic A subunit of the V1 domain and a second highly conserved cysteine residue located at the C-terminus of the same subunit (**Figure 1.8a**). This disulphide bond locks the catalytic site in a closed conformation preventing product release and rebinding of a new ATP molecule. This form of regulation is reversible; the bond can be cleaved by a thiosulphide exchange involving a third cysteine reside in the A subunit.

1.6.2 Regulation of V-ATPase by pump density

V-ATPase activity can also be regulated by mechanisms that control pump density (**Figure 1.8b**) (Pastor-Soler et al, 2003). In renal intercalated cells, proton pump density on the apical membrane controls acid secretion into the distal tubule and collecting duct, and in clear cells of the epididymis, proton pump density ensures an acidic luminal environment essential for sperm maturation. In both these epithelia, V-ATPase recycling between sorting endosomes and the apical membrane is controlled in a pH dependent manner by cAMP generated by the bicarbonate-regulated soluble adenylyl cyclase (sAC) (described in detail below). Briefly, sAC activity is stimulated (and cAMP levels increase) as intracellular pH rises (which will be reflected as an

increase in intracellular bicarbonate). Exactly how the elevated level of cAMP increases pump density at the membrane is not yet clear. However, it is thought that actin might play a role. Subunits B and C of the V1 domain are thought to bind to actin, and inhibition of the actin severing activity of gesolin prevents pH and bicarbonate dependent V-ATPase translocation (Beaulieu et al, 2005).

1.6.3 Regulation of V-ATPase by modulating coupling efficiency

A third way to regulate V-ATPase activity is to modulate its coupling efficiency (**Figure 1.8c**). As discussed above, the H^+/ATP stoichiometry for the V-ATPase is predicted to be between 2 and 3.3. The wide range is thought to reflect variability in coupling efficiency of different isoforms of the V0a subunit. For example, the V-ATPase in the Golgi has a lower coupling efficiency (i.e., fewer protons are translocated for every ATP hydrolyzed) than the V-ATPase in vacuoles. These differences in coupling efficiency have been hypothesized to explain why different compartments have different pH; the Golgi may have more alkaline pH than vacuoles because its V0a subunit supports reduced coupling efficiency. In addition, mutations found in subunits of the V-ATPase affect coupling efficiency. For example, mutations identified in subunit d or A actually increases coupling efficiency. Interestingly, these findings predict that wild type V-ATPases evolved not to maximize coupling, perhaps allowing for regulatory mechanisms which can either increase or decrease coupling efficiency (Forgac, 1989),(Shao & Forgac, 2004).

1.6.4 Regulation of V-ATPase by reversible dissociation of the V1 and V0 domain

Another well-characterized mechanism for regulating V-ATPase activity is the reversible dissociation of the V1 and V0 domains (**Figure 1.8d**) (Kane, 1995). This process has been most extensively studied in yeast and insect cells, where domain dissociation is stimulated by glucose starvation. When glucose is limited, it is thought that yeast inactivate V-ATPase via dissociation to conserve ATP. Dissasembly is rapid (occurs in minutes) and requires an intact microtubule network (Xu & Forgac, 2001). Interestingly, reassembly occurs independent of microtubules suggesting the two processes are controlled independently. Both normal biosynthetic assembly and glucose-dependent reassembly require a novel protein complex called RAVE (regulator of the ATPase of vacuolar and endosomal membranes) (Smardon et al, 2002). Finally, glucose dependent dissociation is also sensitive to the membrane environment in which the V-ATPase resides. A specific subset of V-ATPase complexes undergo dissociation upon glucose removal when localized to the vacuole. However, when these V-ATPase complexes are present in the Golgi (their normal localization), they remain assembled even during glucose depletion.

This mechanism of regulation appears to be conserved in mammalian cells; antigen activation of dendritic cells increases assembly of V-ATPase complexes (Trombetta et al, 2003). The A subunit of the V1 domain has a 90 amino acid region that is conversed among subunits from different species and is thought to play a role

in the dissociation of the complex. Mutation in this region block dissociation without affecting its catalytic activity (Shao & Forgac, 2004).

1.6.5 Other mechanisms for lysosomal pH

During lysosome acidification, V-ATPase activity will be dependent upon the activities of other transporters/channels. Because V-ATPase is an electrogenic pump, transport of protons into the lysosomal lumen generates an inside positive membrane potential, which will limit further proton translocation. Counterion transport pathways allow the lysosomes to dissipate this membrane potential facilitating V-ATPase mediated acidification (Mindell, 2012). Studies in lysosomes isolated from various cell lines suggest that chloride ion influx constitutes one of these counterion transport pathways. The primary chloride conductance in lysosomes is thought to be mediated by ClC. ClC7 (as discussed in Section 1.2.7) is found in lysosomes in a complex with a regulatory partner, Ostm1, which is important for proper trafficking of CLC7 to the lysosomes, as well as its stability and ion transport activity. Lysosomal acidification in microglia is enhanced upon upregulation of CLC7/Ostm1, which is thought to be mediated in a PKA dependent manner (Majumdar et al, 2007). Another mechanism for dissipating the positive membrane potential during acidification would be cation efflux. Efflux of cations facilitates vesicle acidification by neutralizing the positive charge and reducing the membrane potential caused by the pumped protons (Steinberg et al, 2010).

However, it is not completely understood how these transporters or pumps involved in establishing lysosomal acidification. Little is known about how the V-ATPase sets the pH or how these parallel ion transports are regulated. In particular, no pH sensitive signaling cascades have been implicated.

II. Soluble Adenylyl Cyclase (sAC

1.7 cAMP

Cyclic 3', 5'-adenosine monophosphate (cyclic AMP or cAMP) was discovered by Dr. Earl Sutherland in the 1950's while studying the hormonal control of glycogen metabolism (Sutherland & Rall, 1958),(Rall & Sutherland, 1958). Since its discovery, cAMP has been shown to play important roles in a wide range of biological processes. It defines the prototypical "second messenger" relaying information inside the cell in response to different hormones and extracellular ligands (i.e., the first messengers) that bind to cell surface receptors. For this discovery, Dr. Sutherland was awarded the Nobel prize in Physiology or Medicine in 1971.

Intracellular levels of cAMP depend upon its synthesis by adenylyl cyclases (AC), and its degradation by phosphodiesterases (PDE) (Kamenetsky et al, 2006). ACs catalyze the cyclization of ATP to cAMP releasing a pyrophosphate in the reaction, and PDEs terminate the signaling cascade by breaking down cAMP into AMP. In mammals, there are ten genes encoding ACs with differential expression in tissues (Levin & Buck, 2015a). Nine genes (ADCY1-9) encode a family of

transmembrane adenylyl cyclases (tmACs) and a tenth gene (ADCY10) encoding the more recently discovered soluble adenylyl cyclase (sAC). sAC is the focus of this thesis.

There are more than 50 different known isoforms of PDE with differential expression in different tissues and cell types with different sub- cellular localizations. This PDE isoform diversity contributes to specificity in cAMP signaling. In addition to simply diminishing cAMP levels to stop a signaling cascade, PDEs also serve as "firewalls" serving to restrict cAMP to an area so that it can only affect specific downstream effectors (Lomas & Zaccolo, 2014).

1.7.1 Effectors of cAMP

cAMP has different target proteins in different species. In mammalian cells, there are at least 3 known types of cAMP effector proteins: protein kinase A (PKA), exchange proteins activated by cAMP (EPACs), and cyclic nucleotide gated (CNG) ion channels.

The most widely studied target protein of cAMP is PKA. PKA exists as a holoenzyme with two regulatory (R) subunits associated with two catalytic (C) subunits. As cAMP binds to the R subunit, it induces a conformation change that liberates the C subunits, allowing them to phosphorylate serine/threonine residues on a variety of target proteins. This cAMP dependent phosphorylation cascade

regulates, among other things, metabolism, gene expression, cell differentiation, cell growth and division, apoptosis, secretion and neurotransmission, and it plays an integral part in many physiological processes ranging from learning and memory in the brain to contractility and relaxation in the heart and to water uptake in the gut and kidney.

PKA is distributed to specific cAMP signaling compartments by a family of A-kinase anchor proteins (AKAPs). AKAPs are scaffolding proteins that restrict PKA to specific subcellular locations, where it can only phosphorylate local targets. In addition to binding PKA, AKAPs bind other signaling molecules including the PDEs and cyclases.

Another family of cAMP effector proteins is EPACs (Bos, 2003), which are guanine nucleotide exchange factors (GEFs) specific for small GTPase proteins of the Rap family. The GEF activity of EPAC stimulates Rap proteins by facilitating exchange of GTP to replace the bound GDP. Two known EPACs, termed Epac1 and Epac2, bind cAMP and activate Rap1 and Rap2 respectively. While Epac1 is ubiquitously expressed in all tissues; Epac2 has a more limited distribution. Studies have shown EPAC signaling pathways are involved in cell adhesion, cell-cell junction, exocytosis, secretion, cell differentiation and proliferation, gene expression, apoptosis, cardiac contraction and neuronal excitability. The overlap between these identified functions, and the functions historically ascribed to PKA suggests that cAMP mediated effects previously thought to act though PKA, may also involve

EPACs (Gloerich & Bos, 2010). Research using animal models on the functional analyses of EPAC isoforms is just beginning.

While many channels are indirectly affected by cAMP (e.g., via PKA phosphorylation modulating channel activity), there are two families of structurally related ion channels whose activity is regulated by the direct binding of cyclic nucleotides (cAMP and cGMP): cyclic nucleotide-gated channels (cNGCs) (Biel et al, 2009) and the hyperpolarization-activated cyclic nucleotide-gated channels (HCNs) (Wahl-Schott & Biel, 2009). cNGCs are opened directly by binding of cAMP or cGMP; they play a key role in visual and olfactory transduction. HCNs open in response to changes in membrane voltage with cAMP modulating their open probability. HCNs are referred to as “pacemaker channels” since they are involved in the control of cardiac automaticity. HCNs also play an important role in the central and peripheral nervous system.

With the variety of different cAMP effectors distributed throughout a cell, and with cAMP changes happening locally due to the various types of adenylyl cyclases and the “firewall” function of PDEs, the physiological consequences of cAMP depend upon which distinct cAMP pathway gets activated. Due to this modern appreciation that cAMP signaling is compartmentalized, studying cAMP signal transduction means it is imperative to identify the specific adenylyl cyclase, the relevant effector protein, and the right PDE in order to understand cAMP biology.

1.8 Adenylyl Cyclases

Class III cyclases are the most diverse and the most well studied class of cyclases (Linder & Schultz, 2003). It comprises all ACs, as well as guanylyl cyclases from eukaryotes as well as many prokaryotic cyclases.

Class III ACs contain a conserved dimeric core (Tesmer et al, 1999) consisting of two catalytic domains, normally referred to as C1 and C2, which come together to form the active site. The C1 and C2 can be formed from one polypeptide chain (pseudo-heterodimer) or can come from two different poly peptide chains (homodimer). Most bacterial ACs are homodimers which generate two symmetrical active sites at the dimer interface. Mammalian tmAC and sAC have two homologous and structurally similar catalytic domains that come together to form a heterodimer. The C1 and C2 in mammalian ACs is thought to have evolved through gene duplication and subsequent degeneration of the second site into a regulator binding domain.

1.8.1 Transmembrane Adenylyl Cyclase

Transmembrane adenylyl cyclase (tmACs) (Taussig & Gilman, 1995), (Lefkowitz, 1994) contain two cytoplasmic catalytic domain (C1 and C2) and are localized to the plasma membrane by virtue of their two sets of transmembrane domains (M1 and M2). tmACs are regulated *in vivo* by heterotrimeric G- proteins and

by Ca^{2+} (in an isoform-specific manner) which can activate or inhibit tmACs depending on the isoform and the concentration of calcium. tmACs can also be regulated by phosphorylation by kinases. Finally, tmACs can be stimulated pharmacologically by forskolin which binds to the pseudo-active site. It is not know whether there is an endogenous ligand which binds to this site in tmACs.

Compartmentalization of cAMP made it puzzling to think about cAMP that is generated at the plasma membrane by tmACs being able to diffuse throughout the cells and into the nucleus in through a cytoplasm filled with PDEs. Thus, compartmentalization models of cAMP signaling benefited from the identification of sAC and its ability to produce cAMP locally in locations far from the plasma membrane.

1.8.2 Soluble Adenylyl Cyclase [1]

Almost forty years ago, pioneering work of Theodor Braun described a novel, “soluble” adenylyl cyclase (AC) from rat testis (Braun & Dods, 1975). From the initial reports, it became clear that this cyclase was unique; unlike the more widely studied, G protein-regulated transmembrane adenylyl cyclases (tmACs), soluble AC activity was not associated with the plasma membrane (Braun & Dods, 1975); was predicted

[1] The following sections (2.2.2 -2.6) is an updated version of a review published in a peer-reviewed journal. Rahman N, Buck J, Levin LR. 2013. pH sensing via bicarbonate-regulated "soluble" adenylyl cyclase (sAC). Front Physiol 4:343. PMID: 24324443

to be approximately 48 kDa in size (Gordeladze & Hansson, 1981); was hormone and heterotrimeric G protein insensitive (Braun et al, 1977), and its activity appeared to be dependent upon Mn^{2+}-ATP as substrate (Braun & Dods, 1975). It was also shown that it was distinct from the previously identified soluble guanylyl cyclase (Braun et al, 1977; Neer, 1979). Despite extensive searching, soluble AC activity had been detected only in testis (Neer, 1978). A membrane-associated activity found in sperm was similarly hormone and G protein insensitive (Braun & Dods, 1975; Garty & Salomon, 1987; Rojas et al, 1992; Stengel & Hanoune, 1984), and it was hypothesized that during maturation in the testis and/or during the transport of sperm through the epididymis, a single, novel form of adenylyl cyclase would change from being cytosolic to membrane-attached (Braun & Dods, 1975). Subsequent studies confirmed sAC was responsible for soluble activity in testis and the majority of the membrane-associated activity in sperm (Esposito et al, 2004a; Hess et al, 2005a).

1.9 Purification and Cloning of sAC

Numerous attempts to purify this unique cAMP-producing enzyme failed. In 1999, starting from 950-rat testis, our laboratory purified a 48 kDa candidate protein band which eluted with soluble AC activity (Buck et al, 2002; Buck et al, 1999). The amino acid sequences of three peptides derived from this 48 kDa candidate protein revealed it represented a novel protein and were sufficient to isolate its cDNA by degenerate PCR (Buck et al, 1999). The initial screen of a rat testis cDNA library

identified three different clones, the longest of which had an open reading frame predicting the full-length protein (sAC_{fl}) would be 187 kDa. A second cDNA predicted a smaller, truncated sAC isoform, sAC_t, which was subsequently shown to be a bona fide splice variant (Jaiswal & Conti, 2001), and which corresponds to the originally purified protein (Buck et al, 1999).

sAC_t comprises the amino terminal ~50 kDa of sAC_{fl}, and it contains two domains (C1 and C2) homologous to the catalytic domains from other Class III nucleotidyl cyclases (Buck et al, 1999). Closely related catalytic domains are in adenylyl cyclases found in Cyanobacteria, and the biochemical properties of mammalian sAC (described below) are conserved from these bacterial orthologs (Steegborn et al, 2005), which are thought to have evolved over 3 billion years ago.

Initial studies using the cloned sAC cDNA suggested it was abundantly expressed only in testis (Buck et al, 1999); however, subsequent studies using more sensitive RT-PCR (Chen et al, 2000; Farrell et al, 2008), mRNA microarrays (Geng et al, 2005), Western Blotting (Chen et al, 2000), or immunohistochemistry (Chen et al, 2013), revealed that sAC could be detected in nearly all tissues examined. Currently, sAC expression is considered to be ubiquitous. In individual cells, sAC can be found throughout the cytoplasm, inside or at various organelles and intracellular compartments – mitochondria, nuclei, microtubules, centrioles, mitotic spindles, and midbodies (Zippin et al, 2003). As such, sAC's intracellular localization provides an elegant solution to a long-standing conundrum inherent in the historical models for

cAMP signaling. Prior to sAC's discovery and the demonstration that it is widely, if not ubiquitously expressed, and distributed throughout the cell, models for cAMP signaling were dependent upon cAMP production exclusively at the plasma membrane. These models required diffusion of the second messenger through the cytoplasm to its target effector proteins. Current models posit sAC localized at different cellular sites would provide specificity by transducing the cAMP signal exclusively to the appropriate player in close proximity to the cyclase (Bundey & Insel, 2004; Wuttke et al, 2001; Zippin et al, 2003).

1.10 sAC Activity

The early characterization of soluble AC activity revealed it was insensitive to the usual regulators of the more widely studied tmACs, including heterotrimeric G proteins (Braun & Dods, 1975) and the plant diterpene forskolin (Forte et al, 1983; Stengel et al, 1982); these properties were confirmed in the heterologously expressed sAC cDNAs (Buck et al, 1999). In partially purified preparations, soluble testis AC activity was reported to have a K_m for its substrate, ATP, of ~1-2 mM in the presence of the divalent cation Mn^{2+} (Gordeladze & Hansson, 1981; Rojas et al, 1993; Stengel & Hanoune, 1984). Other divalent cations were found to support the enzymatic activity, but none supported activity to the same extent as Mn^{2+} (Braun & Dods, 1975). For example, in the presence of Mg^{2+}, the enzyme's K_m for substrate ATP was reported to be above 15 mM (Stengel & Hanoune, 1984). In these early

studies, there was no real consensus about regulation by Ca^{2+}; in one report, Mn^{2+}-ATP dependent activity was potentiated by Ca^{2+}(Braun et al, 1977), but others found the same activity to be Ca^{2+} insensitive (Stengel & Hanoune, 1984). The membrane-associated, soluble AC-like activity found in sperm was thought to be stimulated by sodium bicarbonate (HCO_3^-) (Garty & Salomon, 1987; Okamura et al, 1985; Visconti et al, 1990), while in guinea pig sperm, Ca^{2+} activation was reported to be dependent upon HCO_3^- (Garbers et al, 1982).

Heterologous expression of full-length (sAC_{fl}) and truncated sAC (sAC_t) isoforms revealed a significant difference in their specific activities (Buck et al, 1999; Jaiswal & Conti, 2003), which was subsequently shown to be due to an autoinhibitory domain present in the longer isoform (Chaloupka et al, 2006). It remains unclear how this autoinhibitory domain regulates sAC activity. sAC_{fl} also contains a unique Heme binding domain, but its contribution to activity also remains unclear (Middelhaufe et al, 2012). Despite these differences, sAC_t and sAC_{fl} share the same C1 and C2 catalytic domains (Buck et al, 1999), and much of their regulation is conserved (Buck et al, 1999; Chaloupka et al, 2006; Chen et al, 2000). Characterization of heterologously expressed and purified sAC_t confirmed many of the biochemical properties identified for purified soluble AC from testis, and they demonstrated that these properties were intrinsic to sAC. Purified sAC_t exhibits a K_m for substrate ATP of ~1 mM in the presence of Mn^{2+}, and while its affinity for Mg^{2+}ATP is in excess of 10 mM, Ca^{2+} (EC_{50} 750 μM) stimulates the enzyme's activity by increasing its affinity for ATP to ~ 1 mM in the presence of Mg^{2+} (Litvin et al, 2003). Its affinity for ATP is

close to the concentration found in cells (Traut, 1994), prompting us to postulate that sAC may be sensitive to physiologically relevant changes in ATP (Litvin et al, 2003). We recently demonstrated this to be the case; sAC, but not tmAC, activity inside cells is sensitive to inhibitors which diminished ATP levels (Zippin et al, 2013b). Cellular ATP levels increase in high glucose, and we showed that overexpression of sAC converts a cell line which normally does not alter cAMP levels in response to glucose into glucose-responsive cells. In addition, we found that in cells which are normally glucose responsive, pancreatic b cells, sAC is required for the ATP-dependent glucose response (Zippin et al, 2013b). Other functions of sAC have been identified based upon phenotypes in sAC knockout mice (Choi et al, 2012; Esposito et al, 2004a; Hess et al, 2005a; Lee et al, 2011; Zippin et al, 2013b) or by taking advantage of pharmacological inhibitors which distinguish between sAC and tmACs (Bitterman et al, 2013a), including functions dependent upon cellular Ca^{2+}. Tumor Necrosis Factor (TNF) (Han et al, 2005) and neurotrophin (NGF) signaling (Stessin et al, 2006) and glucose sensing (Farrell et al, 2008) are mediated via Ca^{2+}-dependent regulation of sAC.

sAC is directly stimulated by the bicarbonate anion (HCO_3^-)(Chen et al, 2000). HCO_3^- stimulates sAC via two mechanisms; it relieves substrate inhibition and elevates V_{max} (Litvin, 2003) by facilitating closure of the active site (Steegborn et al, 2005). As previously predicted (Garbers et al, 1982), HCO_3^- stimulation is synergistic with Ca^{2+} (Litvin, 2003). HCO_3^--dependent regulation of sAC plays a role in sperm activation (Esposito et al, 2004a; Hess et al, 2005a), activity-dependent metabolic

communication between astrocytes and neurons (Choi et al, 2012), and multiple processes in the eye, including aqueous humor formation (Lee et al, 2011), retinal ganglion cell survival (Corredor et al, 2012) and corneal endothelial cell protection (Li et al, 2011).

Due to the ubiquitous presence of carbonic anhydrases (CAs), HCO_3^- regulation means that sAC activity inside cells will be modulated by changes in CO_2 and/or pHi (Buck & Levin, 2011; Tresguerres et al, 2010a). CO_2-dependent regulation of sAC plays a role inside the mitochondrial matrix, where metabolically generated CO_2 modulates the synthesis of ATP by the electron transport chain via sAC-generated cAMP (Acin-Perez et al, 2011; Acin-Perez et al, 2009a; Di Benedetto et al, 2013; Lefkimmiatis et al, 2013), and in airway cilia, where CO_2 regulates the ciliary beat frequency via sAC (Schmid et al, 2007).

1.11 sAC as pH sensor

Although its *in vitro* activity is insensitive to physiologically relevant pH changes (Chen et al, 2000), the pH-dependent equilibrium between CO_2 and HCO_3^- means that cellular sAC activity will be regulated by local changes in pH. In fact, sAC has been shown to play a role in pH dependent movements of the electrogenic, proton pumping vacuolar–ATPase (V-ATPase) in a number of physiological contexts (Pastor-Soler et al, 2003; Paunescu et al, 2008b; Paunescu et al, 2010b; Tresguerres et al, 2010a). In epididymis and proximal tubules of the kidney, V-ATPases

translocate to the apical surface of the cell in response to a pH change in the corresponding lumen. sAC is in a complex with V-ATPase (Paunescu et al, 2008b), and the V-ATPase translocation is mediated by sAC, in a CA dependent manner (Pastor-Soler et al, 2003; Pastor-Soler et al, 2008). This pH dependent signaling is evolutionarily conserved; a similar mechanism, involving CA, sAC and V-ATPase, is responsible for organismal pH homeostasis in shark (Tresguerres et al, 2010c). Interestingly, in shark gills the V-ATPase translocates to the basolateral side of the pH sensing cells. Thus, sAC-dependent V-ATPase mobilization is a conserved mechanism of pH sensing. The appreciation that pH sensing can be achieved via HCO_3^- regulation of sAC instead of being exclusively dependent upon proton sensing suggests there may be additional pH-dependent physiological processes dependent upon sAC.

1.12 pH sensing in the Endosomal-Lysosomal Pathway

The endo-lysosomal system is central to the processes of autophagy and endocytosis (Klionsky, 2007; Mizushima, 2007), and there is growing appreciation of its involvement in a broad range of diseases (Futerman & van Meer, 2004; Nixon et al, 2008). As internalized materials pass from early to late endosomes and finally to lysosomes, the lumen of the endocytic organelles become more acidic. The pH of the lysosome lumen is maintained between 4 and 5 (Pillay et al, 2002), which is the optimal pH for lysosomal enzyme activity.

As mentioned above, regulation of lysosomal pH is a complex process involving multiple channels and transporters. Acidification of lysosomes is accomplished by the electrogenic V-ATPase, (Forgac, 2007). Chloride movement through an opposite conductance pathway (Jentsch, 2007) and efflux of cations (Steinberg et al, 2010) facilitate vesicle acidification by neutralizing the positive charge and reducing the membrane potential caused by the pumped protons. Little is known about how the V-ATPase sets the pH or how these parallel ion transports are regulated. In particular, no pH-sensitive signaling cascades have been implicated.

Cyclic AMP has been shown to modulate lysosomal pH in macrophages (Di et al, 2006), microglia (Majumdar et al, 2007) and retinal pigment epithelium (RPE) cells (Liu et al, 2008). The cAMP effector, Protein Kinase A (PKA) increases chloride conductance (Bae & Verkman, 1990), possibly via the chloride channel CLC7. Lysosomal acidification in microglia is enhanced by upregulation of CLC7 (Majumdar et al, 2011), in what is thought to be a PKA dependent process (Majumdar et al, 2007). However, how the cAMP “second messenger” is made and whether cAMP levels are dependent upon pH remains unknown. It is tempting to postulate that sAC is the pH regulated source of cAMP regulating these processes.

Like lysosomes, both early and late endosomes are maintained within certain pH ranges; early endosomes range between pH ~ 5.9-6.8 whereas late endosomes range between pH ~ 4.9-6.0 (Maxfield & Yamashiro, 1987). Endosomal pH is maintained via similar proteins that control lysosomal pH, but endosomes use distinct

isoforms of V-ATPases and chloride channels (for a complete review, see (Forgac, 2007; Stauber & Jentsch, 2013)). In such cases, different isoforms need to be trafficked to the endosomes or their activity modulated in order to establish and maintain the proper pH. sAC has already been shown to modulate the pH-dependent translocation of the V-ATPase to plasma membranes (Pastor-Soler et al, 2003; Tresguerres et al, 2010a); might sAC-generated cAMP play a role in trafficking V-ATPases or other chloride channels to endosomal/lysosomal membranes and hence establishing intra-vesicular pH?

1.13 Summary

Because HCO_3^-, CO_2 and H^+ are in constant equilibrium due to the ubiquitous presence of carbonic anhydrases (CA), HCO_3^--regulated sAC can function as a sensor of local, intracellular HCO_3, CO_2 and/or pH(Tresguerres et al, 2010a). Previous studies have identified sAC as a HCO_3^- sensor in sperm(Hess et al, 2005a), a CO_2 sensor in cilia of epithelia cells lining the airway(Schmid et al, 2007) and as a pH sensor in epididymis and kidney(Pastor-Soler et al, 2008; Paunescu et al, 2008b). The goal of this work is to elucidate whether pH-regulated soluble Adenylyl Cyclase (sAC) is essential for lysosomal acidification, one of the acidic organelles in the cells and to understand the molecular mechanism whereby sAC generated cAMP regulates lysosomal acidification.

It is well-established that neurodegenerative diseases such as Alzheimers Disease (AD) and Frontotemporal Disease (FTD) reveal neuronal vulnerability to lysosomal dysfunction(Nixon et al, 2008). This work may identify sAC as a potential target for novel treatment strategies for age-related neurodegenerative diseases and lysosomal storage disorders.

CHAPTER TWO: MATERIALS AND METHODS

2.1 Cell lines and animals

Mouse embryonic fibroblasts (MEFs) were immortalized from WT (Wild-Type) and sAC KO (Knock-Out) mice using the 3T3 method or SV40 large T antigen. The cells were grown in Dulbecco's modified Eagle medium (DMEM) supplemented with 1% penicillin/streptomycin (P/S), 10% fetal bovine serum (FBS) and 0.5% glutamine. Huh-7 (human liver cells) were also grown in similar conditions.

Bicarbonate starvation in the presence of atmospheric CO_2 was induced by growing cells overnight with bicarbonate free DMEM (44 mM HEPES) supplemented with 10% FBS and 0.5% glutamine and 1 % P/S.

Primary neuronal cultures were prepared from cortices and hippocampi of embryonic day 15 (E15) sAC heterozygous and wild-type littermate mouse embryos as described in (Tampellini et al, 2009). Briefly, cortices and hippocampi from each embryo were incubated with 0.25% trypsin and triturated to dissociate neurons. Neurons were then plated in serum-free neurobasal media supplemented with B27 and 2 mM l-glutamine on poly-d-lysine-coated plates. Primary neurons are viable for ~3–4 weeks under these culturing conditions. For immunofluorescence, ~4 × 10^5 neurons were plated per well in twenty four-well plates containing coverslips, and for

immunobloting, ~3.3 × 10^6 neurons were plated per 100-mm-diameter dish. Genotyping was performed on cerebellum from the same embryo. Primary neurons were used at 12 DIV for all experiments.

WT and sAC KO mice were studied at 15-18 months together with age-matched controls. All animal work was performed with approval from the Institutional Animal Care and Use Committee (IACUC) of Weill Cornell Medical College and conforms to NIH guidelines for the Care and Use of Laboratory Animals.

2.2 Antibodies and Reagents

Mouse monoclonal antibodies to LC3 (Fe10, nantools) were used for immunoblotting (1:300) studies. LAMP (LAMP-2: ABL-93, 1/200) was purchased from Developmental Studies Hybridoma Bank. LysoTracker Red DND-99 (500 nM), Dextran, Fluorescein and Tetramethylrhodamine, 70,000 MW (2.5 mg/ml) were purchased from Life technologies. Rabbit polyclonal anti-GAPDH (1:5000) and Actin (1:5000) were purchased from Cell Signaling. Ammonium Chloride (NH_4Cl, 20 mM), bafilomycin A1 (200 nM), leupeptin (20 μM), E64d (10 μM), Pepstatin A (20 μM) and acetazolamide (100 μM) were purchased from Sigma. Sp-8-cpt-cAMP (500 μM) was from Biolog Life Science Institute. We applied secondary antibodies conjugated to Alexa Fluo-488 or -546 (IF 1:1000) or to HRP (WB 1:5000, Sigma). KH7 and KH7.15

were synthesized by Chemical Diversity, Inc. (San Diego, CA) and by the Abby and Howard Milstein Synthetic Chemistry Core Facility of Weill Cornell Medical College.

2.3 Immunofluorescence

Immunofluorescence was performed as previously described in (Tampellini et al, 2009). After treatment, cells were fixed in 4% PFA with 2% sucrose for 20 min, permeabilized and blocked in PBS containing 2% normal goat serum, 0.1% saponin and 1% bovine serum albumin (BSA) at room temperature for 1 hr. After washing coverslips 3x with PBST, coverslips were mounted with Fluormont-G (Southern Biotechnology, Birmingham, AL). Cells were viewed using Zeiss LSM 510 laser scanning confocal microscope and a 63 x, 1.4 NA plan apochromat objective equipped with HeNe 633nm / HeNe 543nm / Argon (458, 488 nm) imaging lasers. In dual labeled experiments channels were used sequentially to avoid bleed though. Metamorph software 7.5 (Universal Imaging Co.) was used for quantitative analysis.

500 nM LysoTracker DND-99 was added for 30 min at 37°C to the cells. To quantify Lysotracker immunofluorescence, 50-70 cells/neurons were randomly imaged in total from three different coverslips for each independent experiment. The number of LysoTracker punctate were measured and normalized to cytoplasmic area of the cell. Intensity threshold was set to remove background fluorescence. Quantitative

colocalization analyses were also performed using Metamorph with colocalization analysis plugins.

2.4 Lysosomal pH assay

The measurement of lysosomal pH by confocal microscopy is based on the use of the ratiometric assay of pH-sensitive fluorescein fluorescence to pH-insensitive rhodamine fluorescence as described in (Majumdar et al, 2007). Briefly, cells were plated on glass coverslip containing dishes (Mattek) and overnight with 2.5 mg/ml dextran conjugated to both fluorescein and rhodamine (70,000 mol. wt.; Invitrogen D1951) in complete growth media. Cells were washed 4 times in complete media, and chased for 4 hrs to allow the dextran to traffic to the lysosomes. The cells were then washed with medium 2 buffer (150 mM NaCl, 20 mM HEPES, pH 7.4, 1 mM $CaCl_2$, 5 mM KCl, and 1 mM $MgCl_2$) and were imaged on a heated stage at 37°C. 15-20 images were collected over a period of 5-10 min for each condition. The ratio of fluorescein to rhodamine fluorescence was determined for each individual lysosome. Images were analyzed using MetaMorph image processing software (Molecular Devices). For all experimental sets, crosstalk of the fluorophores was negligible. Calibration curves were generated after fixing and equilibrating the fluorescein-rhodamine-dextran–loaded cells to a range of pH buffers. An independent standard curve was generated for each experimental day. For test groups, cells were

incubated with 30 μM KH7 for 10 hrs and/or 500 μM Sp-8-cpt-cAMP analogue for 1 hr and cells were imaged as mentioned above.

2.5 Electron microscopy

Brain sections were prepared for electron microscopy as previously described (Milner et al, 2011). Briefly, the brains of 15-18 month old wild-type and knock out male mice were anesthetized with an overdoes of Nembutal (150 mg/kg, i.P.) and transcardially perfused with 3.75% acrolein and 2% paraformaldehyde in 0.1 M phosphate buffer. Coronal hippocampal sections (40 μm thick) were embedded in plastic, cut (70 nm thick) on an ultratome and collected on copper mesh grids. Cells were prepared for electron microscopy with the assistance of the WCMC EM Core. To prepare cells for electron microscopy, they were treated as required and fixed with 2% glutaraldehyde for 2 hrs at 4°C followed by post fixation in 1% osmium tetroxide for 1 h at 4 °C. The samples then were embedded in plastic, cut (70-nm thick) and collected on copper grids. Grids were counterstained with 5% uranyl acetate followed by Reynolds lead citrate (sections only) and viewed with a CM10 transmission electron microscope. Grids were photographed and analyzed by a person blind to experimental condition. For the quantitative analysis, images from fifteen entire cells were photographed in each experimental group. Autophagic vacuoles were identified using previous criteria as descried by Nixon et al (Lee et al, 2010) and counted on electron micrographs (x135,000 magnification). Cytosol area

was determined using Image J. Results were expressed as the number of vacuoles per square micrometer.

For immunogold labeling, free-floating sections were labeled with monoclonal R21 (1:50), antibody by the immunogold–silver procedure of Milner et al (Milner et al, 2011). Sections were then incubated in secondary antibodies conjugated to 1 nm gold particles (Amersham Biosciences) in 0.01% gelatin and 0.08% BSA in PBS. The conjugated gold particles were enhanced by treatment with silver solution (IntenSE, Amersham Biosciences). Sections were then embedded in plastic as described above.

2.6 Protein extraction and Immunoblotting

Immunoblotting was performed as previously described in (Choi et al, 2012). Briefly, samples were prepared for SDS-PAGE according to standard protocol. Cells were lysed in buffer containing 50mMTris (pH = 7.4), 150mM NaCl, 1mM EDTA, 1% Triton X-100 and 0.5% Tween-20 with protease and phosphatase inhibitors. Either 10 or 15% gels were run according to protein weight and following electrophoresis proteins were transferred onto 0.45 mm PVDF membranes (Millipore). The membrane was incubated overnight in primary antibody then incubated with HRP conjugated secondary antibody. The blot was developed by ECL-kit (GE Healthcare). Visualization and band quantification were performed with a BioRad gel imager, ChemiDoc XRS system for extra resolutions and sensitivity. Protein concentration in

cellular extracts was quantified using the BioRad DC Protein Assay with absorbance was measured at 750 nm.

2.7 Cellular protein degradation

Total protein degradation in cultured cells was measured by pulse-chase experiments (Auteri et al, 1983; Kaushik & Cuervo, 2009). Briefly, confluent cells were labeled with [^{3}H]-leucine (6 μCi/ml) for 48 hr at 37°C in order to preferentially label long-lived proteins. Following labeling, cells were extensively washed and maintained in complete growth medium (DMEM + 10% fetal bovine serum + 0.5% glutamine) with an excess of unlabeled leucine (2.8 mM; Sigma)to prevent reutilization of radiolabeled leucine. Aliquots of the medium were taken at different time-points and precipitated with 10% Trichloroacetic acid (TCA) and 0.5 mg/ml BSA for an hour. Proteolysis was measured as the percentage of the initial acid insoluble radioactivity (protein) transformed into acid-soluble radioactivity (amino acids and small peptides) over time.

2.8 Statistical analysis

Statistical comparisons were made using two-tailed unpaired *t* tests with significance placed at $p < 0.05$. One set of 3T3 or SV40 MEFs grown separately in individual dishes were considered as one independent experiment ($n = 1$). A set of

primary neuronal cultures s prepared from one mouse embryo was also considered as one independent experiment. Data were expressed as mean ± SEM. Statistical analysis was performed using Excel. Error bars represent standard error of the mean (±SEM).

CHAPTER THREE: RESULTS

3.1 Generalities

Lysosomes degrade extracellular material and intracellular components during endocytosis and autophagy. The hydrolases which degrade the proteins, lipids, and polysaccharides are optimally active in an acidic environment; thus, the pH of the lysosome lumen is maintained around 5 (Pillay et al, 2002). Acidification is mediated by the vacuolar ATPase (V-ATPase), which pumps protons into the lysosomal lumen in an ATP-dependent manner (Breton & Brown, 2013; Ohkuma et al, 1982). This transport generates a charge imbalance, which limits further proton translocation and lysosomal acidification. A number of counter ion transport pathways have been identified that allow the lysosomes to dissipate this membrane potential (Mindell, 2012; Pillay et al, 2002; Steinberg et al, 2010; Xu & Ren, 2015). While these functions provide a mechanism for acidification, they do not explain how lysosomes reach their appropriate pH; i.e., there remains a need for pH “sensors” to set lysosomal pH. A recently identified two-pore ion channel (TPC1) is a pH sensitive sodium channel (Cang et al, 2014) that can regulate acidification during starvation-induced autophagy (Cang et al, 2013). However, TPC1’s role in acidification is limited to starvation-induced autophagy; TPC1 knockout cells grown in the presence of sufficient nutrients have normal lysosomal pH. Therefore, there must be other pH sensitive proteins that regulate acidification during endosome-lysosome biogenesis.

Signaling cascades able to acidify lysosomes include the ubiquitous second messenger cAMP. In pathophysiological situations where lysosomes are insufficiently acidified, pharmacologically increasing intracellular cAMP acidifies them. For example, in retinal pigment epithelial cells (Liu et al, 2008) and fibroblasts (Coffey et al, 2014) mutations causing lysosomal pH to be relatively alkaline can be rescued by exogenous addition of membrane permeable cAMP. Cyclic AMP has also been proposed to mediate physiological acidification; the average pH of lysosomes in resting microglia is ~6, and signals which elevate intracellular cAMP acidify them (Majumdar et al, 2007). In mammalian cells, two distinct classes of adenylyl cyclase generate cAMP. There is a family of widely studied, G-protein regulated, hormonally responsive, transmembrane adenylyl cyclases (tmACs) and the molecularly and biochemically distinct soluble adenylyl cyclase (sAC; ADCY10). sAC is widely expressed, and unlike tmACs, it is directly regulated by bicarbonate (HCO_3^-) anions (Chen et al, 2000; Kleinboelting et al, 2014). Due to ubiquitously expressed carbonic anhydrases (CAs), HCO_3^- is in rapid equilibrium with carbon dioxide (CO_2) and protons (pH). Therefore, HCO_3^--regulated sAC also serves as a CO_2 sensor, and as a CO_2/HCO_3^- sensor, sAC is the source of cAMP impacting a number of physiological processes (Chang & Oude-Elferink, 2014; Levin & Buck, 2015b; Tresguerres et al, 2011), including HCO_3^--induced sperm activation and motility (Esposito et al, 2004b; Hess et al, 2005b), coupling nutrient utilization with ATP generation by sensing metabolically generated CO_2 inside the mitochondrial matrix (Acin-Perez et al, 2009b), maintenance of intraocular pressure (Lee et al, 2011), glucose responsive

insulin release (Zippin et al, 2013a), and CO_2 responsiveness in cilia of bronchi (Chen et al, 2014).

Inside cells, proton movement is facilitated by CA activity (Spitzer et al, 2002; Stewart et al, 1999), and CAs are essential for establishing pH gradients (Tarbashevich et al, 2015). Due to the CA-catalyzed $CO_2/HCO_3^-/H^+$ equilibrium, intracellular HCO_3^- concentrations reflect local pH, and HCO_3^--regulated sAC also functions as an intracellular pH sensor (Chang & Oude-Elferink, 2014; Levin & Buck, 2015b; Rahman et al, 2013). We previously demonstrated this in pH sensing epithelia, where the pH-induced translocation of proton pumping V-ATPase essential for extracellular acid/base regulation is dependent upon sAC. sAC can be found in a complex with V-ATPase (Paunescu et al, 2008a), and pH-dependent V-ATPase translocation to the acid secreting surface is blocked by inhibitors of either CAs or sAC in epididymis (Pastor-Soler et al, 2003; Pastor-Soler et al, 2008) and likely in kidney (Paunescu et al, 2008a; Paunescu et al, 2010a). This pH dependent acid/base regulatory mechanism, involving CA, sAC and V-ATPase, is evolutionarily conserved (Tresguerres, 2014); a similar mechanism is involved in organismal pH regulation in marine invertebrates (Tresguerres et al, 2010b).

We now show that pH regulated sAC is essential for acidification of lysosomes. In the absence of sAC, V-ATPase subunits do not properly co-localize with lysosomes, lysosomes do not fully acidify, and autophagosomes accumulate. Thus, pH sensitive sAC is an essential regulator of lysosomal acidification in

mammalian cells.

3.2 Results

3.2.1 Autophagic vacuoles (AVs) accumulate in the absence of soluble adenylyl cyclase (sAC)

Ultrastructural studies revealed mouse embryo fibroblast cell lines (MEFs) derived from sAC knockout (KO) mice accumulate more autophagic electron dense vesicles compared to MEFs derived from their wild type (WT) littermates (**Figure 3.1**). Macroautophagy (hereafter autophagy) is the catabolic pathway in cells responsible for degrading long-lived proteins, organelles, and protein aggregates (Klionsky, 2007; Mizushima, 2007). It involves sequestration of cytosolic regions into characteristic double-membrane autophagosomes that fuse with lysosomes to form single-membrane degradative autophagolysosomes. Both autophagosomes (AP) and autophagolysosomes (AL) are more abundant in sAC KO MEFs (**Figure 3.1A,B**). Autophagic vacuoles (AVs), defined as APs and ALs, can also be quantitated by immunoblotting for the autophagy markers, LC3-II (Mizushima, 2007) and p62/SQSTM1 (Bjorkoy et al, 2005). Consistent with the ultrastructural studies, steady state levels of both LC3-II and p62 were higher in sAC KO MEFs (**Figure 3.1C,D**) relative to WT MEFs. AV accumulation was not an artifact of the immortalization method; LC3-II and p62 were elevated in an independently derived line of sAC KO

MEFs immortalized using SV40 large T antigen (SV40-MEFs) relative to SV40 immortalized WT MEFs (**Figure 3.2**).

Accumulation of AVs is a hallmark of aging and neurodegenerative diseases (Bahr & Bendiske, 2002b; Nixon et al, 2005). Alzheimer's Disease is a neurodegenerative disease that mostly affects the hippocampus. Using electron microscopy, we quantitated AVs in the dentate gyrus and CA1 regions of the hippocampus from sAC KO and age-matched WT mice. The granule cells of the dentate gyrus from aged sAC KO mice accumulated approximately twice the number of ALs relative to granule cells from WT littermates (**Figure 3.1E,F**). In the pyramidal cells of the CA1 region, both APs and ALs were more abundant in sAC KO mice (**Figure 3.1G,H**). Consistent with these observations in brain, primary neurons isolated from sAC KO mice accumulated more AVs (**Figure 3.3**) and had elevated steady state levels of LC3-II and p62 (**Figure 3.4**) compared to neurons from WT littermates. Pharmacologic inhibition of sAC using the sAC specific inhibitor KH7 (Bitterman et al, 2013b), also increased AVs. Treating WT neurons with KH7 for 4 hours lead to accumulation of AVs (**Figure 3.3B**) and elevated LC3-II and p62 levels (**Figure 3.4**). As expected, the sAC inhibitor had no effect on LC3-II and p62 levels in sAC KO neurons. Inhibition of sAC with KH7 also increased autophagic markers in a human cell line; LC3-II was elevated in Huh7 cells treated with KH7 (**Figure 3.5**). These data identify accumulation of AVs as a general phenotype caused by loss of sAC.

Figure 3.1: Autophagosomes and lysosome-related structures accumulate in the absence of sAC**. (A)** Representative electron micrographs of WT and sAC KO MEFs. Note the accumulation of electron dense organelles in sAC KO cells compared to WT littermates. Scale bars represent 500 nm. Shown below are higher magnification views of boxed areas highlighting examples of autophagic vacuoles in KO mice. **(B)** Quantitative analysis of the number of autophagosomes (AP; white bars) and autophagolysosomes (AL; black bars) in WT and sAC KO MEFs. **p>0.02 n=10 cells/condition. 2 independent experiments. All values are given as mean ± SEM. **(C)** Representative immunoblot of the autophagic markers LC3-II and p62, along with GAPDH which was used for loading control, in 3 independent cultures of WT and sAC KO MEFs. **(D)** Densitometric analysis of LC3-II and p62, normalized to GAPDH, in WT (white bars) and sAC KO (black bars) MEFs. Error bars represent the SEM. n=6, * for p<0.05. **(E)** Representative electron micrographs of hippocampal dentate granule cells in WT and sAC KO aged mice. Shown below are higher magnification views of boxed areas highlighting examples of autophagic vacuoles in KO mice. **(F)** Quantitative analysis of the number of autophagic vacuoles (APs and ALs) in WT and sAC KO granular cells of the dentate gyrus. ***p>0.002, N = 3 mice/condition; n=10 cells/mouse. All values are given as mean ± SEM. **(G)** Representative electron micrographs of the pyramidal cells of the CA1 in WT and sAC KO aged mice. Shown below are higher magnification views of boxed areas highlighting examples of autophagic vacuoles in KO mice. **(H)** Quantitative analysis of the number of vacuoles in WT and sAC KO pyramidal cells of the CA1 of the hippocampus. *p>0.05, N = 3 mice/condition; n=10 cells/mouse. All values are given as mean ± SEM.

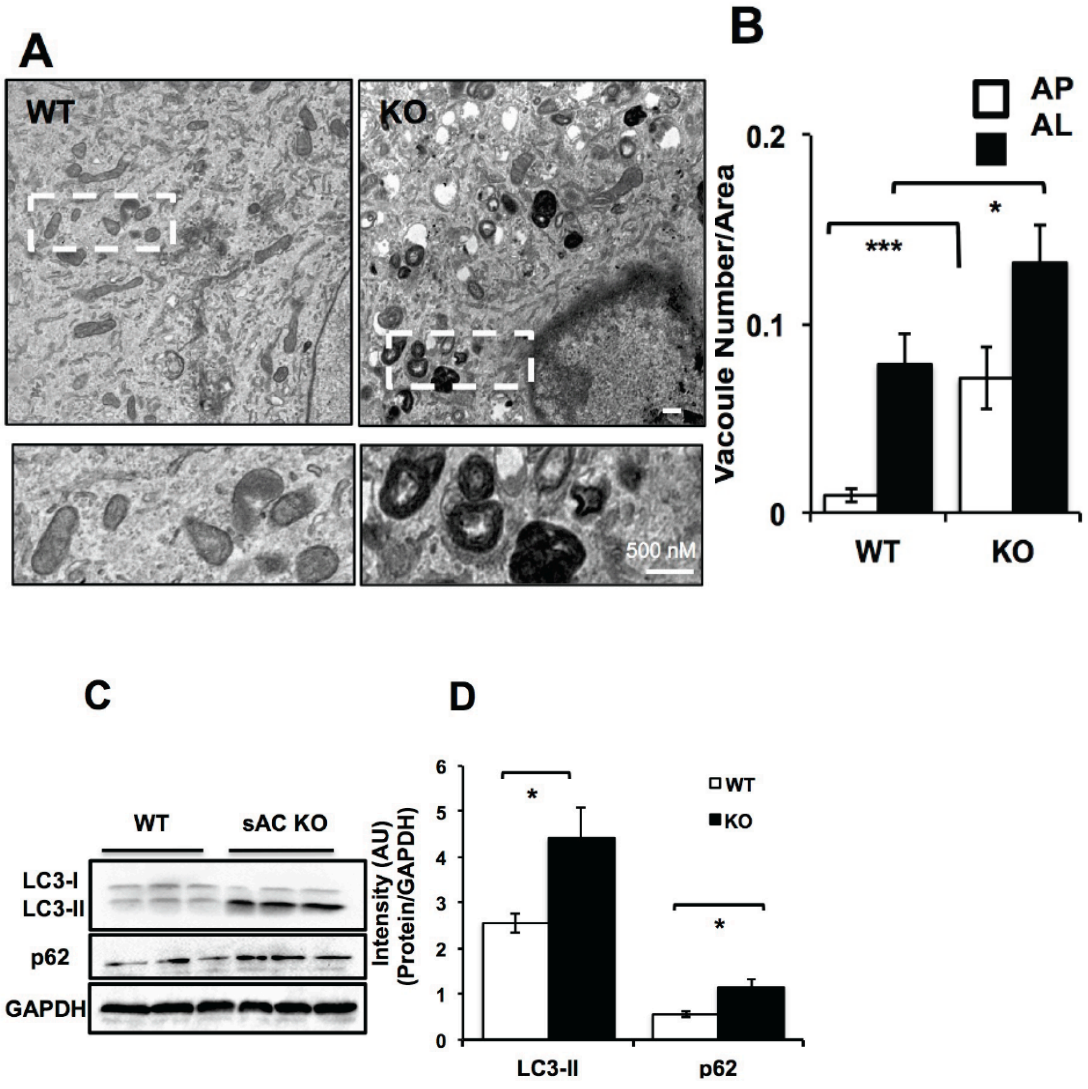
A
WT
KO
500 nM
B
AP
AL
Vacoule Number/Area
0.2
0.1
0
***
*
WT
KO
C
WT
sAC KO
LC3-I
LC3-II
p62
GAPDH
D
Intensity (AU)
(Protein/GAPDH)
6
5
4
3
2
1
0
*
*
WT
KO
LC3-II
p62

Figure 3.1 (continued)

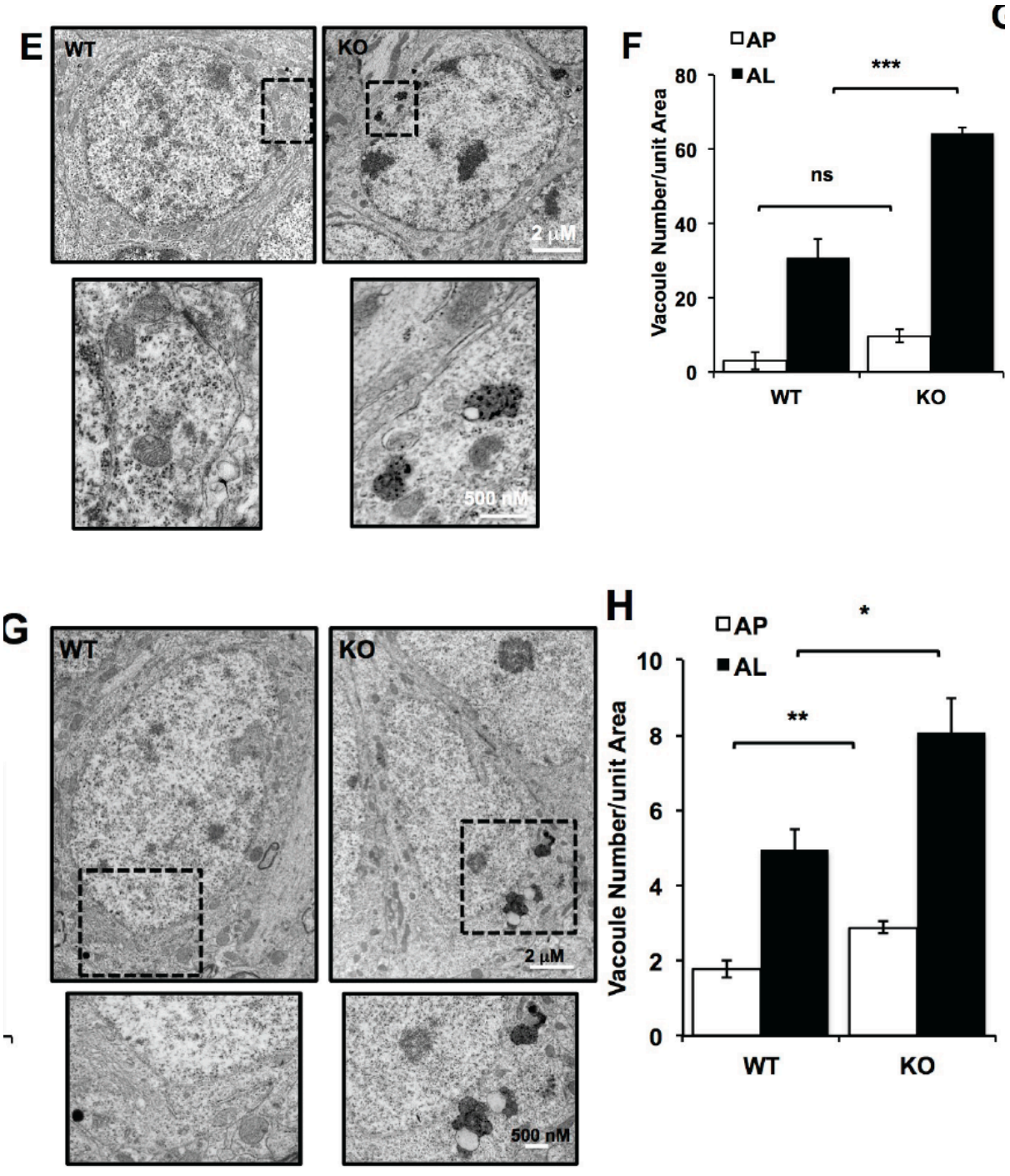

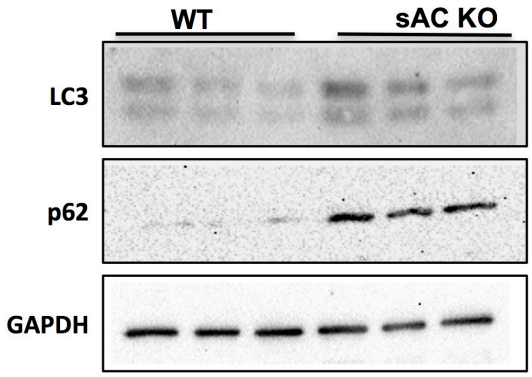

Figure 3.2: Autophagic markers are elevated in an independently derived line of sAC KO MEFs relative WT MEFs. Representative immunoblot of the autophagic markers LC3-II and p62, along with GAPDH which was used for loading control, in an independently derived line of sAC KO MEFs immortalized using SV40 large T antigen (SV40-MEFs). n=3

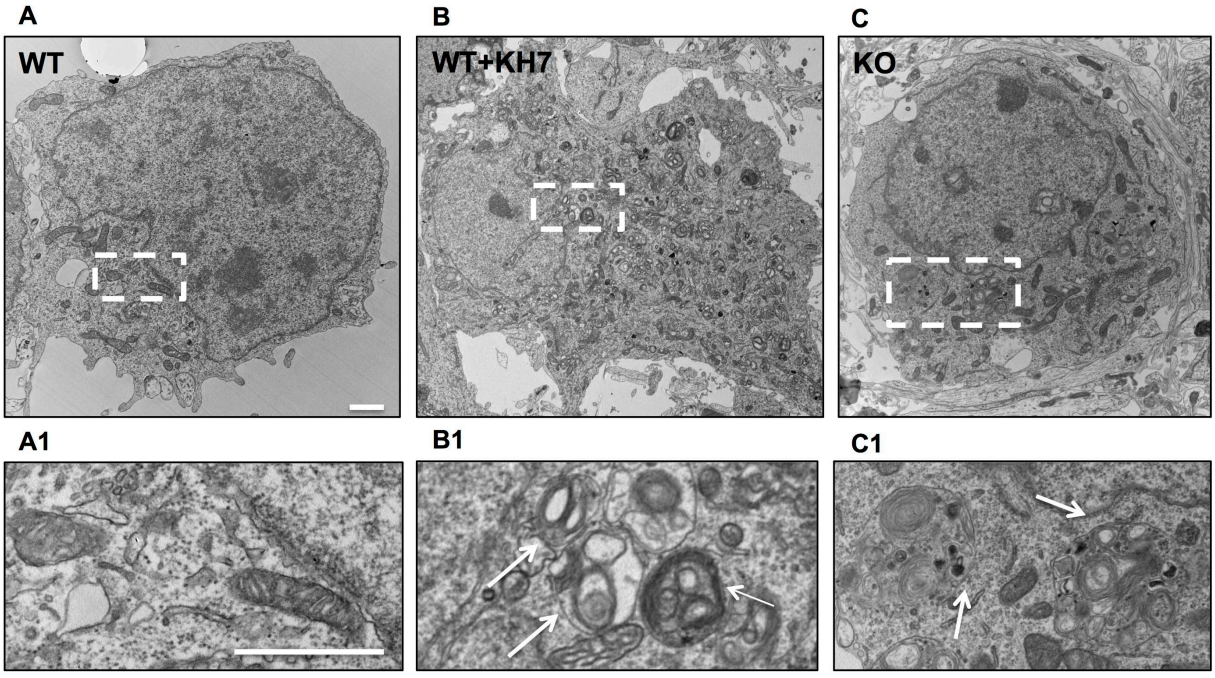

Figure 3.3: Presence of electron dense vacuoles in primary neurons in the absence of sAC **(A)** Representative electron micrographs of 12 DIV WT (**A** and **B**) and sAC KO (**C**) primary neurons. Note the accumulation of electron dense particles (white arrow) in WT neurons treated with 30 μM KH7 for 6 hrs (**B1**) and in sAC KO neurons (**C1**). (Scale bars, 500 nm). **A1-C1** corresponds to high magnification view of the boxed area. (Scale bars, 1 μm).

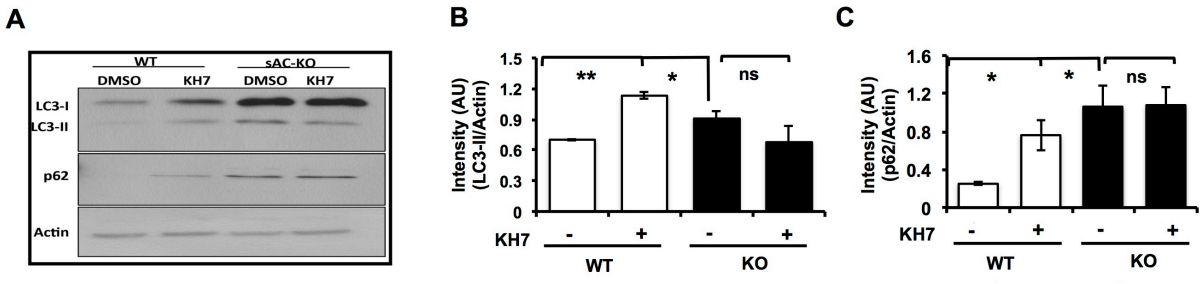

Figure 3.4: Increased of autophagic markers in the absence of sAC in primary neurons **(A)** Representative immunoblot of LC3 and p62 in 12 DIV primary neurons under conditions of no treatment and when treated with 30 μM KH7 for 3 hrs. Protein levels of each protein were normalized to actin as an internal control. **(B)** Densitometric analysis of LC3-II from (A). Error bars represent the SEM. n=6, * for $p<0.05$, **$p<0.001$, ns compared to KO cells. **(C)** Densitometric analysis of immunoblot of p62 from (A). Error bars represent the SEM. n=6, * for $p<0.05$, ns compared to KO cells.

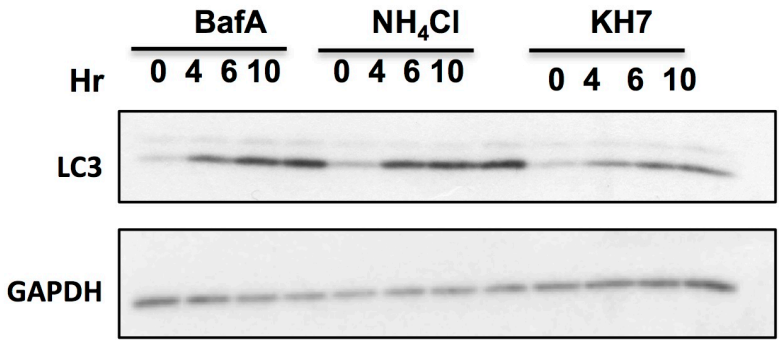

Figure 3.5: Increase of autophagy marker in a human cell line, huh-7. Representative immunoblot of LC3 in Huh-7 human liver cells treated with 30 μM KH7 for 0, 4, 6 and 10 hrs. 200 nM Bafilomycin, BafA (an inhibitor of V-ATPase proton pump) and 20 mM NH_4Cl (which alkalinizes lysosomes) are used as positive controls. Protein levels of each protein was normalized to GAPDH as an internal control n=3-5 per experimental group.

3.2.2 Protein turnover is unaffected in sAC knockout (KO) cells

As the terminal stage of autophagy, autophagolysosomes degrade intracellular components. To determine whether the increased number of autophagolysosomes due to sAC loss altered protein turnover, we performed metabolic labeling experiments. The kinetics of protein turn over were indistinguishable between WT and sAC KO MEFs (**Figure 3.6**). Thus, because more autophagolysosomes result in the same overall rate of proteolysis, degradation inside autophagolysosomes must occur less efficiently.

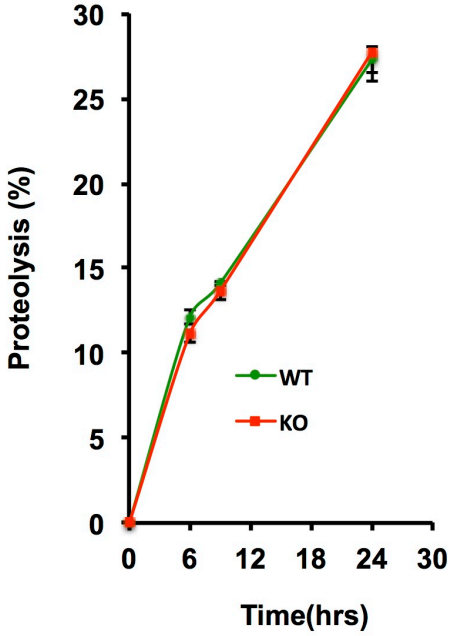

Figure 3.6: Protein turnover is unchanged in sAC KO cells. **(A)** Degradation of long-lived proteins was measured in WT and sAC KO MEFs. After incorporation of [^{3}H]-leucine, cells were incubated in complete growth media for the indicated chase period (n = 15, 4 independent experiments). Shown is proteolysis measured as the percentage of acid-soluble radioactivity (amino acids and small peptides) divided by the initial acid insoluble radioactivity (protein).

The hydrolases which degrade the proteins, lipids, and polysaccharides are optimally active in an acidic environment; thus, the pHs of the lumens of autophagolysosomes and lysosomes are maintained below 5 (Pillay et al, 2002). Because (A) cAMP plays a role in lysosomal acidification (Coffey et al, 2014; Liu et al, 2008; Majumdar et al, 2007); (B) V-ATPases are essential for lysosomal acidification (Breton & Brown, 2013; Xu & Ren, 2015); and (C) previous work identified sAC as an evolutionarily conserved pH regulated signaling enzyme involved in pH dependent regulation of V-ATPase functions (Pastor-Soler et al, 2003; Pastor-Soler et al, 2008; Paunescu et al, 2008a; Paunescu et al, 2010a; Tresguerres et al, 2010b), we hypothesized the diminished degradative capacity of autophagolysosomes in the absence of sAC may result from a defect in lysosomal acidification.

3.2.3 Lysosomal acidification is dependent upon both sAC and intracellular HCO_3^-

LysoTracker is a qualitative acidic pH indicator dye, which is enriched and strongly fluoresces in compartments that have a pH below 5 (Lee et al, 2010). There were less LysoTracker positive puncta in sAC KO MEFs relative to WT MEFs (**Figure 3.7**) indicating that there are fewer acidic organelles in sAC KO cells. Cells can exhibit pH gradients (Martin et al, 2011; Tarbashevich et al, 2015), and although intracellular pH fluctuations are dependent upon CA activity (Tarbashevich et al,

2015), they can be studied in cells grown in the absence of exogenous CO_2/HCO_3^- (i.e., in HEPES-buffered media) (Martin et al, 2011). In HEPES-buffered media, the sole source of intracellular HCO_3^- will be from metabolically generated CO_2, and the intracellular HCO_3^- will be absolutely dependent upon carbonic anhydrase activity (Scheme; **Figure 3.8A**). We took advantage of this CA dependence to explore the contribution of CAs to organellar acidification. When grown in HEPES-buffered media, sAC KO MEFs had fewer LysoTracker positive puncta than WT MEFs (Fig. 3.8B), similar to our observations when the cells were grown under normal conditions (i.e., under 5% CO_2 / 25 mM $NaHCO_3$)(**Figure 3.7**). Interestingly, the number of LysoTracker puncta was also diminished in WT cells grown in HEPES-buffered media in the presence of a carbonic anhydrase inhibitor (CAI) (**Figure 3.8C**). CAI-treated WT cells, which are prevented from forming intracellular HCO_3^-, had fewer LysoTracker positive puncta than the same cells grown in the same media in the absence of CAIs. Importantly, the diminished LysoTracker stainings in both sAC KO MEFs (**Figure 3.8B**) and in CAI-treated WT MEFs (**Figure 3.8C**) were rescued by supplying sAC's product, cAMP. These data demonstrate that in the absence of extracellular CO_2/HCO_3^-, cells have a sufficient supply of protons to acidify organelles and that organellar acidification is dependent upon sAC and upon the presence of intracellular HCO_3^- to regulate it.

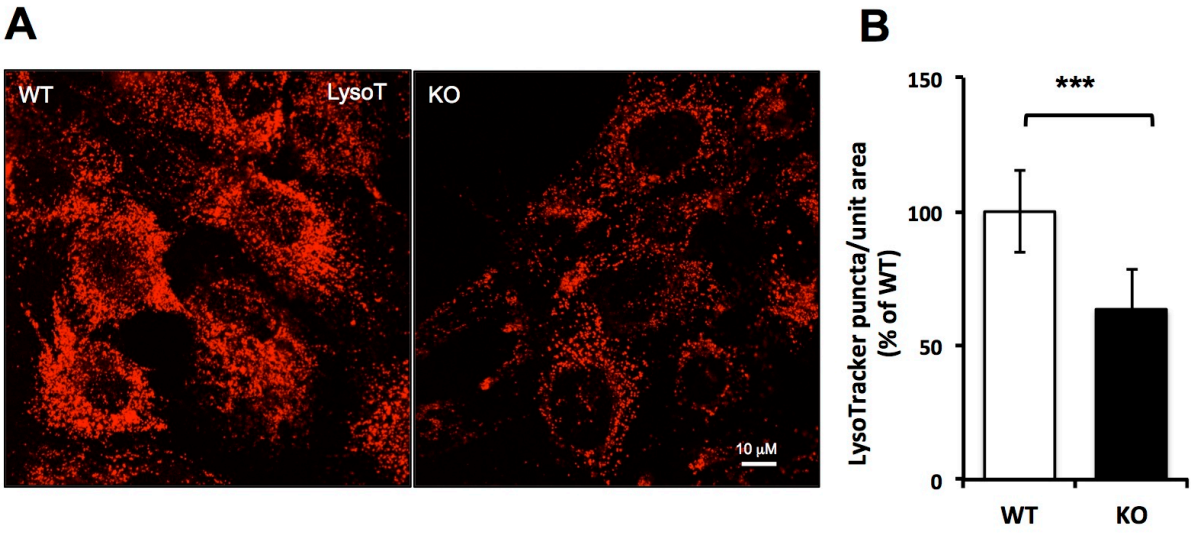

Figure 3.7: sAC KO cells have fewer acidic organelles. **(A)** WT and KO 3T3 MEFs grown in 5% CO_2 and 25 mM HCO_3^- were incubated with 500 nM LysoTracker for 30 minutes and live images were captured. **(B)** Lysotracker puncta were normalized to cytoplasmic cell area. *** for $p<0.001$, n=3 per experimental group. All values are given as mean ± SEM.

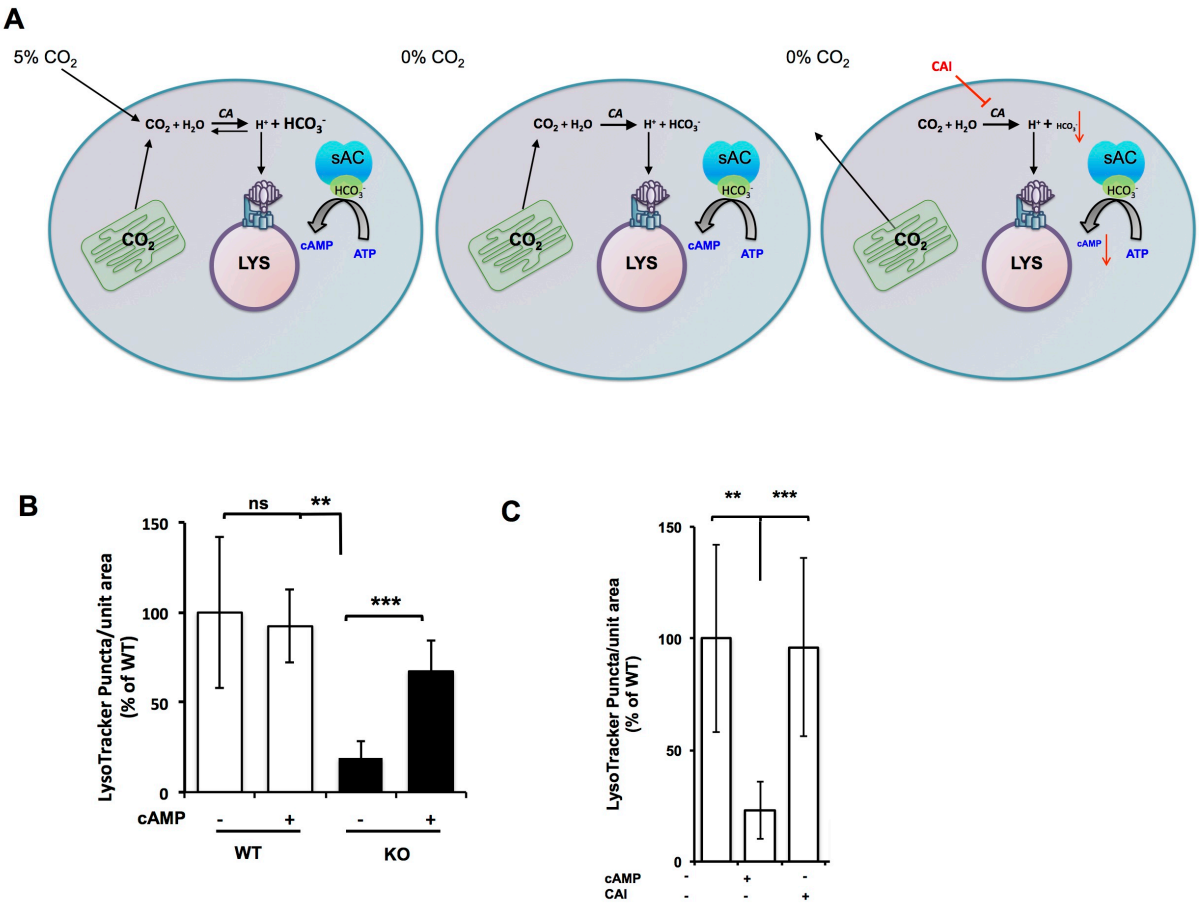

Fig. 3.8: Organellar acidification is dependent upon the presence of intracellular HCO_3^-. **(A)** Schematic of the effect of intracellular HCO_3^- when cells are grown in normal growth media (left panel) HEPES buffered media (center panel) and grown in HEPES-buffered media the presence of a carbonic anhydrase inhibitor (CAI). See text for details. **(B)** WT and KO 3T3 MEFs grown in HEPES buffer (without $NaHCO_3$) in ambient air were incubated with and without 500 μM Sp-8-cpt-cAMP for 60 mins. 500 nM LysoTracker was added for the last 30 mins. LysoTracker puncta/unit area were analyzed. ** for $p<0.02$, *** for $p<0.001$, n=3 per experimental group. All values are given as mean ± SEM. **(C)** WT cells were treated with 100 μM Acetazolamide for 8 hrs in the presence of 500 μM Sp-8-cpt-cAMP for the last 60 mins where indicated. In all cells, 500 nM LysoTracker was added for the last 30 mins. Lysotracker puncta were analyzed ** for $p<0.02$, *** for $p<0.001$, n=3 per experimental group. All values are given as mean ± SEM.

Autophagolysosomes form when autophagosomes fuse with lysosomes. To assess whether the diminished acidic organelles in sAC KO include lysosomes, we first measured colocalization of LysoTracker with the lysosomal-associate membrane proteins, LAMP2 or LAMP1 (**Figure 3.9**). LysoTracker/LAMP2 colocalization was significantly reduced in sAC KO neurons (**Figure 3.9A,B**) relative to WT neurons, and inhibition of sAC using KH7 decreased the LysoTracker/LAMP2 colocalization in WT, but not in sAC KO neurons. KH7 also decreased LysoTracker/LAMP1 colocalization in the human Huh7 cell line (**Figure 3.9C,D**). In Huh7 cells, KH7, but not the inert structurally related KH7.15 (Wu et al, 2006), diminished LysoTracker/LAMP1 colocalization in a time dependent manner.

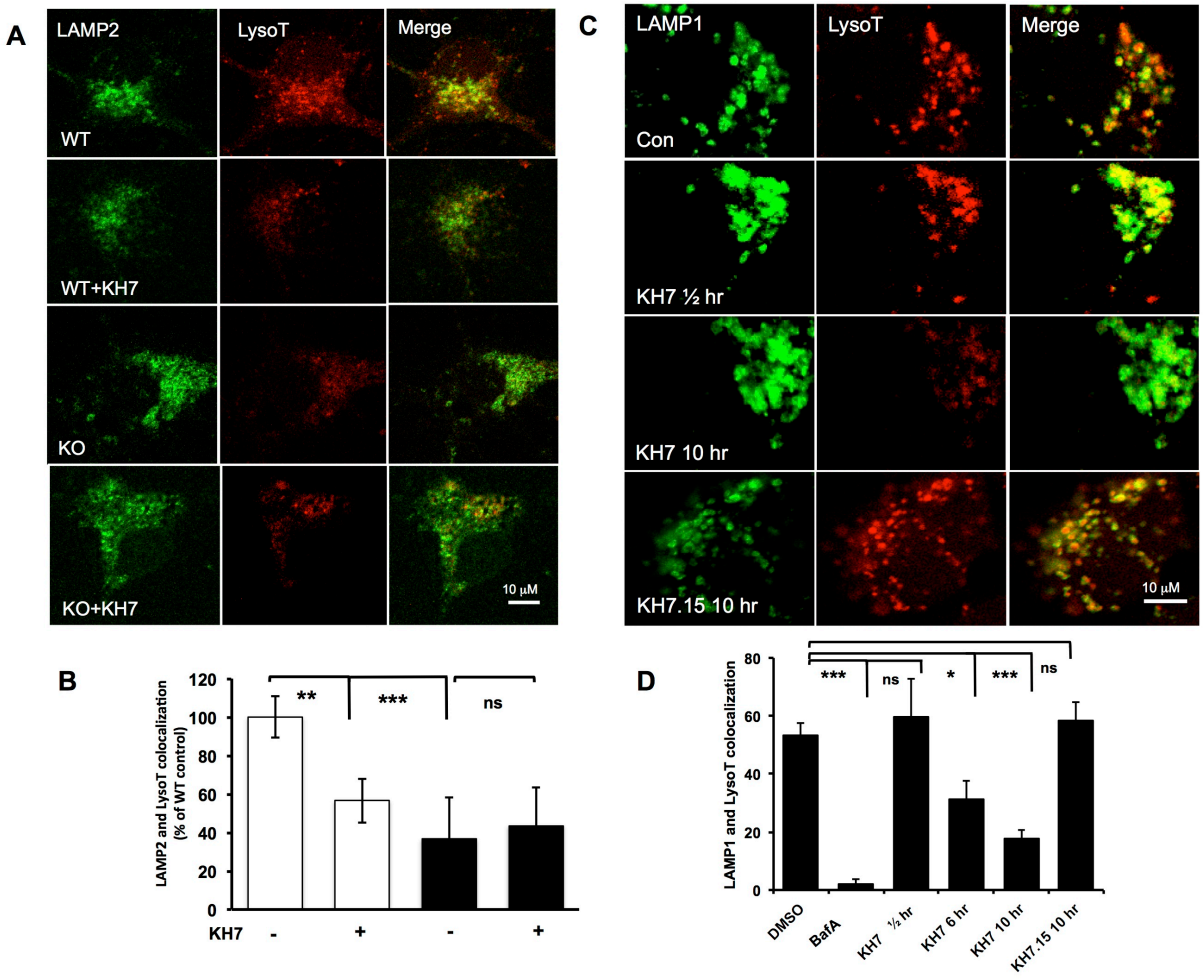

Figure 3.9: In the absence of sAC activity, cells have fewer acidic lysosomes. **(A)** 12 DIV WT and sAC KO neurons were treated with or without KH7 (30 μM 3 hr), incubated with LysoTracker (500 nM, 30 min) and immunolabeled with LAMP2 antibody. **(B)** Quantitative analysis of LysoTracker and LAMP2 colocalization. **p>0.01, ***p>0.001 compared with control untreated cells, ns compared to KO cells, n=3-5 per experimental group. **(C)** Human Huh-7 cells were treated with 30 μM KH7 for the time points indicated with addition of LysoTracker (100 nM, 30 min). 30 μM KH 7.15 (negative control) was added to cells for 10 hrs. Cells were then fixed and immunolabeled with LAMP1 antibody. **(D)** Quantitative analysis of LysoTracker and LAMP1 colocalization. As positive control, the V-ATPase inhibitor, Bafilomycin A (BafA1; 100 nM), was added for 10 hrs to alkalinize lysosomes. *p>0.05, ***p>0.002 compared with control untreated cells, n=3-5 per experimental group.

We next employed ratiometric imaging of fluorescein (pH sensitive) and rhodamine (pH insensitive) dextran beads (Majumdar et al, 2007) to quantify pH of individual lysosomes derived via endosomal maturation pathway. The pH sensitive nature of this dual emission probe is demonstrated in **Figure 3.10**. With decreasing pH, the pH–sensitive fluorescein (green) fluorescence is quenched, while the pH insensitive rhodamine (red) fluorescence remains unchanged; thus, the green/red ratio allows us to identify each lysosome and determine its specific pH. We confirmed the ability of this ratiometric method to measure changes in lysosomal pH by demonstrating alkalinization of lysosomes in WT cells perfused with 20 mM ammonium chloride (NH_4Cl)(**Figure 3.11**). Using this quantitative method, lysosomal pH in WT MEFs was found to average 4.7 ± 0.1, consistent with previously published studies (Cang et al, 2013; Lee et al, 2010; Ohkuma & Poole, 1978) (**Figure 3.12A,B**). In contrast, the average pH of lysosomes in sAC KO MEFs was significantly higher, with their average pH of 5.3 ± 0.1 ($p<0.001$). In addition to having a higher average pH, the distribution of pH values across all lysosomes was broader in sAC KO cells (**Figure 3.12A**). Consistent with these data, lysosomes in an independently derived line of sAC KO MEFs immortalized using SV40 large T antigen (SV40-MEFs) had an elevated mean pH and a wider distribution of pH values relative to WT SV40-immortalized MEFs (**Figure 3.13**), confirming the alkaline lysosomal pH in sAC KO cells was not an artifact of the immortalization method.

We confirmed the elevated lysosomal pH and altered distribution pattern was due to loss of sAC by pharmacologically inhibiting sAC using KH7, and by rescuing the sAC KO phenotype with cAMP. Incubation with the sAC-specific inhibitor, KH7, for 10 hours shifted the distribution and elevated the average pH of lysosomes in WT cells, from 4.7 ± 0.1 to 5.2 ± 0.2 ($p<0.01$), but had no effect on sAC KO cells (**Figure 3.12C,D**). Thus, both genetic and pharmacologic loss of sAC elevates the average pH of lysosomes with fewer lysosomes achieving the acidic pH necessary for optimal degradation. Supplying membrane permeable cAMP for one hour reduced the average pH in KO lysosomes to 4.5 ± 0.3 ($p<0.001$)(**Figure 3.12E,F**), demonstrating that sAC-generated cAMP mediates lysosomal acidification. This one hour cAMP rescue was unaffected by addition of cyclohexamide confirming that cAMP's effects on acidification is not dependent upon new protein synthesis (data not shown).

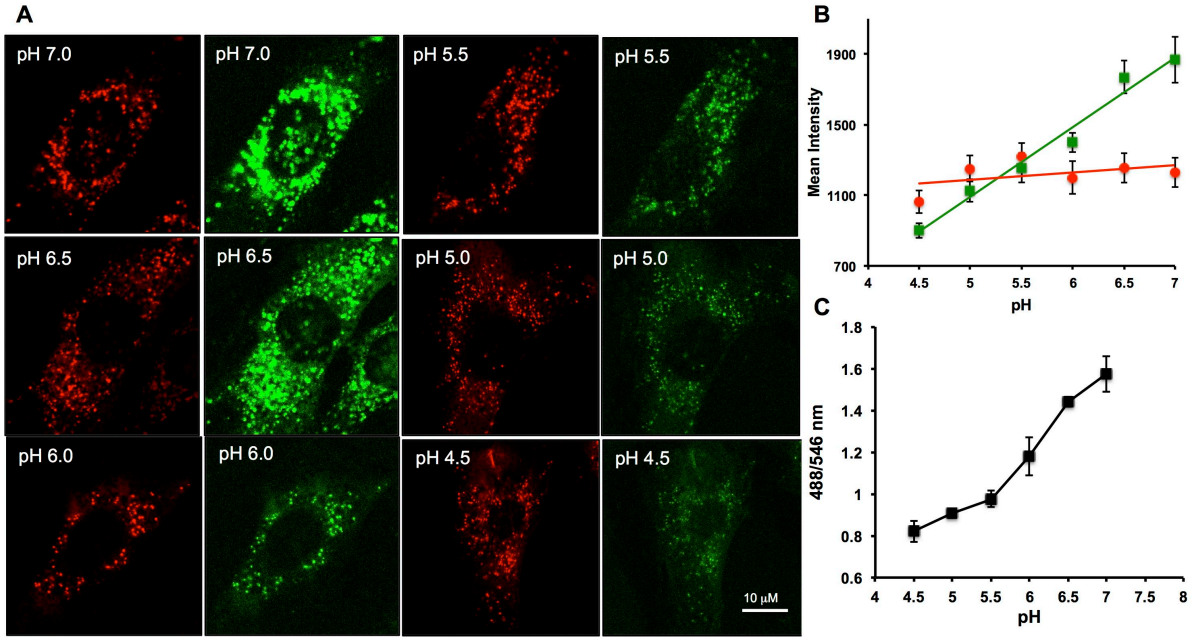

Figure 3.10: The pH-sensitive nature of the dual emission probe **(A)** Representative images of WT MEFs used for ratiometric analysis using the pH sensitive fluorescein and pH-insensitive Rhodamine dextran. Images were collected while permeabilized WT cells were incubated in buffer calibrated at different pH values (pH 7.0, 6.5, 6.0, 5.5, 5.0, 4.5.) **(B)** Graph showing intensities of fluorphore of the dual emission probe. pH sensitive fluorescein is shown in green, and pH-insensitive Rhodamine is shown in red. All values are given as mean ± SEM. **(C)** Graph showing the standard curve from one independent experiment (n=100 lysosomes/pH, values are mean ±SEM).

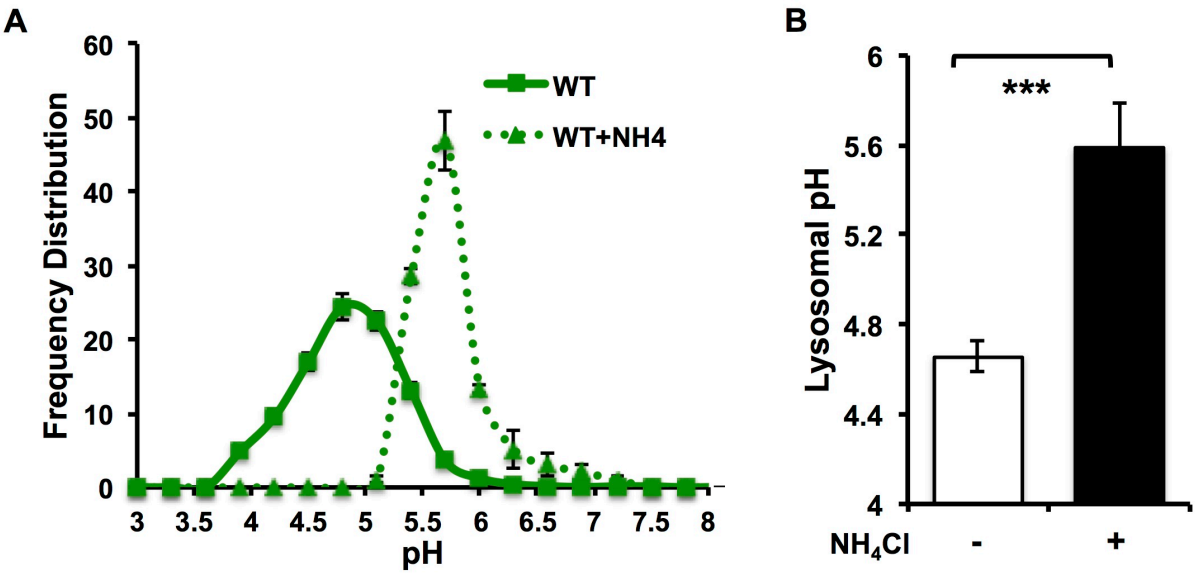

Figure 3.11: Lysosome becomes alanine in the presence of NH_4Cl **(A)** Artificial lysosomal acidification in the presence of 20 mM NH_4Cl for 30 min. WT MEFs were incubated with fluorescein-rhodamine dextran for 16 h followed by a 4-h chase. WT Cells (green curve) were incubated with NH_4Cl (green dashed) and lysosomal pH frequency distribution curve was plotted. WT lysosomes=3141, n=18, 6 independent experiments. WT+NH_4Cl=395, n=3, 1 independent experiment. Error bars represent the SEM.

Figure 3.12: sAC regulates lysosomal pH. **(A)** Frequency distribution of lysosomal pH measured as fluorescein/rhodamine ratios of individual lysosomes in WT (green curve) and sAC KO (red curve) MEFs. Lysosomal pH values were determined from calibration curves generated from permeabilized cells in various pH buffers. Number of lysosomes counted; WT=3141, KO=3559, n=18, 6 independent experiments. Error bars represent the SEM. **(B)** Average lysosomal pH in WT and sAC KO MEFs. **(C)** Frequency distribution of lysosomal pH in WT (green curve) and KO 3T3 MEFs (red curve) treated with 30 μM KH7 (WT+KH7, blue curve, KO+KH7, red dotted) for 10 hours shown alongside the frequency distribution curves of WT and sAC KO MEFs shown in (A). Number of lysosomes counted; WT+KH7= 2036, n=12, 3 independent experiments. KO+KH7=395, n=3, 1 independent experiment. **(D)** Average lysosomal pH in WT and KO cells treated with 30 μM KH7 for 10 hours. Values for minus KH7 are the same as in panel (B). **(E)** Frequency distribution of lysosomal pH in WT (green curve) and sAC KO (red curve) MEFs treated with 500 μM Sp-8-cpt-cAMP (WT+cAMP, green dotted, KO+cAMP, red dashed) for 60 minutes shown alongside the frequency distribution curves of WT and sAC KO MEFs shown in (A). Number of lysosomes counted; KO+cAMP= 2003, n=12, 3 independent experiments. WT+cAMP=579, n=3, 1 independent experiment. Error bars represent the SEM. **(F)** Average lysosomal pH in WT and KO cells treated with 500 μM Sp-8-cpt-cAMP for 60 minutes. Values for minus cAMP are the same as in panel (B). All values are given as mean ± SEM. ** for $p<0.01$, *** for $p<0.001$.

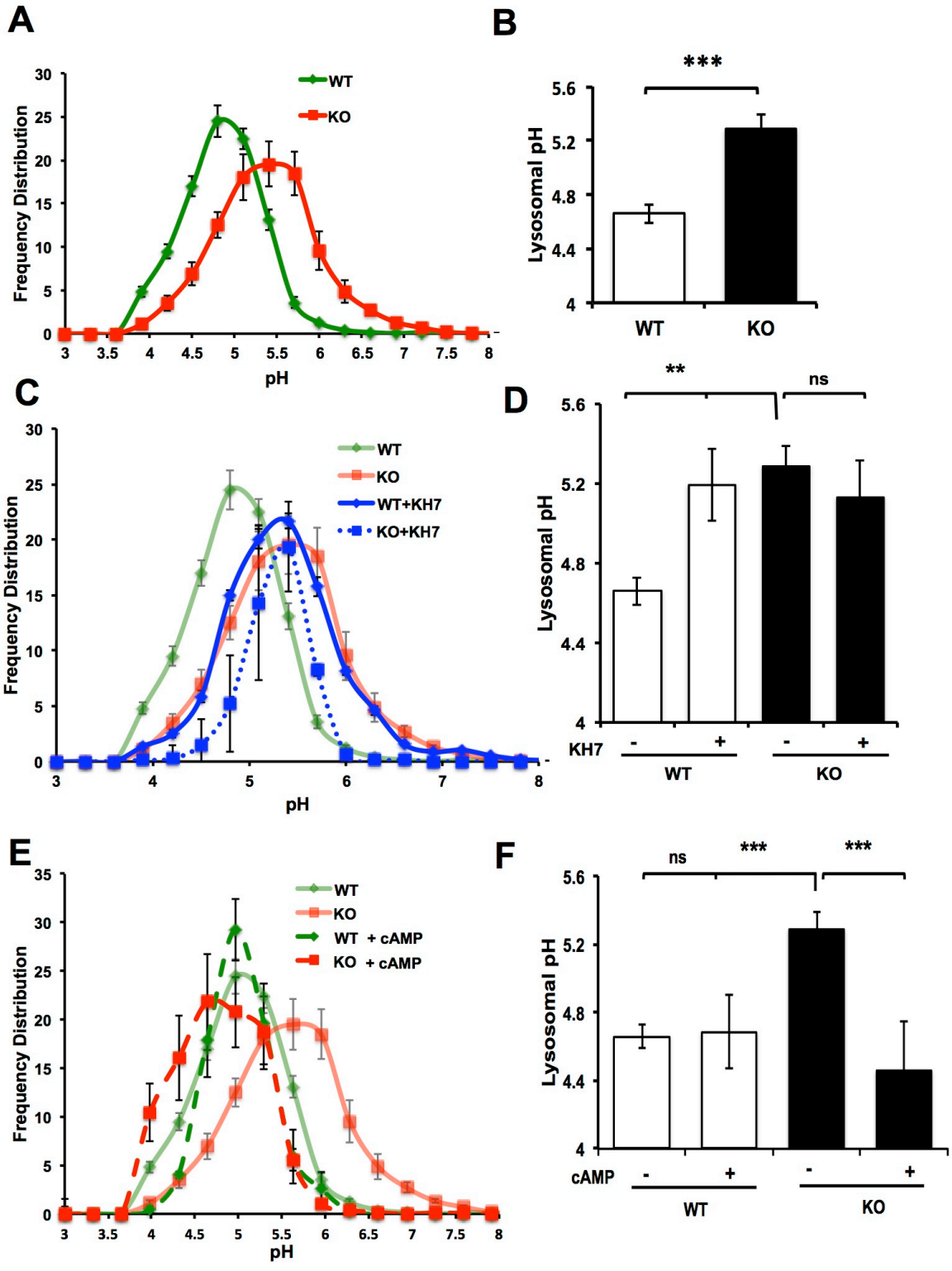
A
Frequency Distribution
pH
WT
KO
B
Lysosomal pH
***
WT
KO
C
Frequency Distribution
pH
WT
KO
WT+KH7
KO+KH7
D
Lysosomal pH
**
ns
KH7
WT
KO
E
Frequency Distribution
pH
WT
KO
WT + cAMP
KO + cAMP
F
Lysosomal pH
ns
***
***
cAMP
WT
KO

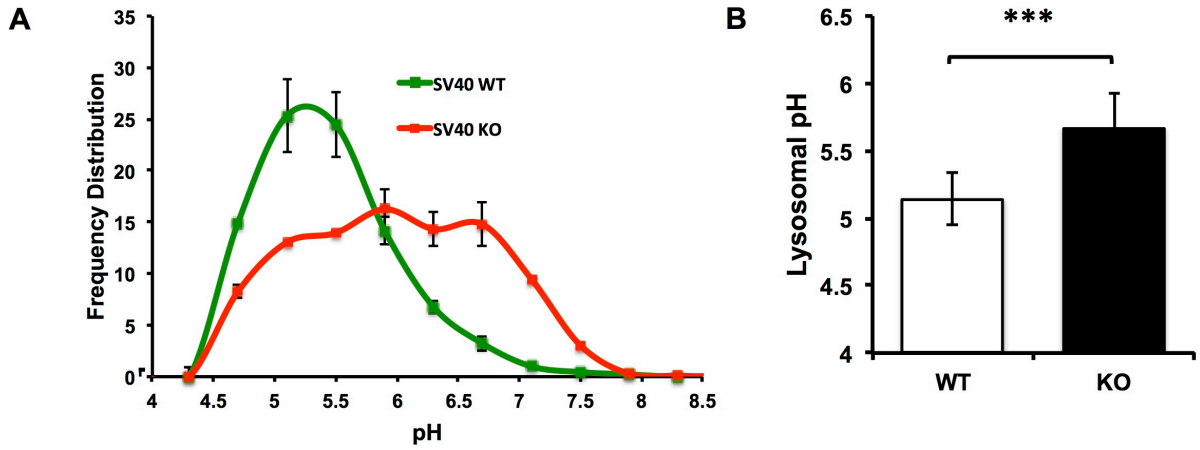

Figure 3.13: sAC regulates lysosomal pH in independently derived SV40 MEFs **(A)** WT and KO SV40 MEFs were loaded with fluorescein-rhodamine-dextran for 16 h followed by a 4-h chase. Frequency distribution of lysosomal pH in WT (green curve) and sAC KO (red curve). Number of lysosomes counted; WT=904, KO =1089, n=6, 2 independent experiments. Error bars represent the SEM. **(B)** Average lysosomal pH in WT and KO SV40 MEFs. All values are given as mean ± SEM. *** for $p<0.001$.

3.2.4 sAC regulates acidification by ensuring proper V-ATPase localization to lysosomes

Lysosomal acidification is dependent upon proper assembly of the proton pumping V-ATPase on the lysosomal membrane as well as regulation of counter ion conductance (Marshansky & Futai, 2008a; Mindell, 2012; Pillay et al, 2002; Steinberg et al, 2010; Xu & Ren, 2015) Because sAC was previously shown to be responsible for pH dependent movements of V-ATPase (Pastor-Soler et al, 2003; Tresguerres et al, 2010b), we asked whether the acidification defect in sAC KO cells might be due to improper V-ATPase localization. The V-ATPase is comprised of multiple subunits

which form two domains, the transmembrane V0 domain and the cytoplasmic V1 domain. To assess V-ATPase localization on lysosomes, we performed double-immunofluorescence labeling of the lysosomal marker LAMP2 with either of two different V1 domain subunits, V1D or V1B2. Protein levels of both V1D and V1B2 were unchanged in WT versus sAC KO cells (Fig. 3.14A). In WT cells, both V1D (Fig. 3.14B) and V1B2 (Fig. 3.14C) colocalized with LAMP2-positive vesicles. In contrast, in sAC KO cells, immunolabeling by both V-ATPase subunit antibodies was diffusely distributed throughout the cytoplasm which did not specifically colocalize with LAMP2. To determine whether this altered staining pattern correlated with the acidification defect, we assessed V-ATPase subunit localization under conditions which rescued the lysosomal acidification in sAC KO cells. Addition of membrane permeable cAMP for 1 hour, which rescued the phenotypic defect in sAC KO cells (Figs. 3.8B and 3.12E,F), restored LAMP2 colocalization with both V-ATPase V1D (Fig. 3.14B) and V1B2 subunits (Fig. 3.14C). Thus, sAC generated cAMP is responsible for proper localization of V-ATPase subunits and acidification of lysosomes.

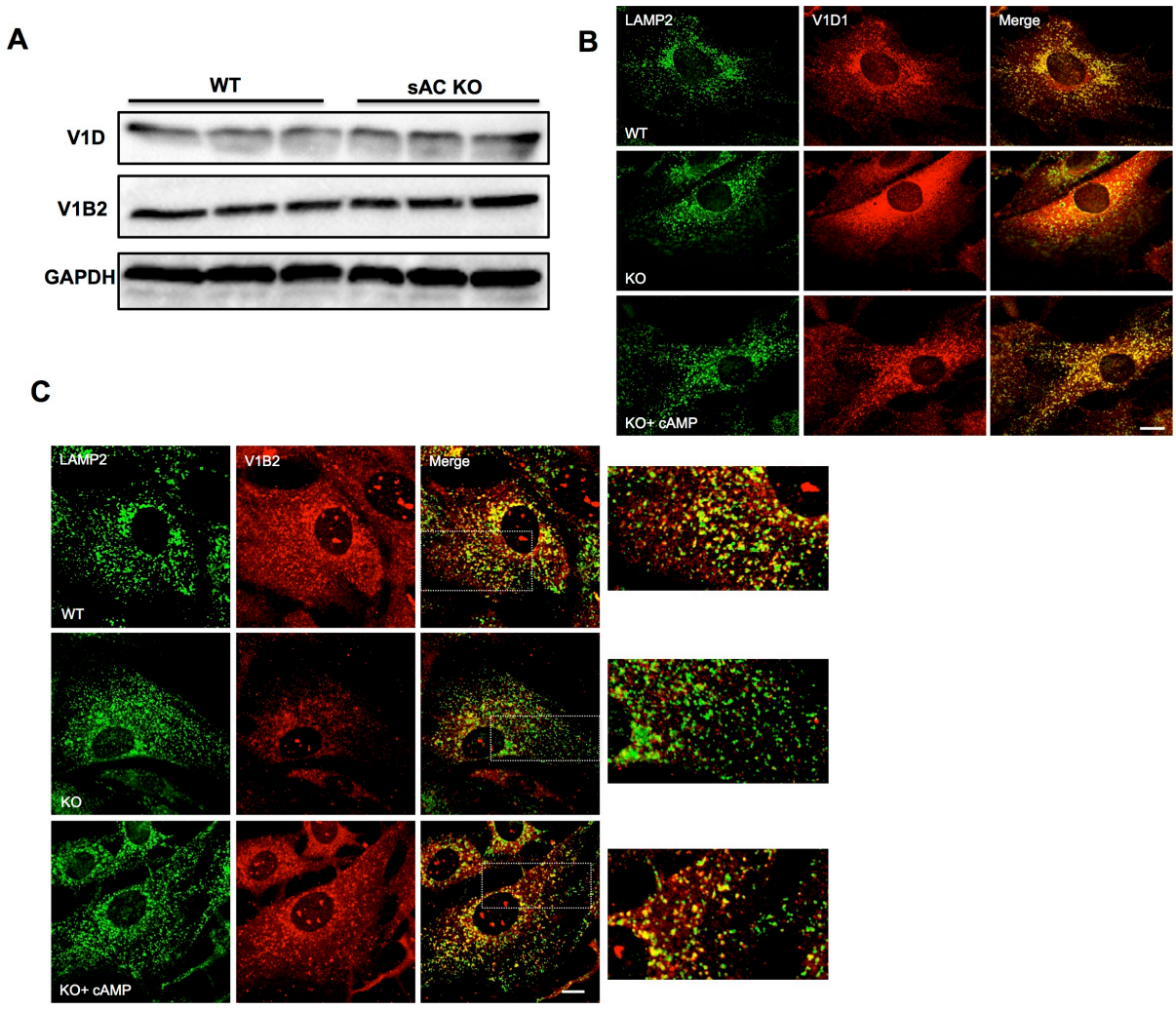

Figure 3.14: sAC regulates V-ATPase localization to lysosomes. **(A)** Representative immunoblot of the V-ATPase subunits, V1D and V1B2 along with GAPDH, which was used for loading control. Shown are whole cell extracts from three independently grown cultures of WT and sAC KO MEFs. n=3. **(B)** Double-immunofluorescence labeling of v-ATPase V1D subunit (red) and LAMP-2 (green) in WT MEFs, sAC KO MEFs, and sAC KO MEFs treated with 500 μM sp-8-cpt-cAMP for 1 hr. Scale bar 10 μm. **(C)** Double-immunofluorescence labeling of v-ATPase V1B2 subunit (red) and LAMP-2 (green) in WT MEFs, sAC KO MEFs, and sAC KO MEFs treated with 500 μM sp-8-cpt-cAMP for 1 hr. Scale bar 10 μm. Shown at right are higher magnification views of boxed areas highlighting colocalization.

3.3 Discussion

Our results demonstrate that sAC activity is essential for proper lysosomal acidification. We also show that organellar pH is dependent upon cytoplasmic HCO_3^-. When cells are grown in the absence of extracellular CO_2/HCO_3^-, blocking generation of intracellular HCO_3^- by inhibiting CAs diminished organellar acidification. The level of organellar acidification in the absence of intracellular HCO_3^- was similar to the levels observed in the absence of sAC, and it was rescued by cAMP, the product of sAC. These data suggest that cytoplasmic HCO_3^- affects organellar acidification by regulating sAC activity. It remains to be seen whether organellar acidification is mediated by local fluctuations in intracellular HCO_3^- and sAC activity. It is tempting to hypothesize that when protons enter a lysosome, they leave behind a local elevation of HCO_3^- which stimulates cytoplasmic sAC in the vicinity of acidifying lysosomes.

Our data also reveal that sAC regulates lysosomal acidification by ensuring proper V-ATPase localization to lysosomes. In addition to the proton pumping V-ATPase, lysosomal acidification is dependent upon counter ion transporters to dissipate the resultant membrane potential, and in microglia, cAMP facilitates lysosomal acidification by stimulating trafficking of a counter ion transporter (Majumdar et al, 2011). In addition to being responsible for proper V-ATPase localization, it remains possible sAC-generated cAMP facilitates acidification by increasing lysosomal localization, or activity, of counter ion transporters.

Increased localization of V1 subunits to the lysosome regulating lysosomal acidification is an evolutionarily conserved mechanism. Lysosomes in resting dendritic cells have a relatively alkaline pH. Upon immune activation, V1 subunits assemble on the lysosome leading to enhanced acidification and antigen proteolysis (Trombetta et al, 2003). Interestingly, in dendritic cell-like microglia cells, activation-induced acidification of lysosomes is mediated by cAMP (Majumdar et al, 2007). In the yeast, *Saccharomyces cerevisiae*, activity of the V-ATPase is regulated by a well-characterized, reversible dissociation/association of the cytoplasmic V1 and transmembrane V0 domains. Association of V1 and V0 domains on the yeast degrative acidic organelle is induced by elevated intracellular HCO_3^- (Dechant et al, 2010). Because the single adenylyl cyclase in yeast is HCO_3^- stimulated (Hess et al, 2014), similar to sAC, it is tempting to hypothesize that yeast adenylyl cyclase participates in the HCO_3^- induced V1 assembly, and V1 assembly on the lysosome is the mechanism of sAC-mediated lysosomal acidification.

As a consequence of aging, post-mitotic cells, such as neurons, have decreased lysosomal proteolytic activity thought to be caused by elevated lysosomal pH (Martinez-Vicente et al, 2005). Aberrant intracellular accumulation of AVs due to lysosomal dysfunction is also a common phenotype shared by lysosomal storage disorders and age-related neurodegenerative diseases, such as Alzheimer's Disease, Parkinson's disease and frontotemporal dementia (Bahr & Bendiske, 2002b), similar to the phenotype we observe in sAC KO mice. Interestingly, addition of cAMP to human Alzheimer's Disease fibroblasts reacidifies their lysosomes and

rescues their autophagic defect (Coffey et al, 2014), suggesting sAC activation may have therapeutic potential for these pathophysiological conditions.

CHAPTER FOUR: DISCUSSION AND CONCLUSION

4.1 Overview:

Lysosomes contribute to variety of cellular functions and the pH of the lysosomal lumen is critical in many of these functions. In addition to controlling the activity of lysosomal proteases for efficient degradation delivered through the endocytic, autophagic and phagocytic pathways, lysosome acidification is also required for fusion with autophagosomes and the release of calcium into the cytosol. Disruptions of either steady-state lysosomal pH or mechanisms that regulate lysosomal pH are thought to underlie many pathological conditions.

Loss of function of specific lysosomal enzymes leads to lysosomal storage diseases; these diseases can have diverse pathologies and commonly appear early in life and often associated with severe neurodegeneration. Lysosomal defects that effect lysosomal function less profoundly have been associated with adult-onset neurodegeneration. The regulation of lysosomal pH is one of the factors contributing to these neurodegenerative symptoms. Correct acidification of the lysosomes is thus critical for the health of the cell.

Maintaining lysosomal pH requires an electrogenic proton pumping V-ATPase as well as the coordinated actions of counter ions. Mutations within these proteins affecting lysosomal pH reveal the critical importance of proper lysosomal pH and the

particular vulnerability of post mitotic cells, such as the neurons and retinal pigmented epithelium (RPE), to pH perturbations.

As more attention is being paid to the importance of lysosomal pH in neurodegeneration and other diseases, ability to measure lysosomal pH reliably has become increasingly important. New commercial dyes are available to measure pH of acidic organelles with each having their own pros and cons. These reagents have been reviewed in detail (Wolfe et al, 2013),(Guha et al, 2014). Accurate measurement of lysosomal pH can be complex and imprecise measurements have clouded the field. Below, I discuss the two reagents used in this study to measure lysosomal pH and assess their specificity for lysosomes and sensitivity for accurately measuring the acidic pH values found in lysosomes.

4.2 Measurement of lysosomal pH

4.2.1 LysoTracker

LysoTracker can be used for qualitative measurement of acidic organelles including lysosomes in live and fixed cells. LysoTracker is a lipophilic dye containing a fluorophore conjugated to a weak amine that once inside an acidic organelle will be protonated and fluoresce. This property allows LysoTracker to freely permeate inside cells and selectively accumulate inside acidic organelles, such as lysosomes, autophagolysosomes and late endosomes. However, there are certain caveats

associated with using LysoTracker. LysoTracker is also a single wavelength dye and changes in the amount of emitted light can arise due to increased organellar pH or increased area/number of these organelles. LysoTracker staining will also be influenced by concentration of the dye being loaded and cell culture conditions.

LysoTracker stained cells can be fixed in paraformaldehyde and studied without a significant loss of fluorescence signal (Raben et al, 2009); however, it has also been reported that fixation might result in weakening the LysoTracker signal (Wolfe et al, 2013). The advantage of fixing is that the signal can be studied in concert with a compartment-specific probe, such as LAMP-2 to identify lysosomes. LysoTracker is not a substitute for a quantitative measurement of lysosomal pH.

Among its advantages, LysoTracker is cheap, readily available and simple to use, in both live and fixed cells. LysoTracker also has the advantage of providing a "snapshot in time" of all acidic organelles in a population of cells. LysoTracker staining is particularly useful to look for changes in the overall pattern of acidic organelles. Thus, a particularly useful application of LysoTracker staining is as a first-pass assay to determine abnormalities in vesicular pH in the presence and absence of pharmacological/genetic manipulations. Additionally, the high signal-to-noise ratio of the dye, its ease of use (cells or tissues can simply be immersed), its ability to be fixed and the endurance of the fluorophore, make the use of LysoTracker particularly well-suited for large screening of cells and tissues that may exhibit organellar acidification defects. In our studies, we have shown that sAC KO cells have

decreased LysoTracker positive puncta compared to WT and KO cells under both live and fixed conditions (**Fig 3.7A,B and 3.8B**) confirming that the dye works reliably under both settings.

LysoTracker can also be used to examine the efficiency of autophagosome/lysosome fusion in live cells (Gonzalez-Polo et al., 2005). Our data show that sAC KO cells have a lysosomal acidification defect. However, it does not differentiate between improper lysosomal acidification or improper maturation of autophagosomes to autophagolysosomes. To determine whether fusion is impaired, further studies needs to be done to colocalize LC3 (a marker for autophagy) with LysoTracker containing organelles. Further studies can use a tfLC3 (tandem fluorescent tagged LC3) (Kimura et al, 2009). This assay is based on the nature of the fluorescent signal of GFP, which is quenched in an acidic environment, whereas the red fluorescent protein (RFP) is not. LC3 tandemly tagged with GFP and RFP shows both GFP and RFP signals before fusion with the lysosome, but once the maturation to an autolysosome occurs, it only exhibits the RFP fluorescence. Therefore, the appearance of puncta with only RFP signals would suggest normal autophagic maturation.

4.2.2 Fluorescein/Rhodamine Dextran

Lysosomal acidification can also be measured quantitatively using pH-sensitive probes. Commonly used probes include Oregon Green® 488, as well as proprietary probes specifically designed to measure lysosomal pH, such as LysoSensor yellow/blue and pHrodo (Life Technologies). While the availability of all these different pH sensitive probes may benefit the studies of organellar acidification, in reality different labs have yielded different results depending on the probe used, making the field of studying lysosomal acidification a little confusing.

A probe commonly used to measure lysosomal pH is Oregon Green® 488 (pKa ~4.7) as optimum sensitivity is achieved when the pKa of the sensor matches the pH of the compartment being investigated. However, Oregon Green® 488 does not have the ability to measure pH via ratiometric measurement, meaning this dye requires co-labeling with another, pH–insensitive fluorophore. LysoSensor yellow/blue–dextran (pKa ~4.2) is another reagent commonly used to measure lysosomal pH. This probe has the advantage of having two probes allowing for ratiometric assay for lysosomal pH. As LysoSensor is a proprietary probe, the structure of this probe is not known.

The pH sensitive probe used in my studies to measure lysosomal acidification was Dextran beads tagged to pH sensitive fluorescein and pH-insensitive Tetramethylrhodamine, 70,000 MW (Life Technologies) (**Fig 3.10**). The large dextran group encourages endocytosis of the probe, and it is important to note that cells were

pulsed with the probe overnight (to ensure high probe signal) and then chased the next day for at least 4 hours. Fluorescein has a pKa of ~6.2 and it is thought to be less ideal for the pH range found in healthy lysosomes (~4.8). Yet pH sensitive fluorescein and pH-insensitive Tetramethylrhodamine probe has also been used successfully to measure lysosomal pH (Majumdar et al, 2007),(Majumdar et al, 2011),(Hayward et al, 2006),(Sturgill-Koszycki & Swanson, 2000), since our hypothesis was that sAC KO lysosomes had an alkaline pH, we wanted to use a probe that would accurately measure elevated lysosomal pH. In my experiments, when I added exogenous cAMP to WT cells, I did not observe a decrease in lysosomal pH, as previously reported by (Liu et al, 2012). It is possible that my experiments were measuring the lowest pH of the particular probe used, and hence, I was unable to distinguish a change in pH at lower pH values.

4.3 sAC as a bicarbonate/pH sensor

Acid-base homeostasis is essential for the survival of a cell. The cytoplasm of a cell is constantly being acidified by cellular metabolism (i.e., generation of CO_2) and the negative resting potential is conducive to influx of protons inside the cell. This poses a challenge for the cell to maintain its intracellular pH. Homeostasis of the cytosol thus will depend on the intracellular bicarbonate, weak acids/bases and macromolecules, such as proteins with their ability to bind protons. A number of different transporters/channels will also act in response to fluctuations of both intra

and extracellular pH, and they will respond to maintain intracellular pH. In eukaryotic cells, which contain compartmentalized organelles, the membranes of distinct organelles are also equipped with channels and transporters to maintain proper luminal pH. Although several studies have established the machinery needed to modulate intra-organellar pH, the mechanism by which cells/organelles sense fluctuations in pH is not understood, i.e. a physiological intracellular pH sensor is missing.

To serve as an efficient intracellular pH sensor, the candidate molecule must be able to detect pH changes within a physiologically relevant range and initiate a signaling cascade to activate an effect that maintains pH homeostasis. It is tempting to postulate sAC as a putative intracellular pH sensor because of its ability to be stimulated by physiological concentration of bicarbonate (sAC has an EC_{50}=11mM (Litvin et al, 2003); calculated intracellular bicarbonate levels are 8-15 mM). Indirectly sensing pH via bicarbonate has two advantages over direct proton sensing. First, because H^+ readily bind to macromolecules, their diffusion though a cytoplasm is slow due to the high concentration of proteins and other macromolecules inside cells. In contrast, the presence of CO_2, HCO_3^- and carbonic anhydrase (CA) in the cytoplasm accelerates the diffusion of H^+ across the cytosol by 2-5 fold, revealing a H^+ gradient moving through out a cell is dependent on changes in CO_2 and HCO_3^- {Levin, 2015 #848}. Second, CO_2 and H_2O are the major end product of energy producing pathways, representing the most fundamental catabolite that needs to be expelled from the cell. CO_2 and H_2O equilibrate instantaneously with HCO_3^- and H^+ in

the presence of CA. Thus in the presence of CA, changes in pH are instantaneously and locally reflected as changes in HCO_3^- and CO_2, allowing pH to be measured indirectly in a timely manner.

sAC's role as a pH sensor was first described in the clear cells of the epididymis (**Figure 4.1**) {Pastor-Soler, 2003 #9}. Sperm are made in the testis and stored in a quiescent state in the cauda of the epididymis. The dormant state of the sperms is achieved due to the cauda being kept at a low pH (6.5 - 6.8, compared to cytosol pH (7.2 - 7.4)) and a low bicarbonate level 2-7 mM (as opposed to 25 mM found in almost all other extracellular fluids). The clear cells of the epididymis are responsible for maintaining the desired low pH and low bicarbonate levels of the cauda. These cells express abundant sAC and V-ATPase. When the luminal pH of the causa epididymis is elevated, sAC in the clear cells is activated in a CA-dependent manner and sAC generated cAMP promotes reacidification of the lumen by increased trafficking of the proton pumping V-ATPase to the clear cell apical membrane (Pastor-Soler et al, 2003),(Pastor-Soler et al, 2008).

sAC dependent V-ATPase trafficking also plays an important role in the proximal tubule of the kidney collecting duct where it is essential for maintaining the acid/base balance in the blood. sAC is found to be in a complex with the V-ATPase (Paunescu et al, 2008b), and here too, V-ATPase translocation is mediated by sAC, in a CA dependent manner (Pastor-Soler et al, 2003; Pastor-Soler et al, 2008). This pH dependent signaling is evolutionarily conserved; a similar mechanism, involving

CA, sAC and V-ATPase, is also responsible for organismal pH homeostasis in dogfish shark (Tresguerres et al, 2010c). Thus, because sensing and regulating pH via sAC-dependent V-ATPase mobilization is a common mechanism, we postulated that the HCO_3^--sAC-V-ATPase is a conserved physiological pH sensor signaling complex that functions to regulate the pH of intracellular compartments. While much has been learned about the channels/transporters contributing to acidification of the lysosomes, sAC would represent the first pH-sensitive signaling enzyme contributing to setting lysosomal pH under normal conditions.

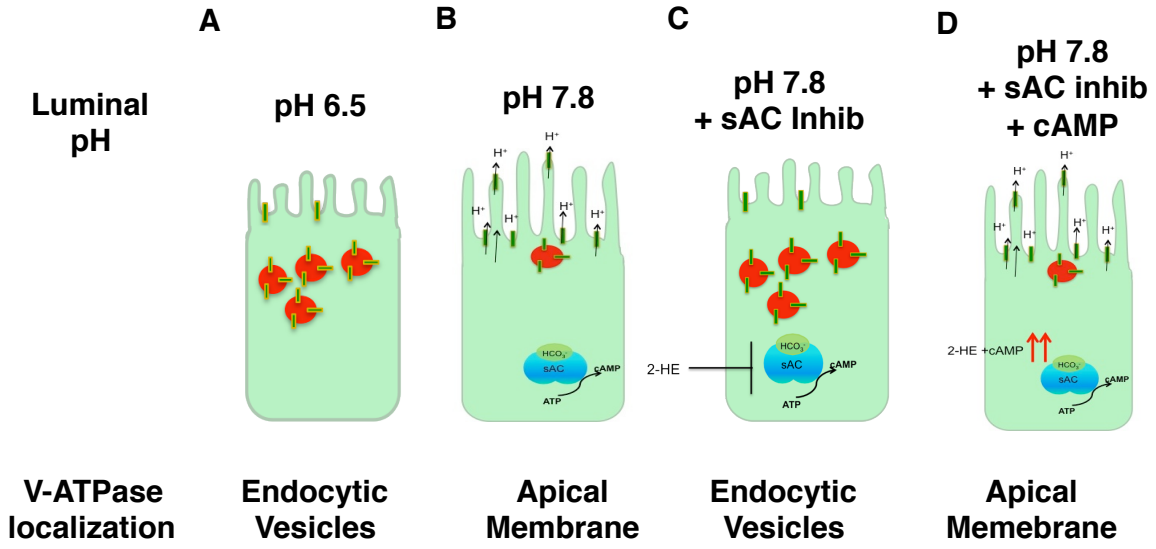

Figure 4.1: Role of sAC in V-ATPase localization in the clear cells from the epididymis. Cells were perfused with PBS at pH 6.5 or pH 7.8 in the presence or absence of sAC inhibitors. **(A)** Majority of the V-ATPases are present in endocytic vesicles in the sub-apical region when luminal pH is at pH 6.5. **(B)** When luminal pH is increased to pH 7.8, V-ATPase are now located mainly in the apical membrane with fewer in the endocytic vesicles. **(C)** At pH 7.8, but in the presence of sAC inhibitor, 2-hydroxyestradiol, the density of V-ATPase in the apical membrane is reduced. Thus, inhibition of sAC prevents the high pH induced apical V-ATPase translocation. **(D)** At pH 7.8, but in the presence of the sAC inhibitor, 2-hydroxyestradiol and exogenous cAMP, the translocation of V-ATPase to the apical membrane is rescued.

4.4 Role of sAC in intra-vesicular acidification in the Endosomal-Lysosomal pathway

The endo-lysosomal system is central to the processes of autophagy and endocytosis (Klionsky, 2007; Mizushima, 2007), and recently a plethora of studies have shown its relevance in a broad range of diseases (Futerman & van Meer, 2004; Nixon et al, 2008). In all eukaryotic cells, endocytic trafficking of proteins/cargoes is associated with increasing acidification of the lumen of the endocytic organelles. Internalized materials pass from early to late endosomes and finally to lysosomes, where pH is maintained between 4 and 5 (Pillay et al, 2002). In post-mitotic cells, such as neurons, lysosomes become unstable over time, and decreased proteolytic activity of the lysosomes, probably due to elevated lysosomal pH, occurs as a consequence of aging (Martinez-Vicente et al, 2005; Rajawat et al, 2009; Terman et al, 2006). Age-related lysosomal dysfunction impairs autophagy resulting in accumulation of partially digested materials and protein aggregates. This is a common phenotype shared by lysosomal storage disorders (LSD) and age-related neurodegenerative diseases such as Alzheimer's Disease (AD), Parkinson's disease (PD) and frontotemporal dementia (FTD) (Bahr & Bendiske, 2002a). Interestingly, addition of cAMP to human Alzheimer's Disease fibroblasts re-acidifies their lysosomes and rescues their autophagic defect (Coffey et al., 2014).

cAMP has also been shown to modulate lysosomal pH in macrophages (Di et al, 2006), microglia (Majumdar et al, 2007) and retinal pigmented epithelium (RPE)

cells (Liu et al, 2008), but its source, the signals leading to its generation, and its mechanism of action are not yet known. Understanding the role of cAMP in lysosomal dysfunction impinges upon real life clinical scenarios. Over the past decade, it has become appreciated that age related neurodegeneration is dependent upon understanding lysosomal function (Nixon et al, 2008). Elevation of lysosomal pH results in accumulation of autophagic materials due to decreased activity of lysosomal cathepsins and reduced degradation of long-lived proteins and old organelles. The sharp pH dependence of lysosomal enzymes makes regulators of pH prime candidates for therapeutic intervention. However, it is still not clearly understood how lysosomal pH is regulated; specifically, we do not understand the role of cAMP in maintaining lysosomal pH.

Here we show that sAC activity is essential for proper lysosomal acidification both in the presence and absence of HCO_3^- buffered media. This is significant because the pre-dominant hypothesis is that bicarbonate concentration remains constant in a cell. However, this cannot be true. HCO_3^- concentrations must be higher near mitochondria where CO_2 is made. Levels of HCO_3^- concentration will also fluctuate depending on other organelles and metabolic processes (Martin et al, 2011; Tarbashevich et al, 2015). It is tempting to propose that during acidification as proton enters the lysosomal lumen due to pumping of the V-ATPase, CA equilibrate cytoplasmic CO_2, HCO_3^- and protons resulting in an increase in the cytoplasmic HCO_3^- which in turn would stimulate sAC.

4.5 Role of sAC in regulating V-ATPase activity in the Endosomal-Lysosomal pathway

As described above, acidification is a required component in the maturation of organelles in the endocytic pathway. There are also diverse acidic organelles present inside cells with different luminal pH. The regulation of luminal acidity is achieved by fine-tuning the composition of the V-ATPase structure depending on isoform composition (as discussed in Section 1.6) and by specific targeting of V-ATPase and/or other acidic machinery to the right organelle.

Reversible assembly/disassembly of V0 and V1 domains is an important mechanism of modulating the activity of V-ATPase. This was well characterized in yeast in response to glucose depletion and the kidney proximal tubule epithelial cells in mammals (Marshansky & Futai, 2008b). *In vivo* dissociation of the V-ATPase is also shown to be dependent on vacuolar luminal pH (Shao & Forgac, 2004), although the identity of the pH sensor controlling dissociation remains to be determined. This suggests that if the luminal pH is too alkaline, dissociation of V-ATPase is blocked. Such a mechanism makes sense as a way to prevent intracellular compartments from becoming too alkaline, which in the case of lysosomes, will result in accumulation of unwanted, undegraded proteins. Because Golgi has a more alkaline pH than lysosomes, this pH dependent dissociation may account for why the V-ATPase complex containing Stvp1 (which normally resides in the Golgi) show no

dissociation when localized to the Golgi but dissociates when targeted to the vacuole (Kawasaki-Nishi et al, 2001).

In mammalian renal epithelial cells, glucose effects on the V-ATPase are mediated by the direct interaction of aldoses (an enzyme in the glycolytic pathway) with the a-subunit from V0 domain and B and E from V1 domain. This interaction results in reversible assembly/disassembly of the V-ATPase. More importantly, reversible association of V-ATPase V1 domain has been demonstrated in mammalian dendritic cells. During maturation of these cells, increased V-ATPase assembly leads to increased lysosomal acidification, activation of proteases, protein degradation and antigen presentation (Trombetta et al, 2003). A similar phenomenon has also been observed in mice or patient fibroblasts carrying the presenilin (PS) mutation, a protein mutated in AD. PS1 -/- cells were found to have alkaline lysosomes due to mistargeting and disassembly of V1 and V0 domains (Lee et al, 2010).

As shown in **Fig 3.14**, we observe that sAC KO cells have decreased colocalization of V1 subunits with LAMP2 positive lysosomes compared to WT cells. This phenotype was rescued by the addition of exogenous cAMP suggesting that cAMP promoted trafficking of V1 subunits to lysosomes leading to increased assembly (**Figure 4.2)**.

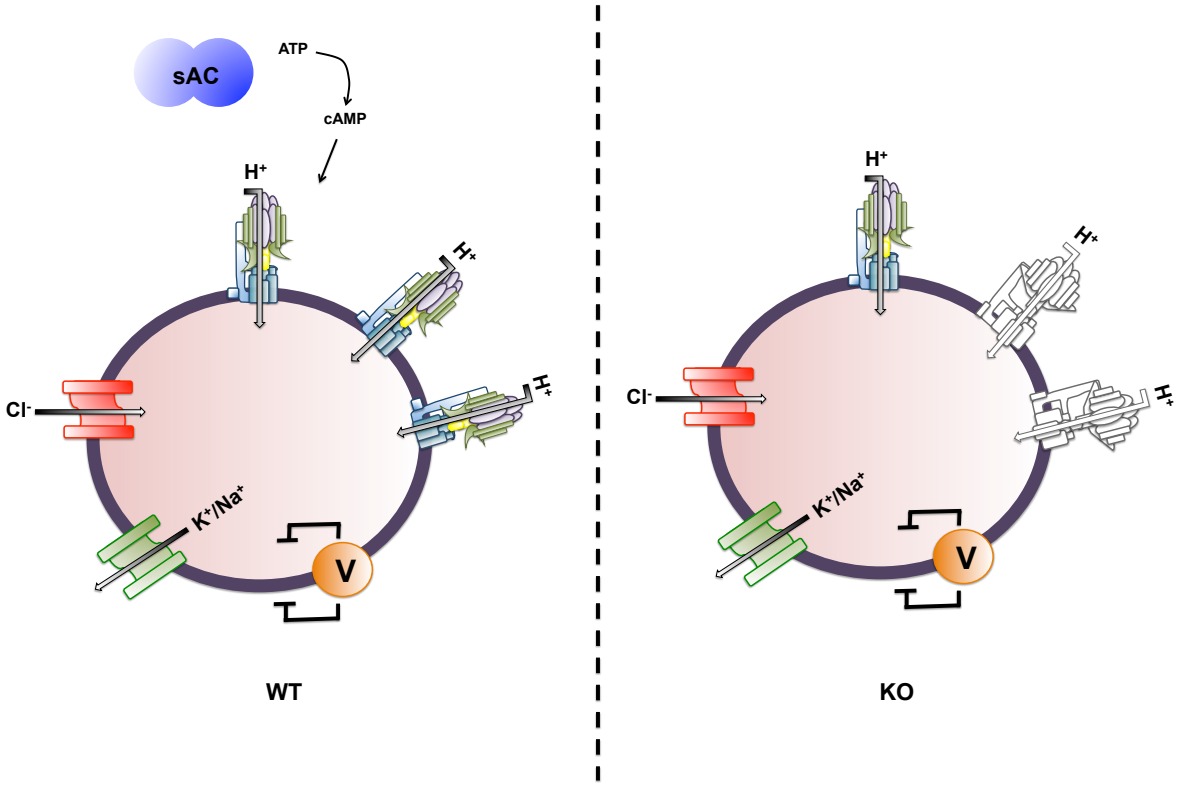

Figure 4.2: Proposed role of sAC mediated V-ATPase translocation into the lysosomal membrane to regulate lysosomal pH. Increased trafficking of the V-ATPase onto the lysosomes will result in increased proton pumping leading to the acidification of the lysosomes in WT lysosomes. In the sAC KO cells, the lysosomes have decreased number of V-ATPase resulting in reduced proton pumping and hence increased lysosomal pH

During normal endocytosis and maturation into lysosomes, a newly formed endosome may not have all the required machinery to fulfill its acidification state. How would a V1 domain properly assemble on to an endo/lysosomal organelle carrying a V0 domain in order to set its correct pH? Perhaps an upstream signal directs the proper assembly of the V-ATPase. This suggests a scenario where protons entering the endosomal lumen through a limited number of V-ATPases present at the membrane create a local elevation of bicarbonate. This local

bicarbonate elevation could increase sAC-generated cAMP, which would promote increased trafficking and assembly of V1/V0 in the endomembrane.

While this study has demonstrated a role of sAC-generated cAMP in mediating lysosomal acidification by regulating trafficking of V-ATPase, we were unable to distinguish whether the sAC KO cells have decreased lysosomal acidification because of a delay in the maturation pathway. I observed (**Fig 3.13**) a subset of lysosomes in the sAC KO cells were able to attain the pH of 4.7; however, the distribution of pH was much broader resulting in more lysosomes having an alkaline pH.

GTPases are a large family of hydrolase enzymes that bind and hydrolyze guanosine triphosphate (GTP) to GDP (guanosine diphosphate). The Ras superfamily of small GTPases function as molecular switches transitioning between the on and off states which is mediated by GTP/GDP cycle. The Arf protein belongs to this family and functions as a molecular switch to regulate vesicular trafficking and organellar structure. Activation of Arf (GTP-bound state, on state) is mediated by GEFs (guanine exchange factor), while deactivation (GDP-bound state, off state) is catalyzed by GAPs (GTPase activating protein). Both Arf6 and its cognate GEF and GAP have been implicated in regulation of the endocytic pathway and organelle biogenesis (Donaldson & Klausner, 1994).

Recent studies have shown that V-ATPase colocalizes with small GTPases in early endosomes in a pH- dependent manner. This interaction is crucial for protein

trafficking between early to late endosomes/lysosomes. Although the interaction allows V-ATPase along with GTPases to modulate vesicle trafficking, it is not known what the upstream signal is. There is a possibility that sAC-mediated trafficking of V-ATPase and the interaction between V-ATPase and GTPases allow for the proper maturation and acidification through the endosomal pathway.

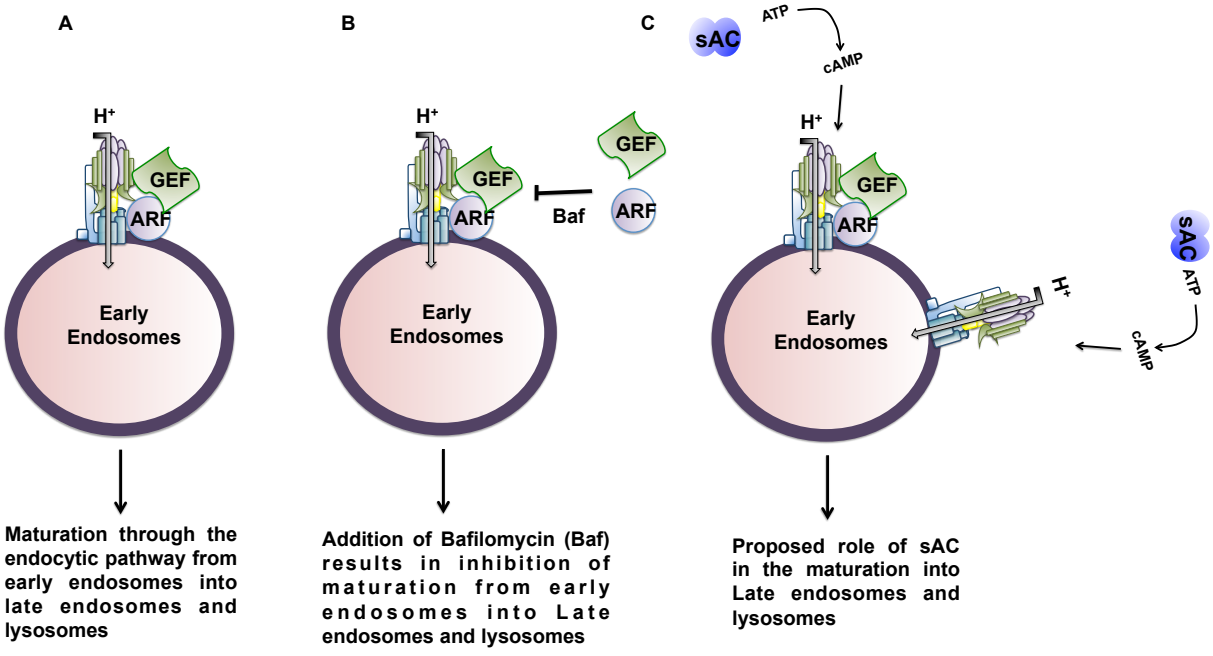

Figure 4.3: Proposed role of sAC in the endocytic pathway as early endosomes mature into late endosomes/lysosomes. (A) Interaction of Arf along with its cognate GEF with V-ATPase in the early endosomes allow for maturation of the early endosomes into late endosomes/lysosomes. (B) Addition of Bafilomycin (Baf), an inhibitor of V-ATPase (which inhibits proton pumping, resulting in alkalization) prevents binding of ARF and GEF. (C) One proposed mechanism of sAC is to increase V-ATPase translocation to enable proper acidification of the early endosomes for maturation through the endocytic pathway.

In kidney physiology, a second place where the CA, sAC and V-ATPase was found to be conserved, proximal tubule epithelial cells play an important role in protein homeostasis via reabsorption of albumin, hormones, chemokines and other low molecular weight proteins. This pathway was found to be dependent on endosomal acidification, with defects in acidification leading to proximal tubulopathies in humans and mice. It has been postulated that the a subunit of the V-ATPase itself is the proton sensor. As V-ATPase in the early endosome acidifies the lumen, it signals the Arf6 and ARNO (GEF) to bind to the early endosomal membrane leading to the 'on' molecular switch. This in turn starts the transition of the early endosomes to late endosomes. This scenario makes sense when the V-ATPase is assembled and active.

4.6 Role of sAC in regulating counter-ion conductance

While sAC seems to regulate lysosomal pH by increased V-ATPase assembly, it does not exclude a role for sAC modulating counterion channels as well. V-ATPase is an electrogenic pump. As protons enter the lumen, a positive potential builds up that will inhibit further proton translocation. This is balanced either by influx of anions like Cl^- into or an efflux of cations, such as Na^+, K^+, or $Ca^{2+,}$ from the lysosomal lumen. Studies by Majumdar et al (Majumdar et al, 2007),(Majumdar et al, 2011) have suggested that cAMP activated PKA can regulate trafficking of CLC-7 (a $2Cl^-/H^+$

exchanger) into lysosomes to increase acidification in microglia. It is not yet known whether the source of cAMP that regulates CLC-7 trafficking is sAC (**Figure 4.4)**.

Another place where sAC can play role in lysosomal acidification is the efflux of cations from the lysosomal lumen. The lysosomal lumen is hyperpolarized due to protons being pumped inside by the V-ATPase. This can lead to an opening of a putative voltage gated channel that can efflux cations from the lumen thus releasing the membrane potential (**Figure 4.4**). The hyperpolarization-activated cyclic nucleotide-gated channels (HCNs) (Biel et al, 2009; Wahl-Schott & Biel, 2009) represent such a putative channel. HCNs open in response to change in membrane voltage, while cAMP binding serves to modulate the open probability of HCN channels.

TRPML1 (transient receptor potential cation channel, mucolipin subfamily) has also been shown to be present in the lysosomes (Mindell, 2012). TRP have been shown to be permeable to both sodium and/or calcium {Venkatachalam, 2015 #1126}. It is plausible that the TRP channel present in the lysosomes is a non-selective cation channel. This will allow the lysosome to efflux extra positive cations and allow lysosomes to properly acidify.

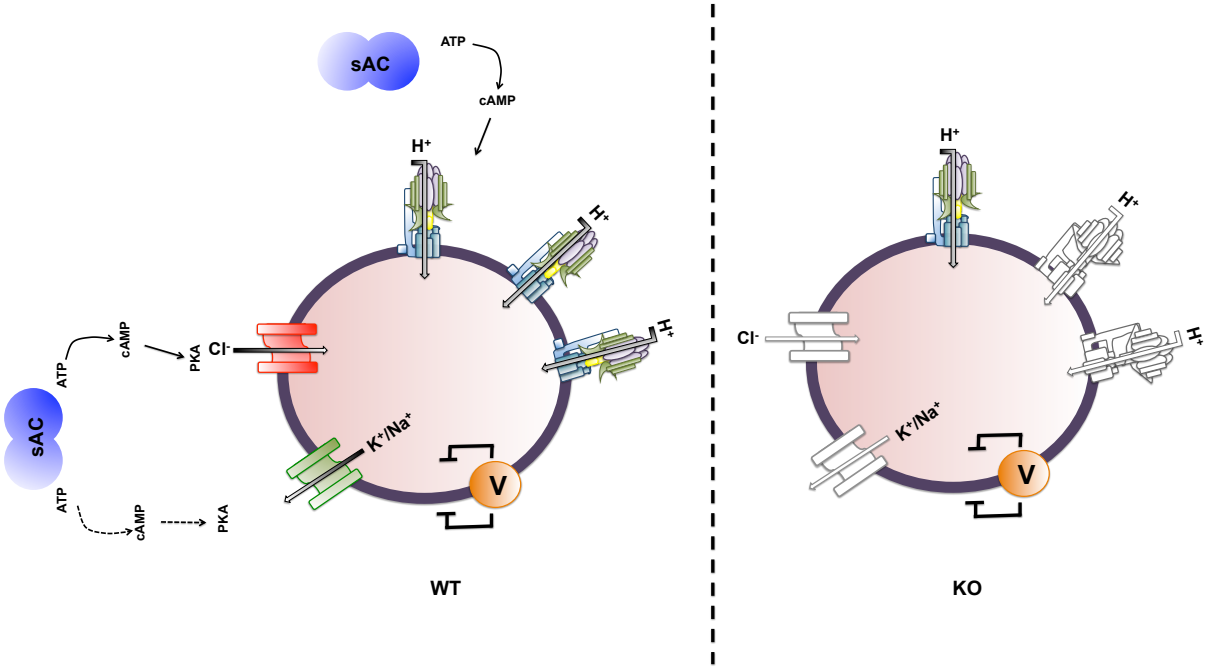

Figure 4.4: Proposed role of sAC in mediating counterion conductance to regulate lysosomal pH. In WT cells, sAC might play a role in the trafficking on cAMP mediated CLC-7 into the lysosomes resulting in an acidic lysosomal pH. A putative role of sAC might also be present in regulating cation efflux from the lysosomes.

4.7 Future Directions

The recognition of sAC's role in regulating lysosomal pH suggests additional physiological processes that merit investigation. For example, it will be interesting to see whether sAC KO mice exhibit increased age-dependent neurodegeneration and behavioral deficit due to lysosomal defects, or whether their vision is affected by lysosomal defects in the RPE. Equally important will be to determine how sAC regulates V-ATPase trafficking to intracellular organelles.

Acidity of lysosomes is closely tied to mechanisms of cellular aging and mitochondrial function (Hughes & Gottschling, 2012). Acidification of a yeast vacuole can affect the function of its mitochondria and thus the life span of the cell. After budding, the mother cell demonstrated an alkaline pH in the vacuole compared to the daughter cell and this decreased in acidity correlated with decreased mitochondrial functions. Restoration of the pH of the yeast vacuole extended the yeast life span.

4.8 Conclusions

In summary, I demonstrate in this thesis that CO2/HCO3-/pH sensing soluble adenylyl cyclase (sAC) regulates lysosomal pH by modulating trafficking of V-ATPase subunits to the lysosomes.

REFERENCES

Acin-Perez R, Gatti DL, Bai Y, Manfredi G (2011) Protein phosphorylation and prevention of cytochrome oxidase inhibition by ATP: coupled mechanisms of energy metabolism regulation. *Cell Metab* 13: 712-719

Acin-Perez R, Salazar E, Kamenetsky M, Buck J, Levin LR, Manfredi G (2009a) Cyclic AMP produced inside mitochondria regulates oxidative phosphorylation. *Cell Metab* 9: 265-276

Acin-Perez R, Salazar E, Kamenetsky M, Buck J, Levin LR, Manfredi G (2009b) Cyclic AMP produced inside mitochondria regulates oxidative phosphorylation. *Cell Metab* 9: 265-276

Altarescu G, Sun M, Moore DF, Smith JA, Wiggs EA, Solomon BI, Patronas NJ, Frei KP, Gupta S, Kaneski CR, Quarrell OW, Slaugenhaupt SA, Goldin E, Schiffmann R (2002) The neurogenetics of mucolipidosis type IV. *Neurology* 59: 306-313

Andrejewski N, Punnonen EL, Guhde G, Tanaka Y, Lullmann-Rauch R, Hartmann D, von Figura K, Saftig P (1999) Normal lysosomal morphology and function in LAMP-1-deficient mice. ***J Biol Chem*** **274: 12692-12701**

Auteri JS, Okada A, Bochaki V, Dice JF (1983) Regulation of intracellular protein degradation in IMR-90 human diploid fibroblasts. ***J Cell Physiol*** **115: 167-174**

Bae HR, Verkman AS (1990) Protein kinase A regulates chloride conductance in endocytic vesicles from proximal tubule. ***Nature*** **348: 637-639**

Bahr BA, Bendiske J (2002a) The neuropathogenic contributions of lysosomal dysfunction. ***J Neurochem*** **83: 481-489**

Bahr BA, Bendiske J (2002b) The neuropathogenic contributions of lysosomal dysfunction. ***J Neurochem*** **83: 481-489**

Bainton DF (1981) The discovery of lysosomes. ***J Cell Biol*** **91: 66s-76s**

Beaulieu V, Da Silva N, Pastor-Soler N, Brown CR, Smith PJ, Brown D, Breton S (2005) Modulation of the actin cytoskeleton via gelsolin regulates vacuolar H+-ATPase recycling. ***J Biol Chem*** **280: 8452-8463**

Berkovic SF, Dibbens LM, Oshlack A, Silver JD, Katerelos M, Vears DF, Lullmann-Rauch R, Blanz J, Zhang KW, Stankovich J, Kalnins RM, Dowling JP, Andermann E, Andermann F, Faldini E, D'Hooge R, Vadlamudi L, Macdonell RA, Hodgson BL, Bayly MA, Savige J, Mulley JC, Smyth GK, Power DA, Saftig P, Bahlo M (2008) Array-based gene discovery with three unrelated subjects shows SCARB2/LIMP-2 deficiency causes myoclonus epilepsy and glomerulosclerosis. ***Am J Hum Genet*** **82: 673-684**

Biel M, Wahl-Schott C, Michalakis S, Zong X (2009) Hyperpolarization-activated cation channels: from genes to function. ***Physiol Rev*** **89: 847-885**

Bitterman JL, Ramos-Espiritu L, Diaz A, Levin LR, Buck J (2013a) Pharmacological distinction between soluble and transmembrane adenylyl cyclases. ***J Pharmacol Exp Ther*** **347: 589-598**

Bitterman JL, Ramos-Espiritu L, Diaz A, Levin LR, Buck J (2013b) Pharmacological distinction between soluble and transmembrane adenylyl cyclases. ***J Pharmacol Exp Ther*** **347: 589-598**

Bjorkoy G, Lamark T, Brech A, Outzen H, Perander M, Overvatn A, Stenmark H, Johansen T (2005) p62/SQSTM1 forms protein aggregates degraded by autophagy and has a protective effect on huntingtin-induced cell death. ***The Journal of Cell Biology*** **171: 603-614**

Bos JL (2003) Epac: a new cAMP target and new avenues in cAMP research. ***Nat Rev Mol Cell Biol*** **4: 733-738**

Braulke T, Bonifacino JS (2009) Sorting of lysosomal proteins. ***Biochim Biophys Acta*** **1793: 605-614**

Braun AP (2008) Identification of ClC-7 as a major pathway for Cl- movement in lysosomes. ***Channels (Austin)*** **2: 309**

Braun T, Dods RF (1975) Development of a Mn-2+-sensitive, "soluble" adenylate cyclase in rat testis. ***Proc Natl Acad Sci U S A*** **72: 1097-1101**

Braun T, Frank H, Dods R, Sepsenwol S (1977) Mn2+-sensitive, soluble adenylate cyclase in rat testis. Differentiation from other testicular nucleotide cyclases. *Biochim Biophys Acta* 481: 227-235

Breton S, Brown D (2013) Regulation of luminal acidification by the V-ATPase. *Physiology (Bethesda)* 28: 318-329

Bright NA, Gratian MJ, Luzio JP (2005) Endocytic delivery to lysosomes mediated by concurrent fusion and kissing events in living cells. *Curr Biol* 15: 360-365

Buck J, Levin LR (2011) Physiological sensing of carbon dioxide/bicarbonate/pH via cyclic nucleotide signaling. *Sensors (Basel)* 11: 2112-2128

Buck J, Sinclair ML, Levin LR (2002) Purification of soluble adenylyl cyclase. *Methods Enzymol* 345: 95-105

Buck J, Sinclair ML, Schapal L, Cann MJ, Levin LR (1999) Cytosolic adenylyl cyclase defines a unique signaling molecule in mammals. *Proc Natl Acad Sci U S A* 96: 79-84

Bundey RA, Insel PA (2004) Discrete intracellular signaling domains of soluble adenylyl cyclase: camps of cAMP? *Sci STKE* 2004: pe19

Calcraft PJ, Ruas M, Pan Z, Cheng X, Arredouani A, Hao X, Tang J, Rietdorf K, Teboul L, Chuang KT, Lin P, Xiao R, Wang C, Zhu Y, Lin Y, Wyatt CN, Parrington J, Ma J, Evans AM, Galione A, Zhu MX (2009) NAADP mobilizes calcium from acidic organelles through two-pore channels. *Nature* 459: 596-600

Cang C, Bekele B, Ren D (2014) The voltage-gated sodium channel TPC1 confers endolysosomal excitability. *Nat Chem Biol* 10: 463-469

Cang C, Zhou Y, Navarro B, Seo YJ, Aranda K, Shi L, Battaglia-Hsu S, Nissim I, Clapham DE, Ren D (2013) mTOR regulates lysosomal ATP-sensitive two-pore Na(+) channels to adapt to metabolic state. *Cell* 152: 778-790

Canuel M, Bhattacharyya N, Balbis A, Yuan L, Morales CR (2009) Sortilin and prosaposin localize to detergent-resistant membrane microdomains. *Exp Cell Res* 315: 240-247

Chaloupka JA, Bullock SA, Iourgenko V, Levin LR, Buck J (2006) Autoinhibitory regulation of soluble adenylyl cyclase. *Mol Reprod Dev* 73: 361-368

Chang JC, Oude-Elferink RP (2014) Role of the bicarbonate-responsive soluble adenylyl cyclase in pH sensing and metabolic regulation. *Front Physiol* 5: 42

Chen J, Martinez J, Milner TA, Buck J, Levin LR (2013) Neuronal expression of soluble adenylyl cyclase in the mammalian brain. *Brain Res* 1518: 1-8

Chen X, Baumlin N, Buck J, Levin LR, Fregien N, Salathe M (2014) A soluble adenylyl cyclase form targets to axonemes and rescues beat regulation in soluble adenylyl cyclase knockout mice. *Am J Respir Cell Mol Biol* 51: 750-760

Chen Y, Cann MJ, Litvin TN, Iourgenko V, Sinclair ML, Levin LR, Buck J (2000) Soluble adenylyl cyclase as an evolutionarily conserved bicarbonate sensor. *Science* 289: 625-628

Choi HB, Gordon GR, Zhou N, Tai C, Rungta RL, Martinez J, Milner TA, Ryu JK, McLarnon JG, Tresguerres M, Levin LR, Buck J, MacVicar BA (2012) Metabolic communication between astrocytes and neurons via bicarbonate-responsive soluble adenylyl cyclase. *Neuron* 75: 1094-1104

Cipriano DJ, Wang Y, Bond S, Hinton A, Jefferies KC, Qi J, Forgac M (2008) Structure and regulation of the vacuolar ATPases. *Biochim Biophys Acta* 1777: 599-604

Coffey EE, Beckel JM, Laties AM, Mitchell CH (2014) Lysosomal alkalization and dysfunction in human fibroblasts with the Alzheimer's disease-linked presenilin 1 A246E mutation can be reversed with cAMP. *Neuroscience* 263: 111-124

Corredor RG, Trakhtenberg EF, Pita-Thomas W, Jin X, Hu Y, Goldberg JL (2012) Soluble adenylyl cyclase activity is necessary for retinal ganglion cell survival and axon growth. *J Neurosci* 32: 7734-7744

de Duve C (2005) The lysosome turns fifty. *Nat Cell Biol* 7: 847-849

Dechant R, Binda M, Lee SS, Pelet S, Winderickx J, Peter M (2010) Cytosolic pH is a second messenger for glucose and regulates the PKA pathway through V-ATPase. *EMBO J* 29: 2515-2526

Di A, Brown ME, Deriy LV, Li C, Szeto FL, Chen Y, Huang P, Tong J, Naren AP, Bindokas V, Palfrey HC, Nelson DJ (2006) CFTR regulates phagosome acidification in macrophages and alters bactericidal activity. *Nat Cell Biol* 8: 933-944

Di Benedetto D, Di Vita G, Romano C, Giudice ML, Vitello GA, Zingale M, Grillo L, Castiglia L, Musumeci SA, Fichera M (2013) 6p22.3 deletion: report of a patient with autism, severe intellectual disability and electroencephalographic anomalies. *Mol Cytogenet* 6: 4

Donaldson JG, Klausner RD (1994) ARF: a key regulatory switch in membrane traffic and organelle structure. *Curr Opin Cell Biol* 6: 527-532

Eskelinen EL, Schmidt CK, Neu S, Willenborg M, Fuertes G, Salvador N, Tanaka Y, Lullmann-Rauch R, Hartmann D, Heeren J, von Figura K, Knecht E,

Saftig P (2004) Disturbed cholesterol traffic but normal proteolytic function in LAMP-1/LAMP-2 double-deficient fibroblasts. *Mol Biol Cell* 15: 3132-3145

Esposito G, Jaiswal BS, Xie F, Krajnc-Franken MA, Robben TJ, Strik AM, Kuil C, Philipsen RL, van Duin M, Conti M, Gossen JA (2004a) Mice deficient for soluble adenylyl cyclase are infertile because of a severe sperm-motility defect. *Proc Natl Acad Sci U S A* 101: 2993-2998

Esposito G, Jaiswal BS, Xie F, Krajnc-Franken MA, Robben TJ, Strik AM, Kuil C, Philipsen RL, van Duin M, Conti M, Gossen JA (2004b) Mice deficient for soluble adenylyl cyclase are infertile because of a severe sperm-motility defect. *Proc Natl Acad Sci U S A* 101: 2993-2998

Farrell J, Ramos L, Tresguerres M, Kamenetsky M, Levin LR, Buck J (2008) Somatic 'soluble' adenylyl cyclase isoforms are unaffected in Sacy tm1Lex/Sacy tm1Lex 'knockout' mice. *PLoS One* 3: e3251

Forgac M (1989) Structure and function of vacuolar class of ATP-driven proton pumps. *Physiol Rev* 69: 765-796

Forgac M (2007) Vacuolar ATPases: rotary proton pumps in physiology and pathophysiology. *Nat Rev Mol Cell Biol* 8: 917-929

Forte LR, Bylund DB, Zahler WL (1983) Forskolin does not activate sperm adenylate cyclase. *Mol Pharmacol* 24: 42-47

Futerman AH, van Meer G (2004) The cell biology of lysosomal storage disorders. *Nat Rev Mol Cell Biol* 5: 554-565

Garbers DL, Tubb DJ, Hyne RV (1982) A requirement of bicarbonate for Ca2+-induced elevations of cyclic AMP in guinea pig spermatozoa. *J Biol Chem* 257: 8980-8984

Garty NB, Salomon Y (1987) Stimulation of partially purified adenylate cyclase from bull sperm by bicarbonate. *FEBS Lett* 218: 148-152

Geng W, Wang Z, Zhang J, Reed BY, Pak CY, Moe OW (2005) Cloning and characterization of the human soluble adenylyl cyclase. *Am J Physiol Cell Physiol* 288: C1305-1316

Ghosh P, Dahms NM, Kornfeld S (2003) Mannose 6-phosphate receptors: new twists in the tale. *Nat Rev Mol Cell Biol* 4: 202-212

Glick D, Barth S, Macleod KF (2010) Autophagy: cellular and molecular mechanisms. *J Pathol* 221: 3-12

Gloerich M, Bos JL (2010) Epac: defining a new mechanism for cAMP action. *Annu Rev Pharmacol Toxicol* 50: 355-375

Gordeladze JO, Hansson V (1981) Purification and kinetic properties of the soluble Mn2+-dependent adenylyl cyclase of the rat testis. *Mol Cell Endocrinol* 23: 125-136

Graves AR, Curran PK, Smith CL, Mindell JA (2008) The Cl-/H+ antiporter ClC-7 is the primary chloride permeation pathway in lysosomes. *Nature* 453: 788-792

Guha S, Coffey EE, Lu W, Lim JC, Beckel JM, Laties AM, Boesze-Battaglia K, Mitchell CH (2014) Approaches for detecting lysosomal alkalinization and impaired degradation in fresh and cultured RPE cells: Evidence for a role in retinal degenerations. *Exp Eye Res* 126: 68-76

Han H, Stessin A, Roberts J, Hess K, Gautam N, Kamenetsky M, Lou O, Hyde E, Nathan N, Muller WA, Buck J, Levin LR, Nathan C (2005) Calcium-sensing soluble adenylyl cyclase mediates TNF signal transduction in human neutrophils. *J Exp Med* 202: 353-361

Hayward R, Saliba KJ, Kirk K (2006) The pH of the digestive vacuole of Plasmodium falciparum is not associated with chloroquine resistance. *J Cell Sci* 119: 1016-1025

Hess KC, Jones BH, Marquez B, Chen Y, Ord TS, Kamenetsky M, Miyamoto C, Zippin JH, Kopf GS, Suarez SS, Levin LR, Williams CJ, Buck J, Moss SB (2005a) The "soluble" adenylyl cyclase in sperm mediates multiple signaling events required for fertilization. *Developmental cell* 9: 249-259

Hess KC, Jones BH, Marquez B, Chen Y, Ord TS, Kamenetsky M, Miyamoto C, Zippin JH, Kopf GS, Suarez SS, Levin LR, Williams CJ, Buck J, Moss SB (2005b) The "soluble" adenylyl cyclase in sperm mediates multiple signaling events required for fertilization. *Dev Cell* 9: 249-259

Hess KC, Liu J, Manfredi G, Muhlschlegel FA, Buck J, Levin LR, Barrientos A (2014) A mitochondrial CO2-adenylyl cyclase-cAMP signalosome controls yeast normoxic cytochrome c oxidase activity. *FASEB J* 28: 4369-4380

Hughes AL, Gottschling DE (2012) An early age increase in vacuolar pH limits mitochondrial function and lifespan in yeast. *Nature* 492: 261-265

Ishidoh K, Kominami E (2002) Processing and activation of lysosomal proteinases. *Biol Chem* 383: 1827-1831

Jaiswal BS, Conti M (2001) Identification and functional analysis of splice variants of the germ cell soluble adenylyl cyclase. *J Biol Chem* 276: 31698-31708

Jaiswal BS, Conti M (2003) Calcium regulation of the soluble adenylyl cyclase expressed in mammalian spermatozoa. *Proc Natl Acad Sci U S A* 100: 10676-10681

Jentsch TJ (2007) Chloride and the endosomal-lysosomal pathway: emerging roles of CLC chloride transporters. *J Physiol* 578: 633-640

Kamenetsky M, Middelhaufe S, Bank EM, Levin LR, Buck J, Steegborn C (2006) Molecular details of cAMP generation in mammalian cells: a tale of two systems. *J Mol Biol* 362: 623-639

Kane PM (1995) Disassembly and reassembly of the yeast vacuolar H(+)-ATPase in vivo. *J Biol Chem* 270: 17025-17032

Kasper D, Planells-Cases R, Fuhrmann JC, Scheel O, Zeitz O, Ruether K, Schmitt A, Poet M, Steinfeld R, Schweizer M, Kornak U, Jentsch TJ (2005) Loss of the chloride channel ClC-7 leads to lysosomal storage disease and neurodegeneration. *Embo J* 24: 1079-1091

Kaushik S, Cuervo AM (2009) Methods to monitor chaperone-mediated autophagy. *Methods Enzymol* 452: 297-324

Kawasaki-Nishi S, Nishi T, Forgac M (2001) Yeast V-ATPase complexes containing different isoforms of the 100-kDa a-subunit differ in coupling efficiency and in vivo dissociation. *J Biol Chem* 276: 17941-17948

Kimura S, Fujita N, Noda T, Yoshimori T (2009) Monitoring autophagy in mammalian cultured cells through the dynamics of LC3. *Methods Enzymol* 452: 1-12

Kleinboelting S, Diaz A, Moniot S, van den Heuvel J, Weyand M, Levin LR, Buck J, Steegborn C (2014) Crystal structures of human soluble adenylyl cyclase reveal mechanisms of catalysis and of its activation through bicarbonate. *Proc Natl Acad Sci U S A* 111: 3727-3732

Klionsky DJ (2007) Autophagy: from phenomenology to molecular understanding in less than a decade. *Nat Rev Mol Cell Biol* 8: 931-937

Klumperman J, Raposo G (2014) The complex ultrastructure of the endolysosomal system. *Cold Spring Harb Perspect Biol* 6: a016857

Kornak U, Kasper D, Bosl MR, Kaiser E, Schweizer M, Schulz A, Friedrich W, Delling G, Jentsch TJ (2001) Loss of the ClC-7 chloride channel leads to osteopetrosis in mice and man. *Cell* 104: 205-215

Kornfeld S, Mellman I (1989) The biogenesis of lysosomes. *Annu Rev Cell Biol* 5: 483-525

Lange PF, Wartosch L, Jentsch TJ, Fuhrmann JC (2006) ClC-7 requires Ostm1 as a beta-subunit to support bone resorption and lysosomal function. *Nature* 440: 220-223

Lee JH, Yu WH, Kumar A, Lee S, Mohan PS, Peterhoff CM, Wolfe DM, Martinez-Vicente M, Massey AC, Sovak G, Uchiyama Y, Westaway D, Cuervo AM, Nixon RA (2010) Lysosomal proteolysis and autophagy require presenilin 1 and are disrupted by Alzheimer-related PS1 mutations. *Cell* 141: 1146-1158

Lee YS, Tresguerres M, Hess K, Marmorstein LY, Levin LR, Buck J, Marmorstein AD (2011) Regulation of anterior chamber drainage by bicarbonate-sensitive soluble adenylyl cyclase in the ciliary body. *J Biol Chem* 286: 41353-41358

Lefkimmiatis K, Leronni D, Hofer AM (2013) The inner and outer compartments of mitochondria are sites of distinct cAMP/PKA signaling dynamics. *J Cell Biol* 202: 453-462

Lefkowitz RJ (1994) Rodbell and Gilman win 1994 Nobel Prize for Physiology and Medicine. *Trends Pharmacol Sci* 15: 442-444

Levin LR, Buck J (2015a) Physiological roles of acid-base sensors. *Annu Rev Physiol* 77: 347-362

Levin LR, Buck J (2015b) Physiological roles of Acid-base sensors. *Annu Rev Physiol* 77: 347-362

Li S, Allen KT, Bonanno JA (2011) Soluble adenylyl cyclase mediates bicarbonate-dependent corneal endothelial cell protection. *Am J Physiol Cell Physiol* 300: C368-374

Linder JU, Schultz JE (2003) The class III adenylyl cyclases: multi-purpose signalling modules. *Cell Signal* 15: 1081-1089

Litvin TN (2003) A Novel Mechanism of Adenylyl Cyclase Activation Conserved from Cyanobacteria to Man. *Weill Medical College and Graduate School of Cornell University*: 129

Litvin TN, Kamenetsky M, Zarifyan A, Buck J, Levin LR (2003) Kinetic properties of "soluble" adenylyl cyclase. Synergism between calcium and bicarbonate. *J Biol Chem* 278: 15922-15926

Liu J, Lu W, Guha S, Baltazar GC, Coffey EE, Laties AM, Rubenstein RC, Reenstra WW, Mitchell CH (2012) Cystic fibrosis transmembrane conductance regulator contributes to reacidification of alkalinized lysosomes in RPE cells. *Am J Physiol Cell Physiol* 303: C160-169

Liu J, Lu W, Reigada D, Nguyen J, Laties AM, Mitchell CH (2008) Restoration of lysosomal pH in RPE cells from cultured human and ABCA4(-/-) mice: pharmacologic approaches and functional recovery. *Invest Ophthalmol Vis Sci* 49: 772-780

Lomas O, Zaccolo M (2014) Phosphodiesterases maintain signaling fidelity via compartmentalization of cyclic nucleotides. *Physiology (Bethesda)* 29: 141-149

Luzio JP, Hackmann Y, Dieckmann NM, Griffiths GM (2014) The biogenesis of lysosomes and lysosome-related organelles. *Cold Spring Harb Perspect Biol* 6: a016840

Luzio JP, Pryor PR, Bright NA (2007) Lysosomes: fusion and function. *Nat Rev Mol Cell Biol* 8: 622-632

Majumdar A, Capetillo-Zarate E, Cruz D, Gouras GK, Maxfield FR (2011) Degradation of Alzheimer's amyloid fibrils by microglia requires delivery of ClC-7 to lysosomes. *Mol Biol Cell* 22: 1664-1676

Majumdar A, Cruz D, Asamoah N, Buxbaum A, Sohar I, Lobel P, Maxfield FR (2007) Activation of microglia acidifies lysosomes and leads to degradation of Alzheimer amyloid fibrils. *Mol Biol Cell* 18: 1490-1496

Marshansky V, Futai M (2008a) The V-type H+-ATPase in vesicular trafficking: targeting, regulation and function. *Curr Opin Cell Biol* 20: 415-426

Marshansky V, Futai M (2008b) The V-type H+-ATPase in vesicular trafficking: targeting, regulation and function. *Curr Opin Cell Biol* 20: 415-426

Martin C, Pedersen SF, Schwab A, Stock C (2011) Intracellular pH gradients in migrating cells. *Am J Physiol Cell Physiol* 300: C490-495

Martinez-Vicente M, Sovak G, Cuervo AM (2005) Protein degradation and aging. *Exp Gerontol* 40: 622-633

Maxfield FR, Yamashiro DJ (1987) Endosome acidification and the pathways of receptor-mediated endocytosis. *Adv Exp Med Biol* 225: 189-198

Middelhaufe S, Leipelt M, Levin LR, Buck J, Steegborn C (2012) Identification of a haem domain in human soluble adenylate cyclase. *Biosci Rep* 32: 491-499

Milner TA, Waters EM, Robinson DC, Pierce JP (2011) Degenerating processes identified by electron microscopic immunocytochemical methods. *Methods Mol Biol* 793: 23-59

Mindell JA (2012) Lysosomal acidification mechanisms. *Annu Rev Physiol* 74: 69-86

Mizushima N (2007) Autophagy: process and function. *Genes Dev* 21: 2861-2873

Mizushima N, Ohsumi Y, Yoshimori T (2002) Autophagosome formation in mammalian cells. *Cell Struct Funct* 27: 421-429

Neer EJ (1978) Physical and functional properties of adenylate cyclase from mature rat testis. *J Biol Chem* 253: 5808-5812

Neer EJ (1979) Interaction of soluble brain adenylate cyclase with manganese. *J Biol Chem* 254: 2089-2096

Nishino I, Fu J, Tanji K, Yamada T, Shimojo S, Koori T, Mora M, Riggs JE, Oh SJ, Koga Y, Sue CM, Yamamoto A, Murakami N, Shanske S, Byrne E, Bonilla E, Nonaka I, DiMauro S, Hirano M (2000) Primary LAMP-2 deficiency causes X-linked vacuolar cardiomyopathy and myopathy (Danon disease). *Nature* 406: 906-910

Nixon RA, Wegiel J, Kumar A, Yu WH, Peterhoff C, Cataldo A, Cuervo AM (2005) Extensive involvement of autophagy in Alzheimer disease: an immuno-electron microscopy study. *J Neuropathol Exp Neurol* 64: 113-122

Nixon RA, Yang DS, Lee JH (2008) Neurodegenerative lysosomal disorders: a continuum from development to late age. *Autophagy* 4: 590-599

Ohkuma S, Moriyama Y, Takano T (1982) Identification and characterization of a proton pump on lysosomes by fluorescein-isothiocyanate-dextran fluorescence. *Proc Natl Acad Sci U S A* 79: 2758-2762

Ohkuma S, Poole B (1978) Fluorescence probe measurement of the intralysosomal pH in living cells and the perturbation of pH by various agents. *Proc Natl Acad Sci U S A* 75: 3327-3331

Okamura N, Tajima Y, Soejima A, Masuda H, Sugita Y (1985) Sodium bicarbonate in seminal plasma stimulates the motility of mammalian spermatozoa through direct activation of adenylate cyclase. *J Biol Chem* 260: 9699-9705

Pastor-Soler N, Beaulieu V, Litvin TN, Da Silva N, Chen Y, Brown D, Buck J, Levin LR, Breton S (2003) Bicarbonate-regulated adenylyl cyclase (sAC) is a sensor that regulates pH-dependent V-ATPase recycling. *J Biol Chem* 278: 49523-49529

Pastor-Soler NM, Hallows KR, Smolak C, Gong F, Brown D, Breton S (2008) Alkaline pH- and cAMP-induced V-ATPase membrane accumulation is mediated by protein kinase A in epididymal clear cells. *Am J Physiol Cell Physiol* 294: C488-494

Paunescu TG, Da Silva N, Russo LM, McKee M, Lu HA, Breton S, Brown D (2008a) Association of soluble adenylyl cyclase with the V-ATPase in renal epithelial cells. *Am J Physiol Renal Physiol* 294: F130-138

Paunescu TG, Da Silva N, Russo LM, McKee M, Lu HA, Breton S, Brown D (2008b) Association of soluble adenylyl cyclase with the V-ATPase in renal epithelial cells. *Am J Physiol Renal Physiol* 294: F130-138

Paunescu TG, Ljubojevic M, Russo LM, Winter C, McLaughlin MM, Wagner CA, Breton S, Brown D (2010a) cAMP stimulates apical V-ATPase accumulation, microvillar elongation, and proton extrusion in kidney collecting duct A-intercalated cells. *Am J Physiol Renal Physiol* 298: F643-654

Paunescu TG, Ljubojevic M, Russo LM, Winter C, McLaughlin MM, Wagner CA, Breton S, Brown D (2010b) cAMP stimulates apical V-ATPase accumulation,

microvillar elongation, and proton extrusion in kidney collecting duct A-intercalated cells. *Am J Physiol Renal Physiol* 298: F643-654

Peters A, Palay SL, Webster Hd (1991) *The fine structure of the nervous system : neurons and their supporting cells*, 3rd edn. New York: Oxford University Press.

Pillay CS, Elliott E, Dennison C (2002) Endolysosomal proteolysis and its regulation. *Biochem J* 363: 417-429

Poet M, Kornak U, Schweizer M, Zdebik AA, Scheel O, Hoelter S, Wurst W, Schmitt A, Fuhrmann JC, Planells-Cases R, Mole SE, Hubner CA, Jentsch TJ (2006) Lysosomal storage disease upon disruption of the neuronal chloride transport protein ClC-6. *Proc Natl Acad Sci U S A* 103: 13854-13859

Pryor PR, Mullock BM, Bright NA, Gray SR, Luzio JP (2000) The role of intraorganellar Ca(2+) in late endosome-lysosome heterotypic fusion and in the reformation of lysosomes from hybrid organelles. *J Cell Biol* 149: 1053-1062

Raben N, Shea L, Hill V, Plotz P (2009) Monitoring autophagy in lysosomal storage disorders. *Methods Enzymol* 453: 417-449

Rahman N, Buck J, Levin LR (2013) pH sensing via bicarbonate-regulated "soluble" adenylyl cyclase (sAC). *Front Physiol* 4: 343

Rajawat YS, Hilioti Z, Bossis I (2009) Aging: central role for autophagy and the lysosomal degradative system. *Ageing Res Rev* 8: 199-213

Rall TW, Sutherland EW (1958) Formation of a cyclic adenine ribonucleotide by tissue particles. *J Biol Chem* 232: 1065-1076

Reczek D, Schwake M, Schroder J, Hughes H, Blanz J, Jin X, Brondyk W, Van Patten S, Edmunds T, Saftig P (2007) LIMP-2 is a receptor for lysosomal mannose-6-phosphate-independent targeting of beta-glucocerebrosidase. *Cell* 131: 770-783

Rink J, Ghigo E, Kalaidzidis Y, Zerial M (2005) Rab conversion as a mechanism of progression from early to late endosomes. *Cell* 122: 735-749

Rojas FJ, Bruzzone ME, Moretti-Rojas I (1992) Regulation of cyclic adenosine monophosphate synthesis in human ejaculated spermatozoa. II. The role of calcium and bicarbonate ions on the activation of adenylyl cyclase. *Hum Reprod* 7: 1131-1135

Rojas FJ, Patrizio P, Do J, Silber S, Asch RH, Moretti-Rojas I (1993) Evidence for a novel adenylyl cyclase in human epididymal sperm. *Endocrinology* 133: 3030-3033

Saftig P, Klumperman J (2009) Lysosome biogenesis and lysosomal membrane proteins: trafficking meets function. *Nat Rev Mol Cell Biol* 10: 623-635

Saftig P, Schroder B, Blanz J (2010) Lysosomal membrane proteins: life between acid and neutral conditions. *Biochem Soc Trans* 38: 1420-1423

Sardiello M, Palmieri M, di Ronza A, Medina DL, Valenza M, Gennarino VA, Di Malta C, Donaudy F, Embrione V, Polishchuk RS, Banfi S, Parenti G, Cattaneo E, Ballabio A (2009) A gene network regulating lysosomal biogenesis and function. *Science* 325: 473-477

Schmid A, Sutto Z, Nlend MC, Horvath G, Schmid N, Buck J, Levin LR, Conner GE, Fregien N, Salathe M (2007) Soluble adenylyl cyclase is localized to cilia and contributes to ciliary beat frequency regulation via production of cAMP. *J Gen Physiol* 130: 99-109

Schroder J, Lullmann-Rauch R, Himmerkus N, Pleines I, Nieswandt B, Orinska Z, Koch-Nolte F, Schroder B, Bleich M, Saftig P (2009) Deficiency of the tetraspanin CD63 associated with kidney pathology but normal lysosomal function. *Mol Cell Biol* 29: 1083-1094

Settembre C, Fraldi A, Medina DL, Ballabio A (2013) Signals from the lysosome: a control centre for cellular clearance and energy metabolism. *Nat Rev Mol Cell Biol* 14: 283-296

Shao E, Forgac M (2004) Involvement of the nonhomologous region of subunit A of the yeast V-ATPase in coupling and in vivo dissociation. *J Biol Chem* 279: 48663-48670

Smardon AM, Tarsio M, Kane PM (2002) The RAVE complex is essential for stable assembly of the yeast V-ATPase. *J Biol Chem* 277: 13831-13839

Spitzer KW, Skolnick RL, Peercy BE, Keener JP, Vaughan-Jones RD (2002) Facilitation of intracellular H(+) ion mobility by CO(2)/HCO(3)(-) in rabbit ventricular myocytes is regulated by carbonic anhydrase. *J Physiol* 541: 159-167

Stauber T, Jentsch TJ (2013) Chloride in vesicular trafficking and function. *Annu Rev Physiol* 75: 453-477

Steegborn C, Litvin TN, Hess KC, Capper AB, Taussig R, Buck J, Levin LR, Wu H (2005) A novel mechanism for adenylyl cyclase inhibition from the crystal structure of its complex with catechol estrogen. *J Biol Chem* 280: 31754-31759

Steinberg BE, Huynh KK, Brodovitch A, Jabs S, Stauber T, Jentsch TJ, Grinstein S (2010) A cation counterflux supports lysosomal acidification. *J Cell Biol* 189: 1171-1186

Stengel D, Guenet L, Desmier M, Insel P, Hanoune J (1982) Forskolin requires more than the catalytic unit to activate adenylate cyclase. *Mol Cell Endocrinol* 28: 681-690

Stengel D, Hanoune J (1984) The sperm adenylate cyclase. *Ann N Y Acad Sci* 438: 18-28

Stessin AM, Zippin JH, Kamenetsky M, Hess KC, Buck J, Levin LR (2006) Soluble adenylyl cyclase mediates nerve growth factor-induced activation of Rap1. *J Biol Chem* 281: 17253-17258

Stewart AK, Boyd CA, Vaughan-Jones RD (1999) A novel role for carbonic anhydrase: cytoplasmic pH gradient dissipation in mouse small intestinal enterocytes. *J Physiol* 516 (Pt 1): 209-217

Sturgill-Koszycki S, Swanson MS (2000) Legionella pneumophila replication vacuoles mature into acidic, endocytic organelles. *J Exp Med* 192: 1261-1272

Sutherland EW, Rall TW (1958) Fractionation and characterization of a cyclic adenine ribonucleotide formed by tissue particles. *J Biol Chem* 232: 1077-1091

Tampellini D, Rahman N, Gallo EF, Huang Z, Dumont M, Capetillo-Zarate E, Ma T, Zheng R, Lu B, Nanus DM, Lin MT, Gouras GK (2009) Synaptic activity

reduces intraneuronal Abeta, promotes APP transport to synapses, and protects against Abeta-related synaptic alterations. *J Neurosci* 29: 9704-9713

Tanaka Y, Guhde G, Suter A, Eskelinen EL, Hartmann D, Lullmann-Rauch R, Janssen PM, Blanz J, von Figura K, Saftig P (2000) Accumulation of autophagic vacuoles and cardiomyopathy in LAMP-2-deficient mice. *Nature* 406: 902-906

Tarbashevich K, Reichman-Fried M, Grimaldi C, Raz E (2015) Chemokine-Dependent pH Elevation at the Cell Front Sustains Polarity in Directionally Migrating Zebrafish Germ Cells. *Curr Biol* 25: 1096-1103

Taussig R, Gilman AG (1995) Mammalian membrane-bound adenylyl cyclases. *J Biol Chem* 270: 1-4

Terman A, Gustafsson B, Brunk UT (2006) The lysosomal-mitochondrial axis theory of postmitotic aging and cell death. *Chem Biol Interact* 163: 29-37

Tesmer JJ, Sunahara RK, Johnson RA, Gosselin G, Gilman AG, Sprang SR (1999) Two-metal-Ion catalysis in adenylyl cyclase. *Science* 285: 756-760

Traut TW (1994) Physiological concentrations of purines and pyrimidines. *Mol Cell Biochem* 140: 1-22

Tresguerres M (2014) sAC from aquatic organisms as a model to study the evolution of acid/base sensing. *Biochim Biophys Acta* 1842: 2629-2635

Tresguerres M, Buck J, Levin LR (2010a) Physiological carbon dioxide, bicarbonate, and pH sensing. *Pflugers Arch* 460: 953-964

Tresguerres M, Levin LR, Buck J (2011) Intracellular cAMP signaling by soluble adenylyl cyclase. *Kidney Int* 79: 1277-1288

Tresguerres M, Parks SK, Salazar E, Levin LR, Goss GG, Buck J (2010b) Bicarbonate-sensing soluble adenylyl cyclase is an essential sensor for acid/base homeostasis. *Proc Natl Acad Sci U S A* 107: 442-447

Tresguerres M, Parks SK, Salazar E, Levin LR, Goss GG, Buck J (2010c) Bicarbonate-sensing soluble adenylyl cyclase is an essential sensor for acid/base homeostasis. *Proc Natl Acad Sci U S A* 107: 442-447

Trombetta ES, Ebersold M, Garrett W, Pypaert M, Mellman I (2003) Activation of lysosomal function during dendritic cell maturation. *Science* 299: 1400-1403

van Meel E, Klumperman J (2008) Imaging and imagination: understanding the endo-lysosomal system. *Histochem Cell Biol* 129: 253-266

Visconti PE, Muschietti JP, Flawia MM, Tezon JG (1990) Bicarbonate dependence of cAMP accumulation induced by phorbol esters in hamster spermatozoa. *Biochim Biophys Acta* 1054: 231-236

Vladutiu GD, Rattazzi MC (1979) Excretion-reuptake route of beta-hexosaminidase in normal and I-cell disease cultured fibroblasts. *J Clin Invest* 63: 595-601

Waguri S, Dewitte F, Le Borgne R, Rouille Y, Uchiyama Y, Dubremetz JF, Hoflack B (2003) Visualization of TGN to endosome trafficking through fluorescently labeled MPR and AP-1 in living cells. *Mol Biol Cell* 14: 142-155

Waheed A, Pohlmann R, Hasilik A, von Figura K, van Elsen A, Leroy JG (1982) Deficiency of UDP-N-acetylglucosamine:lysosomal enzyme N-

acetylglucosamine-1-phosphotransferase in organs of I-cell patients. *Biochem Biophys Res Commun* 105: 1052-1058

Wahl-Schott C, Biel M (2009) HCN channels: structure, cellular regulation and physiological function. *Cell Mol Life Sci* 66: 470-494

Wartosch L, Fuhrmann JC, Schweizer M, Stauber T, Jentsch TJ (2009) Lysosomal degradation of endocytosed proteins depends on the chloride transport protein ClC-7. *Faseb J* 23: 4056-4068

Wolfe DM, Lee JH, Kumar A, Lee S, Orenstein SJ, Nixon RA (2013) Autophagy failure in Alzheimer's disease and the role of defective lysosomal acidification. *Eur J Neurosci* 37: 1949-1961

Wu KY, Zippin JH, Huron DR, Kamenetsky M, Hengst U, Buck J, Levin LR, Jaffrey SR (2006) Soluble adenylyl cyclase is required for netrin-1 signaling in nerve growth cones. *Nature Neuroscience* 9: 1257-1264

Wuttke MS, Buck J, Levin LR (2001) Bicarbonate-regulated soluble adenylyl cyclase. *Jop* 2: 154-158

Xu H, Ren D (2015) Lysosomal physiology. *Annu Rev Physiol* 77: 57-80

Xu T, Forgac M (2001) Microtubules are involved in glucose-dependent dissociation of the yeast vacuolar [H+]-ATPase in vivo. *J Biol Chem* 276: 24855-24861

Zhang F, Jin S, Yi F, Li PL (2009) TRP-ML1 functions as a lysosomal NAADP-sensitive Ca2+ release channel in coronary arterial myocytes. *J Cell Mol Med* 13: 3174-3185

Zippin JH, Chen Y, Nahirney P, Kamenetsky M, Wuttke MS, Fischman DA, Levin LR, Buck J (2003) Compartmentalization of bicarbonate-sensitive adenylyl cyclase in distinct signaling microdomains. *The FASEB journal : official publication of the Federation of American Societies for Experimental Biology* 17: 82-84

Zippin JH, Chen Y, Straub SG, Hess KC, Diaz A, Lee D, Tso P, Holz GG, Sharp GW, Levin LR, Buck J (2013a) CO2/HCO3(-)- and calcium-regulated soluble adenylyl cyclase as a physiological ATP sensor. *J Biol Chem* 288: 33283-33291

Zippin JH, Chen Y, Straub SG, Hess KC, Diaz A, Lee D, Tso P, Holz GG, Sharp GW, Levin LR, Buck J (2013b) CO2/HCOFormula- and Calcium-regulated Soluble Adenylyl Cyclase as a Physiological ATP Sensor. *J Biol Chem* 288: 33283-33291